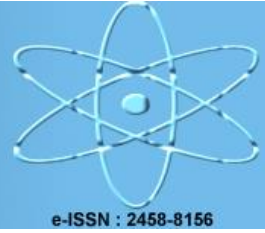




# EJENS

European Journal of Engineering and Natural Sciences



e-ISSN : 2458-8156

## Estimation of Optimum Insulation Thickness for the Buildings in Different Climate Zones of Türkiye

Atila G. Devecioğlu\*, Vedat Oruç

<sup>1</sup>Department of Mechanical Engineering, Faculty of Engineering, Dicle University, 21280, Diyarbakır, Türkiye.

\*Corresponding Author email: atillad@dicle.edu.tr

### Abstract

The application of insulation on outer walls of buildings is investigated in this study. The provinces of Istanbul, Ankara, Van and Erzurum are selected as 3<sup>rd</sup>, 4<sup>th</sup>, 5<sup>th</sup> and 6<sup>th</sup> zones, respectively in Türkiye for the investigation. The optimum insulation thickness ( $x_{opt}$ ) values are computed using heating degree-day method. The extruded polystyrene (XPS) and glass wool are separately used as insulation materials in the analysis. According to the obtained results,  $x_{opt}$  of glass wool is higher compared to XPS material while the payback periods for glass wool are found to be shorter for all studied provinces. In addition, the amount of saved energy due to the application of  $x_{opt}$  increases as going from 3<sup>rd</sup> zone (Istanbul) to 6<sup>th</sup> zone (Erzurum). The saved energy is seen to be over 80% due to the presence of  $x_{opt}$ . The saved energy amount is also determined to be greater using glass wool than XPS for the presence of insulation material with optimum thickness in all studied cities. The glass wool can be suggested as a potential insulation material than XPS for these investigated provinces considering quicker payback period, higher energy savings and suitable value of overall heat transfer coefficient.

### Keywords

building insulation, glass wool, HDD, optimum insulation thickness, XPS

### 1. INTRODUCTION

In line with the Paris Agreement and the European Green Deal, building programming rules have been revised to increase technical, storage, and economic changes to support Türkiye's net-zero energy goal. According to the new building protocol introduced in Türkiye, heating energy needs will be calculated separately for cooling energy. The calculation method is based on the monthly method according to EN ISO 52016-1. This regulation aims to reduce CO<sub>2</sub> emissions by 600 million tons annually [1]. With the new regulation, the number of climate zones has been increased from 4 to 6, allowing for more sensitive insulation to regional conditions. The new regulation sets indoor design temperatures at 20°C (winter) and 26°C (summer). Hourly, monthly meteorological data, and solar radiation data have been updated according to climate zones. The new standard aims to reduce energy consumption from 120–150 kWh/m<sup>2</sup> to 70–90 kWh/m<sup>2</sup>. Furthermore, the total heat transfer coefficient of the wall ( $U$ ) values of buildings have been improved, ranging from 0.25–0.45 W/m<sup>2</sup>K for walls, 0.2–0.35 W/m<sup>2</sup>K for roofs, and 0.25–0.40 W/m<sup>2</sup>K for floors. The  $U$ -value of windows has been reduced to 1.8 W/m<sup>2</sup>K, making the use of Low-E/solar glass mandatory [2].

Most of the energy is consumed in residences, public buildings and commercial buildings. Sector-based energy consumption of the last 20 years in Türkiye is shown in Figure 1. While approximately 34% of the energy consumed in Türkiye in 2005 was developed in residences, public buildings and commercial buildings, this rate decreased to 32% in 2023 [3].

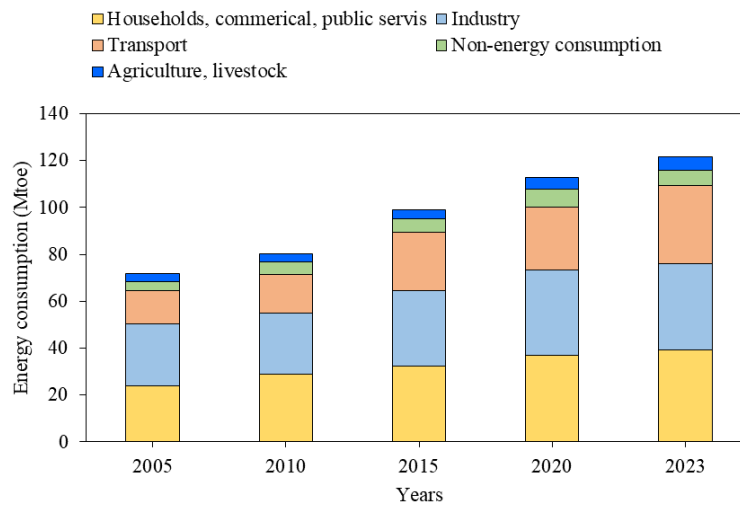


Figure 1. The energy consumption information for the last 20 years of Türkiye depending on application field

Insulation is a critical component in building design, aimed at reducing heat transfer through the building envelope including walls, roofs, floors, and windows. The insulation enhances energy efficiency, reduces heating and cooling energy requirement, and improves indoor thermal comfort by minimizing heat loss in winter and heat gain in summer. Furthermore, a suitable insulation contributes to environmental sustainability due to reduced energy consumption and associated greenhouse gas emissions. In residential and commercial buildings, the building envelope accounts for 50–60% of total heat loss or gain hence, insulation plays a major role in providing energy savings of up to 50%. In addition to energy efficiency, insulation leads to benefits such as fire resistance, sound control, and condensation control, which makes it essential for establishing sustainable and comfortable indoor mediums.

A critical aspect of insulation design is to determine the optimum insulation thickness ( $x_{opt}$ ), which balances the initial insulation cost with the long-term energy savings. In fact,  $x_{opt}$  depends on factors such as climate, insulation material properties (e.g., thermal conductivity), fuel types, and economic parameters (e.g., insulation costs and energy prices). Generally,  $x_{opt}$  is calculated using life-cycle cost analysis (LCCA) which consider both economic and environmental impacts over the building's lifespan. The degree-days or degree-hours approach methods estimate annual heating and cooling loads, while advanced techniques account for dynamic thermal conditions. These computations demonstrate that  $x_{opt}$  maximizes energy savings without excessive material costs, with payback periods often ranging from 1 to 5 years, according to the variables such as region and insulation type.

There are related investigations in the available literature. For example, the degree-hours method is used to calculate  $x_{opt}$  for external walls in Türkiye's warmest zone, which emphasizes the greater impact of insulation on cooling loads [4]. The results indicated  $x_{opt}$  of 3.2–3.8 cm for cooling and 1.6–2.7 cm for heating, with energy savings of 8.47–12.19 \$/m<sup>2</sup> and payback periods of 3.39–5.47 years. In another study, LCCA is applied to optimize insulation thickness [5]. The results indicate economic savings of up to 21 \$/m<sup>2</sup> for rock wool and polystyrene in Palestine, with payback periods of 1–2.3 years. It highlights the economic feasibility of insulation in reducing energy costs. The impact of dynamic heat transfer and electricity tariffs on optimum insulation thickness, is investigated [6]. It is found that wall orientation has a minor effect on total cost and thickness, with optimal thicknesses ranging from 5.4–19.2 cm.

A dynamic thermal model is used to determine  $x_{opt}$  under varying structural materials [7]. It is determined that  $x_{opt}$  values are 5.4–19.2 cm and payback periods are 3.56–8.85 years, with substantial energy savings. A 100 m<sup>2</sup> residential house was modelled using Design Builder to determine  $x_{opt}$  for external walls in Kirkuk, Iraq (hot climate) and Konya, Türkiye (cold climate) [8]. The analysis evaluated XPS, EPS, rock wool, and glass wool, with

electricity and natural gas as energy sources for Kirkuk and Konya, respectively, finding XPS to be the most effective insulation material. The values of  $x_{opt}$  were 7 cm and 9 cm for Kirkuk, and 7 cm and 15 cm for Konya, achieving energy savings of 6.7% and 8.3% with XPS at 9 cm and 11 cm, respectively.

An analysis is performed across 16 cities from four climate zones using life-cycle cost analysis and heating degree-days [9]. It is determined that  $x_{opt}$  values range from 2 to 17 cm, with energy savings between 22% and 79%. Payback periods vary from 1.3 to 4.5 years depending on the city and fuel type used (coal, natural gas, fuel oil, LPG, or electricity). In a recent study,  $x_{opt}$  for expanded and extruded polystyrene is evaluated in diverse Indian climates [10]. The results are reporting  $x_{opt}$  values as 0.0428–0.891 m for cooling and 0.0063–0.1522 m for heating, and payback periods as 1.49–6.52 years. It also includes emission analysis, highlighting reductions in greenhouse gas emissions. The HDD method is applied across all Turkish provinces to find  $x_{opt}$  for various materials (glass wool, rock wool, XPS, EPS) [11]. The energy savings, payback period, and CO<sub>2</sub> emissions reductions are also evaluated in the study. The results demonstrate  $x_{opt}$  varied between 0.07 m and 0.23 m, depending on HDD, with payback periods as short as 0.11–0.38 years for the best cases. The values of  $x_{opt}$  are calculated via heating degree day and cooling degree day methods and lifecycle cost analysis over 30 years [12]. The optimum insulation thickness values are reported as 10.5 cm–17.3 cm for walls, 6–9.8 cm for floors, and up to 26.8 cm for ceilings; energy savings in the range of 13–22% depending on region.

In the present investigation, four zones (Istanbul, Ankara, Van, and Erzurum) in Türkiye are selected to determine  $x_{opt}$  for the outer wall of buildings using HDD method. The studied insulation materials are XPS and glass wool (GW). The natural gas is considered as heating energy source in the analysis. The energy savings and payback periods corresponding to  $x_{opt}$  are computed. Finally, the results are compared and discussed to suggest the suitable insulation case for the studied provinces.

## 2. MATERIALS AND METHODS

The extruded polystyrene (XPS) and glass wool (GW) are used as insulation materials on outer walls of the buildings in Istanbul (3<sup>rd</sup> zone), Ankara (4<sup>th</sup> zone), Van (5<sup>th</sup> zone) and Erzurum (6<sup>th</sup> zone) which are the provinces of Türkiye. The natural gas is considered as heating energy source for the analysis. The heat losses ( $q$ ) in W/m<sup>2</sup> through an exterior wall surface is given by

$$q = U \cdot (T_i - T_o) \quad (1)$$

where  $U$  is the total heat transfer coefficient of the wall in W/m<sup>2</sup>·K,  $T_i$  is the indoor air temperature and  $T_o$  is the outdoor air temperature. The value of  $U$  for external wall containing an insulation layer is calculated as

$$U = \frac{1}{R_i + R_w + R_{ins} + R_o} \quad (2)$$

where  $R_i$  and  $R_o$  represent the convection thermal resistance of the indoor and outdoor environments, which are 0.13 and 0.04 m<sup>2</sup>·K/W, respectively,  $R_w$  is the thermal resistance of the uninsulated wall and  $R_{ins}$  is thermal resistance of the insulating material which is found as

$$R_{ins} = \frac{x}{k} \quad (3)$$

where  $x$  and  $k$  are the thickness and the thermal conductivity of the insulation element, respectively. Then, the total resistance of the uninsulated wall ( $R_{w,t}$ ) can be obtained as

$$R_{w,t} = R_i + R_w + R_o \quad (4)$$

The elements in the exterior wall are shown schematically in Figure 2. The specifications of the wall elements can be seen in Table 1, hence  $R_w$  is found to be 0.333 m<sup>2</sup>·K/W while  $R_{w,t}$  is obtained as 0.503 m<sup>2</sup>·K/W. Some properties of investigated insulation materials are given in Table 2 where  $\rho$  is the density of material and  $C_i$  is the price of material per unit volume in \$/m<sup>3</sup>.

Table 1. The specifications of wall components

Wall components	Thickness, $x$ (m)	Thermal conductivity, $k$ (W/m·K)	Thermal resistance, $R$ (m <sup>2</sup> ·K/W)
Interior plaster	0.02	0.87	0.023
Brick	0.13	0.45	0.289
Exterior plaster	0.03	1.40	0.021

Table 2. Some information for the investigated insulation materials

Insulation	$k$ (W/m·K)	$C_i$ (\$/m <sup>3</sup> )	$\rho$ (kg/m <sup>3</sup> )
XPS	0.031	115	28
GW	0.038	60	24

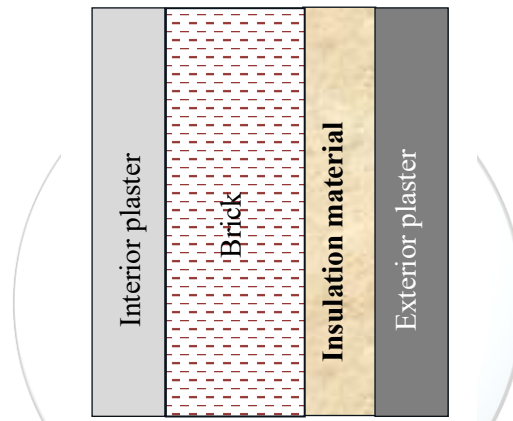


Figure 2. The schematic sketch for exterior wall elements

The optimum insulation thickness ( $x_{opt}$ ) can be computed using heating degree-day (HDD) values as [5]

$$x_{opt} = 293.94 \left( \frac{\text{HDD} \cdot C_F \cdot \text{PWF} \cdot k}{\text{LHV} \cdot C_i \cdot \eta} \right)^{\frac{1}{2}} - k \cdot R_{w,t} \quad (5)$$

where HDD values are 1786, 2599, 3465, and 4640 for İstanbul, Ankara Van, and Erzurum, respectively.  $C_F$  is the cost of natural gas taken as 0.3 \$/m<sup>3</sup> in the calculations while  $C_i$  and  $k$  are the values of insulation materials given in Table 2. Additionally, LHV is the lower heating value of natural gas (34485 kJ/m<sup>3</sup>) and  $\eta$  is the efficiency of heating system accepted as 90% for the computations. PWF in Eq. (5) is the present worth factor that can be obtained as

$$\text{PWF} = \frac{(1+r)^N - 1}{r \cdot (1+r)^N} \quad (6)$$

where  $N$  is the lifetime which is assumed as 15 years in the investigation and  $r$  is the real interest rate calculated as

$$r = \frac{i-g}{1+g} \quad (7)$$

where  $i$  is the annual interest rate (37%) and  $g$  is the inflation rate (35%) for Türkiye.

The annual energy saving,  $C_s$  in \$/(m<sup>2</sup>·year) is the difference between the annual heating cost amounts for the uninsulated wall and insulated wall cases, respectively. Hence, the economic payback period of insulation cost (PP) is calculated in year as follows

$$PP = \frac{C_{ins}}{c_s} \tag{8}$$

where the cost of insulation ( $C_{ins}$ ) is calculated in  $\$/m^2$  as

$$C_{ins} = C_i x \tag{9}$$

where  $C_i$  is unit cost of the insulation material in  $\$/m^3$  (Table 2) and  $x$  is the insulation thickness. The detailed information on the computation method of the investigated parameters can be found, for example in [5,13].

### 3. RESULTS AND DISCUSSION

The behavior of the energy cost, the insulation cost and the total cost (i.e., sum of energy cost and insulation cost) is determined depending on various insulation thickness values for the provinces of Istanbul (3<sup>rd</sup> zone), Ankara (4<sup>th</sup> zone), Van (5<sup>th</sup> zone), and Erzurum (6<sup>th</sup> zone). The results are demonstrated as sample cases in Figure 3 utilizing extruded polystyrene (XPS) for Istanbul and Van while glass wool (GW) for Ankara and Erzurum. The common behavior in these plots is that energy cost is reduced substantially with increasing insulation thickness. As expected, the insulation cost increases as insulation has greater thickness. However, the total cost decreases initially up to a certain insulation thickness but it starts to augment beyond that point. In fact, the insulation thickness at which total cost has the minimum amount is called as optimum insulation thickness,  $x_{opt}$ . Hence, the outer walls of the buildings should be insulated with suitable materials considering computed value of  $x_{opt}$ . A thickness greater than  $x_{opt}$  is not meaningful due to the increased total cost.

Figure 3 shows clearly that energy cost without insulation (i.e., insulation thickness is zero) has the highest amount for all cases. Moreover, the cost of energy without insulation is lowest for Istanbul followed by Ankara, Van, and Erzurum with the amounts of 39.62, 57.65, 76.86, and 102.92  $\$/m^2$ , respectively. This behavior is due to selected zones as mentioned above such that the coldest region is 6<sup>th</sup> zone (Erzurum) while the warmest region is 3<sup>rd</sup> zone (Istanbul) in the present investigation.

As a sample illustration, the case of Istanbul using XPS can be focused. First of all, total cost reaches its minimum value of 15.06  $\$/m^2$  at insulation thickness of 5.8 cm which corresponds to  $x_{opt}$  (the cost of XPS insulation is 6.67  $\$/m^2$  for this situation). Obviously, the energy cost without insulation is 39.62 is  $\$/m^2$ , but it is significantly reduced to about 8.40  $\$/m^2$  at  $x_{opt}=5.8$  cm. Hence, the cost of energy (i.e., amount of energy consumption) is lowered about by 78% as a result of application of XPS insulation having  $x_{opt}$ . Similar observation can be noted for other cases in Figure 3 with different numerical amounts as discussed.

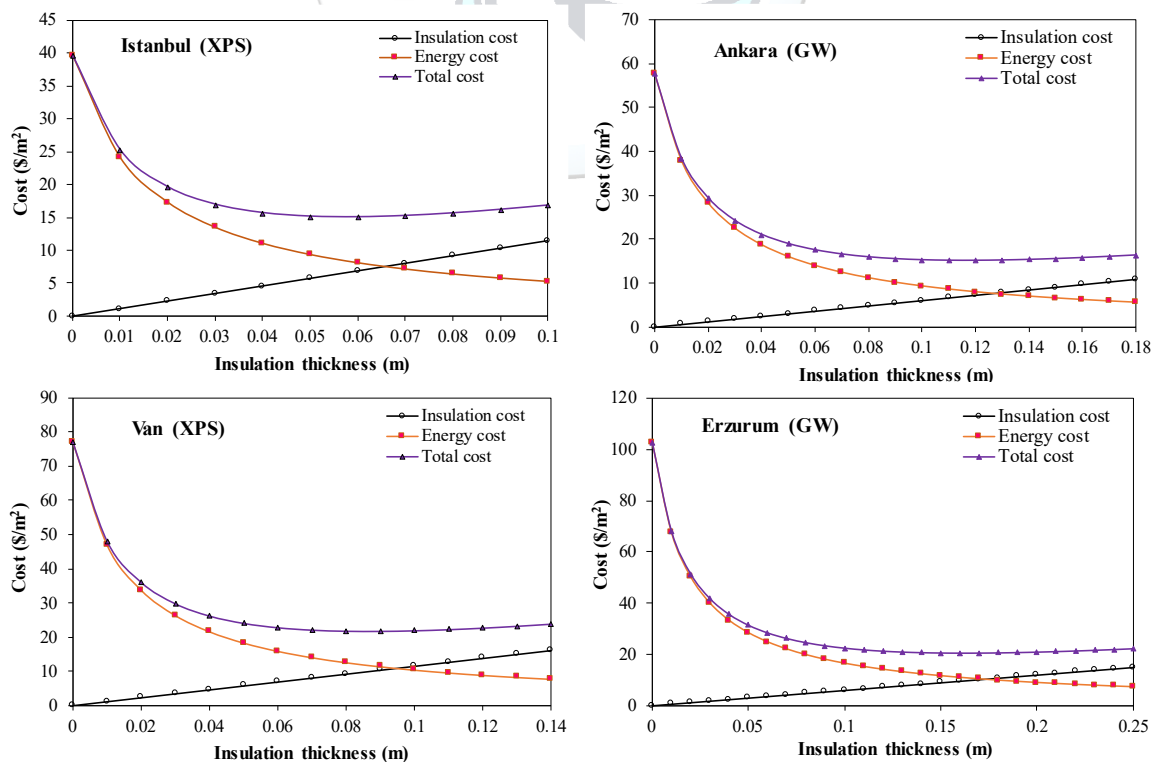


Figure 3. Variation of energy cost, insulation cost, and total cost with insulation thickness for sample cases

The optimum insulation thickness ( $x_{opt}$ ) values are detected considering both cases of XPS and GW as insulation material on the outside wall of the building in the considered provinces. The corresponding total heat transfer coefficient of the wall ( $U$ ) as well as payback period (PP) values which are calculated with Eq. (2) and Eq. (8), respectively and the results are listed in Table 3. As a sample situation using GW in Istanbul, the following computations corresponding to optimum insulation thickness ( $x_{opt} = 9.3$  cm) can be recalled as insulation cost,  $C_{ins}$  is 5.58 \$/m<sup>2</sup>, annual cost without insulation is 2.97 \$/m<sup>2</sup>·year, annual cost with insulation is 0.51 \$/m<sup>2</sup>·year (i.e., annual saved cost,  $C_S$  occurs as 2.46 \$/m<sup>2</sup>·year), and therefore PP is calculated as 2.27 years (Eq. 8). Table 3 denotes clearly that  $x_{opt}$  increases as HDD becomes greater for a given insulation material type. Moreover,  $x_{opt}$  of GW is thicker than that of XPS for all cities. The behaviours of both  $U$  and PP are similar such that they are reduced as HDD increases (i.e., when going from 3<sup>rd</sup> zone to 6<sup>th</sup> zone), in other words as  $x_{opt}$  becomes bigger whatever the type of insulation material. In addition,  $U$  and PP are smaller for a given province using GW than XPS. Although thicker values of  $x_{opt}$  in GW case, the quicker payback periods for all provinces are noticeable. Besides, the value of  $U$  should be below 0.25 W/m<sup>2</sup>·K for 5<sup>th</sup> and 6<sup>th</sup> zones while the maximum values of  $U$  should be 0.45 and 0.4 W/m<sup>2</sup>·K for 3<sup>rd</sup> and 4<sup>th</sup> zones, respectively according to the recent regulations [1, 2]. It is evidently seen in Table 3 that  $U$  values using XPS for Van and Erzurum violate the mentioned regulations since  $U > 0.25$  W/m<sup>2</sup>·K while Istanbul and Ankara satisfy the requirement as  $U < 0.45$  W/m<sup>2</sup>·K. On the other hand, when GW is utilized, all of the four provinces demonstrate suitable  $U$  values required by the new standard of heat insulation rules [1, 2]. Therefore, as well as considering its shorter payback periods, GW can be suggested to be applied as an insulation material on the outside wall of buildings in Türkiye due to the development of favorable  $U$  values.

Table 3. Results for the optimum insulation thickness application

XPS					GW			
City	HDD	$x_{opt}$ (m)	$U$ (W/m <sup>2</sup> ·K)	PP (year)	City	$x_{opt}$ (m)	$U$ (W/m <sup>2</sup> ·K)	PP (year)
İstanbul	1786	0.058	0.423	2.84	İstanbul	0.093	0.338	2.27
Ankara	2599	0.073	0.351	2.36	Ankara	0.116	0.280	1.89
Van	3465	0.086	0.304	2.04	Van	0.137	0.243	1.63
Erzurum	4640	0.103	0.262	1.76	Erzurum	0.162	0.210	1.41

As it is seen from Table 3,  $x_{opt}$  is highly dependent on HDD as well as type of insulation material. Thus, the relationship between  $x_{opt}$  and HDD for both XPS and GW is depicted in Figure 4. Obviously,  $x_{opt}$  is higher as HDD linearly increases whatever the insulation material. On the other hand,  $x_{opt}$  of GW is thicker compared to XPS for a given HDD value. Then, data for GW in Figure 4 can be expressed with the following equation

$$x_{opt} = 2 \times 10^{-5}HDD + 0.052 \quad (10)$$

Similarly, the following expression can be fitted well to the variation of  $x_{opt}$  with HDD using XPS

$$x_{opt} = 2 \times 10^{-5}HDD + 0.031 \quad (11)$$

Eqs. (10, 11) could be useful to estimate  $x_{opt}$  for other provinces using GW or XPS since these expressions already include the effect of zone through HDD values.

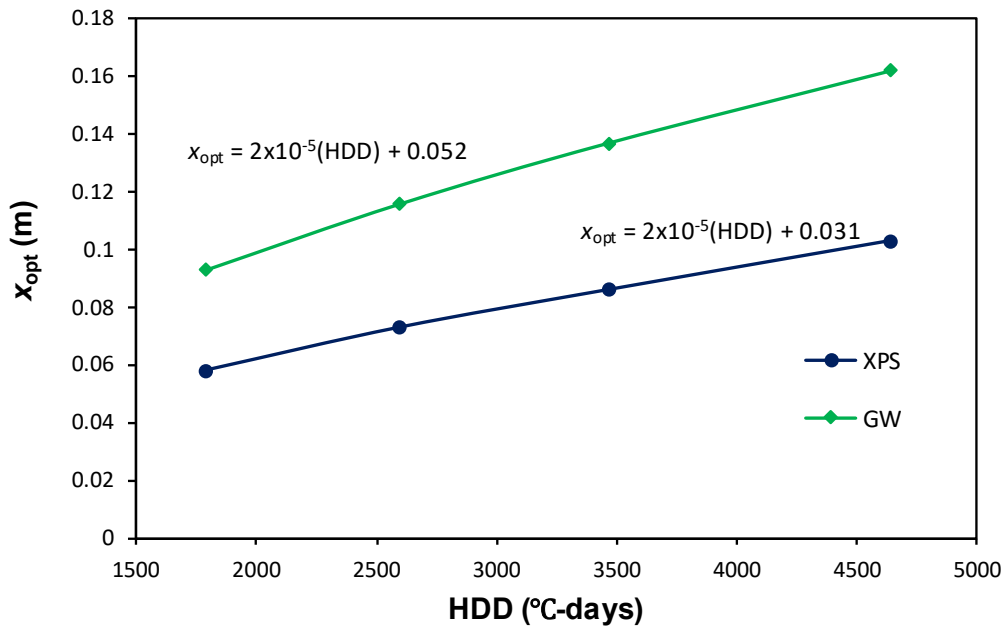


Figure 4. The dependence of  $x_{opt}$  on heating degree days for the studied insulation materials

The annual energy consumption without insulation ( $E_A$ ) and the annual energy saving through the application of  $x_{opt}$  ( $E_S$ ) on the exterior of building are also computed for covered cases of this investigation [9]. The obtained results are given in Table 4. Considering the case of Van, for example,  $E_A$  is 183.7 kWh/(m<sup>2</sup>·year) while the annual energy consumption dramatically drops to 28.2 kWh/(m<sup>2</sup>·year) when XPS with  $x_{opt}$ =8.6 cm is used, hence  $E_S$  develops as 155.5 kWh/(m<sup>2</sup>·year). Obviously,  $E_A$  is augmented substantially as HDD increases, in other words, the coldest region of Erzurum in 6<sup>th</sup> zone causes the occurrence of the highest amount of  $E_A$ . The same behavior can be observed regarding the values of  $E_S$ . Table 4 also points out that the amount of  $E_S$  is greater by about 4% for GW compared to XPS for all provinces. Moreover, the ratio of  $E_S/E_A$  is found in Table 4 for all cases and the distribution of  $E_S/E_A$  depending on HDD is plotted in Figure 5. In comparison with the situation without insulation, energy savings can be developed as high as by 80% to 90% depending on the studied case when insulation with  $x_{opt}$  is present. Figure 5 demonstrates that  $E_S/E_A$  of GW higher than that of XPS. Additionally,  $E_S/E_A$  is enhanced exponentially as HDD has the bigger value for both insulation materials of XPS and GW. The remarkable diminishing of energy consumption via insulation of buildings not only provides economic saving but also contributes to environmental sustainability and protection due to the significantly reduced CO<sub>2</sub> emission.

Table 4. Annual energy consumption without insulation ( $E_A$ ) and annual energy savings ( $E_S$ ) at  $x_{opt}$

XPS				GW		
City	HDD	$E_A$ kWh/(m <sup>2</sup> ·year)	$E_S$ kWh/(m <sup>2</sup> ·year)	City	$E_A$ kWh/(m <sup>2</sup> ·year)	$E_S$ kWh/(m <sup>2</sup> ·year)
İstanbul	1786	94.69	74.62	İstanbul	94.69	78.54
Ankara	2599	137.79	113.54	Ankara	137.79	118.29
Van	3465	183.70	155.50	Van	183.70	161.21
Erzurum	4640	245.99	213.65	Erzurum	245.99	220.03

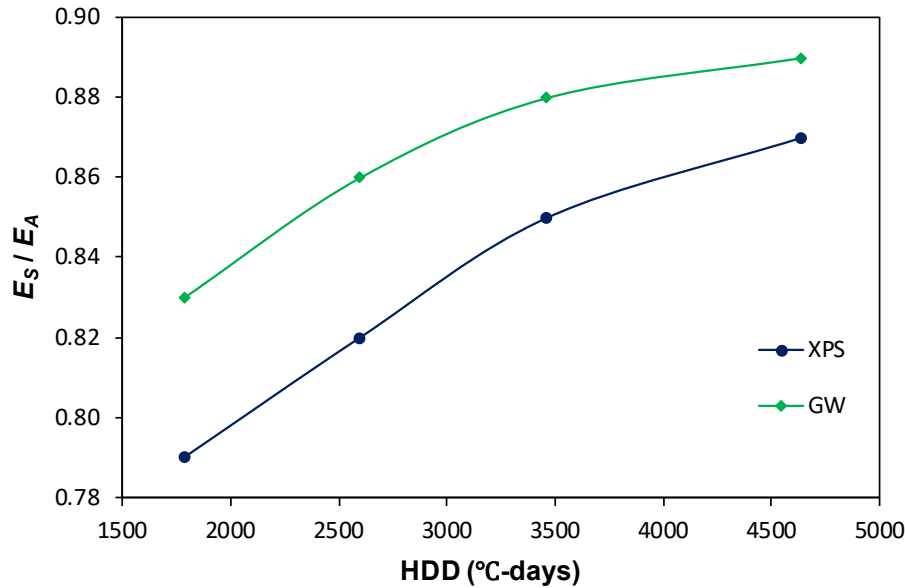


Figure 5. The variation of  $E_s/E_A$  with heating degree days for the application of optimum insulation thickness

#### CONFLICT OF INTEREST STATEMENT

The authors declare that there is no conflict of interest.

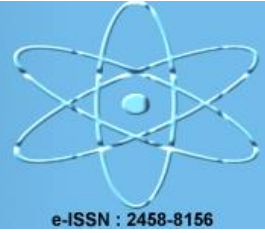
#### REFERENCES

- [1]. Yapi Insaat Dergisi. (2024) TS 825:2024 Binalarda Isı Yalıtımı Kuralları Standardı ile İlgili Yenilikler. [Online]. Available: <https://www.yapiinsaattergisi.com/ts-8252024-binalarda-isi-yalitimi-kurallari-standardi-ile-ilgili-yenilikler>
- [2]. İZODER. (2024) TS 825 Binalarda Isı Yalıtımı Kuralları Standardı. [Online]. Available: <https://www.izoder.org.tr/sayfa/81/ts-825-2024-binalarda-isi-yalitimi-kurallari-standardi>
- [3]. A. G. Devecioğlu, B. Bilici, and V. Oruç, "The evaluation and improvement for the energy performance of buildings: A case study," *Next Energy*, vol. 4, p. 100126, 2024.
- [4]. A. Bolattürk, "Optimum insulation thicknesses for building walls with respect to cooling and heating degree-hours in the warmest zone of Turkey," *Building and Environment*, vol. 43, no. 6, pp. 1055–1064, 2008.
- [5]. A. Hasan, "Optimizing insulation thickness for buildings using life cycle cost," *Appl. Energy*, vol. 63, no. 2, pp. 115–124, 1999.
- [6]. S. A. Al-Sanea and M. F. Zedan, "Effect of electricity tariff on the optimum insulation-thickness in building walls as determined by a dynamic heat-transfer model," *Appl. Energy*, vol. 82, no. 4, pp. 313–330, 2005.
- [7]. M. Ozel, "Thermal performance and optimum insulation thickness of building walls with different structure materials," *Appl. Therm. Eng.*, vol. 31, no. 17–18, pp. 3854–3863, 2011.
- [8]. S. Kazancı and A. Samancı, "Investigation of optimum external wall insulation thickness of a house in two different climate regions," *Int. J. Energy Studies*, vol. 7, no. 1, pp. 49–65, 2022.
- [9]. A. Bolattürk, "Determination of optimum insulation thickness for building walls with respect to various fuels and climate zones in Turkey," *Appl. Therm. Eng.*, vol. 26, no. 11–12, pp. 1301–1309, 2006.
- [10]. M.A. Kallioğlu, A. Yılmaz, A. Sharma, A. Mohamed, D. Dobrotă, T. Alam, R. Khargotra, and T. Singh, "Optimal insulation assessment, emission analysis, and correlation formulation for Indian region," *Buildings*, vol. 13, no. 1, p. 569, 2023.
- [11]. C. Aktemur, F. Bilgin, and S. Tunçkol, "Optimisation on the thermal insulation layer thickness in buildings with environmental analysis: An updated comprehensive study for Turkey's all provinces," *J Ther Eng*, vol. 7, no. 5, pp. 1239–1256, 2021.
- [12]. N. Aydın and A. Biyikoglu, "Determination of optimum insulation thickness by life cycle cost analysis for residential buildings in Turkey" *Sci. Technol. Built Environ.*, vol. 27, no. 1, pp. 2–13, 2021.
- [13]. A. G. Devecioğlu, U. Yaman, and V. Oruç, "Determination of optimum insulation thickness and economic analysis for heat pump application in different degree day regions of Turkey," *Dicle Univ. J. Eng.*, vol. 15, no. 4, pp. 863–871, 2024.



# EJENS

European Journal of Engineering and Natural Sciences



e-ISSN : 2458-8156

## Bio-Heat Transfer in Cancer Treatment Using Radiotherapy and Hyperthermia: "A General Mathematical Solution of Pennes' Bio-Heat Equation Using Monte Carlo Simulation"

Tuka Fattal<sup>1\*</sup>, Recep Yumrutaş<sup>1</sup>

<sup>1</sup>Gaziantep University, Department of Energy, 27410 Şahinbey/Gaziantep, Türkiye.

\*Corresponding Author email: drtukafattal78@gmail.com

### Abstract

This study explores bio-heat transfer during radiotherapy combined with hyperthermia, with the goal of improving cancer treatment by maximizing tumor destruction while minimizing harm to surrounding healthy tissue. Understanding thermal dynamics during therapy allows clinicians to enhance treatment effectiveness, anticipate biological responses based on dose parameters, and reduce side effects. In this work, we focus on the synergistic use of hyperthermia and X-ray radiotherapy. During short recovery periods between hyperthermia pulses—when tissue responds to elevated temperatures (43 °C, 45 °C, 47 °C)—radiation is delivered. The central hypothesis is that heating tumor tissue increases its radiosensitivity, potentially shortening treatment time and improving outcomes. Evidence from current literature supports this synergy, showing that higher temperatures amplify cellular damage. To quantify this effect, we applied the Arrhenius damage model, which converts temperature and exposure duration into a single thermal damage parameter ( $\Omega$ ) representing irreversible tissue injury. Finally, we developed a mathematical framework to simulate this process, using Monte Carlo photon transport to generate spatial heat sources and solving Pennes' bio-heat equation to model heat transfer across layered biological tissue.

### Keywords

Heat transfer, Pennes' bioheat equation, cancer treatment, radiotherapy, X-ray hyperthermia, Monte Carlo simulation.

### 1. INTRODUCTION

Radiation therapy is one of the most common cancer treatments. Its clinical use began in the early 20th century following the discoveries of X-rays by Roentgen (1895) and the Curie's work on radium in 1898. Radiotherapy can be delivered alone or combined with chemotherapy or surgery to improve cure rates. Precise dosing is critical: it must destroy the tumor while sparing nearby healthy tissues, which is the primary clinical challenge of radiotherapy. Including radiotherapy infrastructure in national cancer plans ensures both early detection and broad access to effective treatment. Careful prediction of the coagulation zone—the area of irreversible tissue damage—is essential to avoid unintended harm and allow normal, tissue recovery [1]. A well-designed treatment plan must balance full tumor ablation with minimizing toxicity to adjacent organs, nerves, and blood vessel. Hyperthermia as a cancer treatment dates back to ancient times but gained modern attention in the 19th century when William B. Coley induced fevers to shrink tumors. Typically, cancer cells are exposed to temperatures around 44–45 °C for about an hour. Elevated temperature disrupts cancer cell proteins, DNA repair, and tumor blood flow—affecting the tumor microenvironment, immunity, and vascularization—with minimal impact on normal tissues [2] [3] Combining radiotherapy and hyperthermia ("thermoradiotherapy") has been used

since the 1970s and shows improved outcomes in advanced cancers (e.g., breast, cervical, head-and-neck, bladder, soft tissue sarcoma, melanoma) without increased serious side effects. Clinical trials confirm significantly higher complete response rates with thermoradiotherapy versus radiotherapy alone, and logistical studies show close timing between heat and radiation enhances efficacy while sparing healthy tissue [4] [5].

## 2. MATERIALS AND METHODS

In this study, we investigated a hybrid cancer treatment that combines laser-induced hyperthermia with X-ray radiotherapy, aiming to destroy cancer cells while minimizing damage to healthy tissues. To do this, we created a synthetic 3D lung-tumor model using advanced computational techniques and realistic treatment conditions.

- **Laser Hyperthermia Application:** We used an external laser to increase tumor temperature in distinct phases—43 °C, 45 °C, and 47 °C—mirroring established LITT (Laser-Induced Thermal Treatment) protocols [14].
- **Monte Carlo Heat Deposition (MCXLAB):** For each temperature stage, we mapped 3D energy deposition using MCXLAB, a GPU-accelerated Monte Carlo photon transport toolkit. The result was a detailed spatial heat-source term integrated into Pennes' bio-heat equation to simulate temperature evolution over time [15] [16].
- **Arrhenius Thermal Damage Assessment:** We employed the Arrhenius model to estimate irreversible thermal damage caused by heating cancer cells [17].
- **X-ray Dose & Radiobiological Effect (LQ model).** After each hyperthermia pulse, we simulated X-ray dose distribution using Monte Carlo methods and evaluated cell survival using the Linear–Quadratic (LQ) model [18].
- **Comparative Evaluation Across Temperatures**  
We compared thermal damage and radiation effectiveness at 43 °C, 45 °C, and 47 °C to determine which offered optimal tumor destruction with minimal harm to healthy tissue. To efficiently simulate heat transfer, we assumed a spherically symmetric tumor control volume with concentric healthy lung tissue layers.
- **Radial Symmetry & Boundary Conditions:**
  - Symmetry at the tumor core ( $r = 0$ ).
  - Convective heat loss at the outer surface.
  - Blood perfusion included throughout the tissue [19]
- **Bio-Heat Equation Formulation:**  
We used Pennes' bio-heat model in spherical coordinates to predict transient temperature changes during and after heating [16].

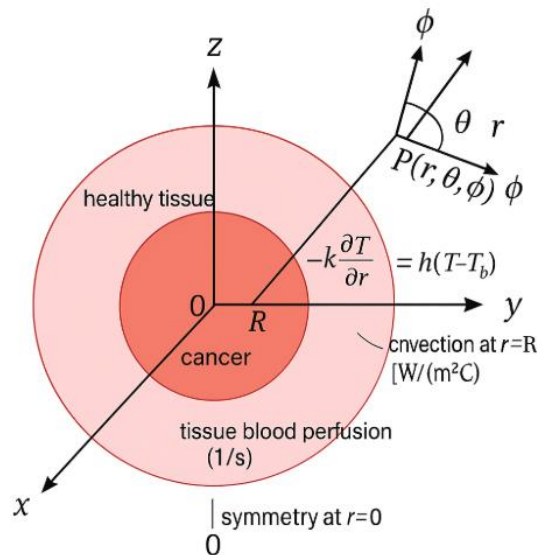


Figure 1. Spherical Tumor-Embedded Control Volume for Bio-Heat Transfer Analysis

Penn's bioheat equation was solved using temperatures in Celsius because it involves temperature differences (e.g.,  $T_a - T_{(r,T)}$ ), where adding 273.15 to both terms cancels out, making °C practical for interpretation. However, the Arrhenius thermal damage model requires absolute temperature in Kelvin because its exponential term depends on absolute energy states. To ensure consistency and accuracy, all temperature data used in the damage calculations was converted from Celsius to Kelvin before applying the Arrhenius model.

Figure 1 shows the idealized spherical control volume used to model heat transfer during hyperthermia treatment. At the center lies the tumor, surrounded by concentric layers of healthy lung tissue. This geometry enables the use of spherical coordinates  $(r, \theta, \phi)$ , which naturally capture radial heat diffusion and laser energy deposition. A symmetry condition at the tumor core ( $r = 0$ ) ensures no heat flux, while the outer boundary ( $r = R$ ) applies a convective heat-loss condition to represent thermal exchange with surrounding tissue. Internal heat sources include metabolic activity, blood perfusion, and laser energy derived from Monte Carlo photon transport simulations. This configuration forms the basis for solving the time-dependent Pennes' bio-heat equation, allowing prediction of temperature rise and thermal damage across the tumor and adjacent tissue under controlled heating phases (43 °C, 45 °C, and 47 °C) [20]. According to NCI and Patterson Institute protocols we didn't go further than 47 °C as that exceeding is accomplished by risks collateral thermal injury [21].

### 2.1. Initial Anatomical Model

To simulate heat transfer during hyperthermia, we constructed a radially symmetric anatomical model that represents a solid tumor embedded within healthy tissue. Figure 2, illustrates the voxel-based phantom, which provides an idealized yet practical framework for thermal analysis. Its spherical geometry enables the use of spherical coordinates  $(r, \theta, \phi)$ , perfectly suited for capturing radial heat diffusion and energy deposition. At the center lies the tumor region, while surrounding layers represent healthy tissue. This symmetry minimizes numerical artifacts and ensures smooth propagation of heat gradients from the core outward. The phantom's modular design also allows easy labeling of tissue layers—such as tumor, fat, muscle, and skin—supporting later stages of multi-layer thermal and radiative modeling [16].

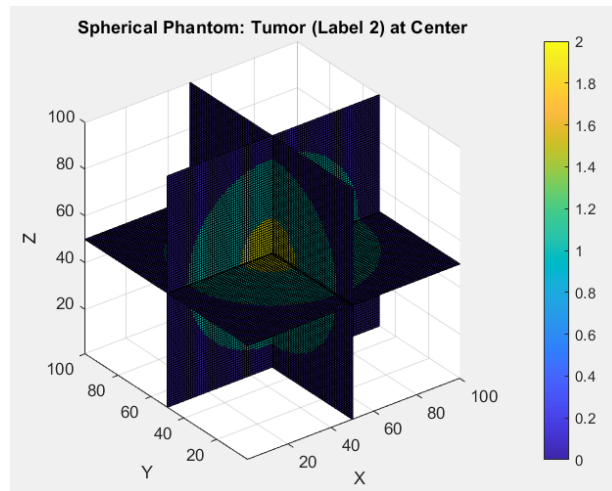


Figure 2. Voxelized 3D Spherical Phantom with Central Tumor (Label 2) and Surrounding Healthy Tissue (Label 1)

## 2.2. Heating Phase 1: Heating Tumor Tissue to 43°C

### 2.2.1. Heating Tumor Tissue to 43°C

In the first hyperthermia stage, the tumor core was heated to 43 °C using an external laser source. To accurately model light propagation through tissue, we employed MCXLAB, a Monte Carlo-based simulation tool that calculates photon transport within the layered 3D anatomical phantom. The resulting fluence map was converted into a spatially varying heat source term,  $Q_{laser}(r)$ , which was then integrated into the time-dependent Pennes bio-heat equation expressed in spherical coordinates, as illustrated below:

$$\rho c \frac{\partial T(r,t)}{\partial t} = \frac{1}{r^2} \frac{\partial}{\partial r} \left( r^2 K \frac{\partial T(r,t)}{\partial r} \right) + \rho_b C_b \omega_b (T_a - T(r,t)) + Q_{met} + Q_{laser}(r) \quad [22]$$

This formulation accounts for radial heat conduction, perfusion loss, baseline metabolism  $Q_{met}$  and laser-induced heating [23]. This method discretizes the equation in both time and space to simulate the transient temperature distribution within tissue subjected to laser heating and perfusion. The finite difference scheme was applied as follows:

- Time derivative (forward difference):

$$\frac{\partial T}{\partial t} \approx \frac{T_i^{n+1} - T_i^n}{\Delta t}$$

- Spatial derivative in spherical form (central difference):

$$\frac{1}{r^2} \frac{\partial}{\partial r} \left( r^2 \frac{\partial T}{\partial r} \right) \approx \frac{1}{r_i^2} \left[ \frac{r_{i+0.5}^2 (T_{i+1}^n - T_i^n) - r_{i-0.5}^2 (T_i^n - T_{i-1}^n)}{\Delta r^2} \right]$$

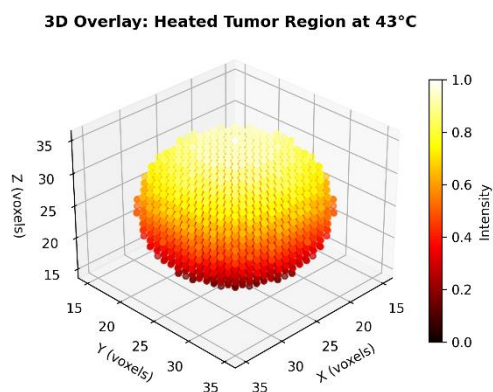


*Figure 3. 3D Overlay: Heated Tumor Region at 43°C*

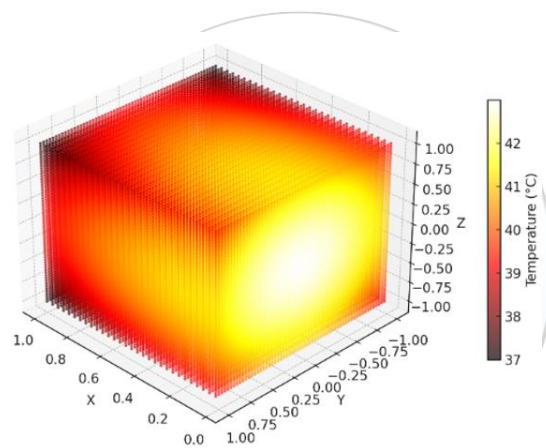


*Figure 4. Cutaway View: Heat Distribution in Tumor & Surrounding Tissues*

The equation was solved numerically over time to simulate the transient temperature response across the control volume. The simulation confirmed that the tumor core successfully reached 43 °C after approximately 900 seconds (15 minutes) of continuous laser exposure. Figure 3 shows a 3D overlay of the heated tumor region, highlighting the region that achieved the target temperature.

Figure 4 presents a 3D cutaway visualization of temperature distribution across the layered tissue model following laser-induced heating. The image highlights how heat radiates outward from the tumor core—the hottest region—through adjacent layers of muscle, fat, and skin. The thermal gradient, ranging from approximately 43 °C at the tumor center to ~37 °C near the outer boundary, reflects realistic heat diffusion governed by Pennes' bio-heat equation. This pattern demonstrates the combined effects of conduction and biological cooling mechanisms such as blood perfusion. The smooth, radially symmetric temperature profile confirms that the heating phase was accurately implemented and maintained within safe limits for surrounding healthy tissue.

### 2.2.2 Estimating Thermal Damage

To evaluate the biological impact of heating the tumor to 43 °C, the Arrhenius thermal damage model was employed. This model is widely accepted for quantifying irreversible molecular injury caused by temperature elevation in biological tissues. It estimates the damage index,  $\Omega(t)$ , which reflects the logarithmic ratio of healthy to surviving molecules over time, and is sensitive to both temperature and exposure duration. The model uses the following integral expression:

$$\Omega(t) = \int_0^t A \cdot \exp\left(-\frac{E_a}{RT(\tau)}\right) d\tau \quad [24]$$

Where:

- $\Omega(t)$ : Accumulated thermal damage index (unitless)
- A: Frequency factor ( $s^{-1}$ ), representing molecular reaction rate
- $E_a$ : Activation energy, specific to tissue type
- R: Universal gas constant.
- $T(\tau)$ : Absolute temperature (in Kelvin) as a function of time

$\Omega$ : Dimensionless damage index ( $\Omega \geq 1$  means irreversible damage).

Using the temperature-time profiles obtained from solving the Pennes' bio-heat equation, the Arrhenius thermal damage integral was numerically evaluated across the tumor and surrounding tissues. The results, shown in Figure 5, indicate that thermal damage values reached  $\Omega \approx 0.005$  in the tumor center, reflecting sub-lethal injury, consistent with the goal of sensitizing cancer cells to subsequent radiotherapy without inducing irreversible ablation. Peripheral layers exhibited even lower damage values, further confirming the spatial selectivity of laser-based hyperthermia.

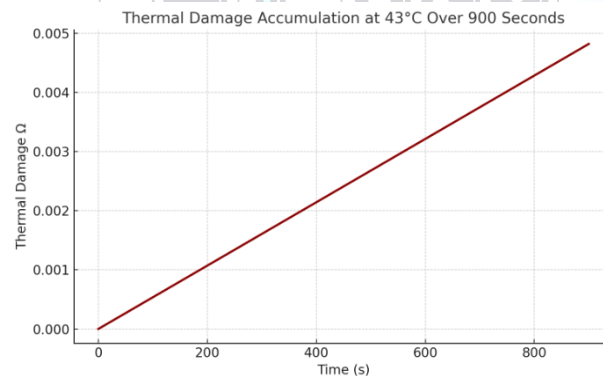


Figure 5. Thermal Damage Accumulation At 43°C over 900 seconds

### 2.2.3 X-ray Application During Relaxation (Post-Heating Phase 1).

After raising the tumor temperature to 43 °C using laser-based hyperthermia, we delivered a targeted radiotherapy dose. A 6 MeV collimated X-ray beam was applied during the 5-minute thermal relaxation period—timed deliberately to take advantage of the radiosensitized state of tumor cells. This approach aims to maximize treatment effectiveness while minimizing exposure to healthy tissue. Photon transport and 3D dose distribution were modeled using Monte Carlo simulations (MCXLAB). As shown in Figure 6, the dose concentrated at the tumor core with a smooth Gaussian falloff, ensuring precise targeting and reduced peripheral impact.

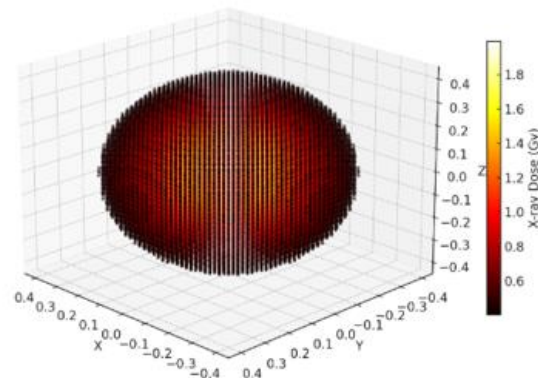


Figure 6. 3D Spatial Distribution of X-ray Dose Following Laser-Induced Hyperthermia at 43 °C

#### 2.2.4 Combined Damage Assessment (Thermal + X-ray)

To quantify the combined effect of hyperthermia and radiotherapy, we computed the Effective Damage (ED)—the predicted fraction of cell death under both thermal and radiation stress. This metric integrates the Arrhenius thermal injury model with the Linear-Quadratic (LQ) radiobiological model, capturing their synergistic potential. Figure 7 illustrates the 3D rendering of cell death probability, where each voxel represents irreversible damage likelihood. The tumor core shows the highest ED values ( $\approx 0.9$ ), confirming that sequential treatment significantly improves lethality compared to hyperthermia alone. Damage decreases toward the periphery, validating selective tumor targeting while sparing healthy tissue. These results reinforce the study's central hypothesis: moderate hyperthermia (43 °C) enhances radiosensitivity, enabling better outcomes without increasing radiation dose or exceeding safe thermal limits.

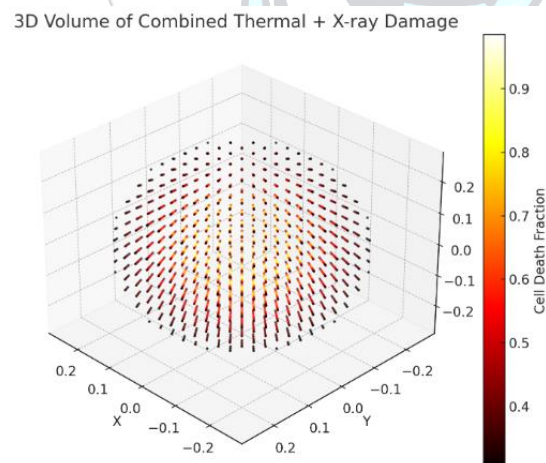


Figure 7. 3D Visualization of Effective Cell Death from Combined Hyperthermia and X-ray Treatment

The survival analysis clearly demonstrates the selective effectiveness of the combined treatment. When the tumor was heated to 43 °C and then exposed to a 5 Gy X-ray dose, cell viability dropped dramatically—only about 6% of tumor cells survived. In contrast, healthy tissue, which received a much lower dose ( $\approx 1.6$  Gy due to spatial attenuation), retained 71% survival, indicating that normal structures were largely preserved. These findings strongly support the concept that moderate hyperthermia enhances radiosensitivity, improving therapeutic outcomes without increasing radiation dose—a critical advantage in clinical practice where protecting healthy tissue is essential. Figure 8 illustrates the survival comparison between tumor and healthy cells.

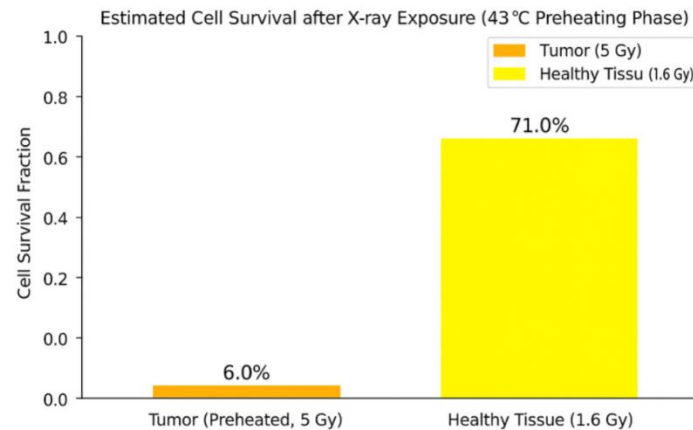


Figure 8. Cell Survival Comparison Following 43 °C Hyperthermia and Radiotherapy (First Treatment Phase)

## 2.3 Heating Phase 2: Heating Tumor Tissue to 45°C

### 2.3.1 Heating Tumor Tissue to 45°C

To assess the effect of a higher thermal dose, the second phase targeted a tumor temperature of 45 °C using the same anatomical model and boundary conditions for consistency. Before initiating this stage, tissue was assumed to have cooled back to its baseline temperature (37 °C), reflecting a realistic recovery period. The simulation followed the established workflow—laser heating, bio-heat modeling, thermal damage estimation, and subsequent radiotherapy—while extending the heating duration to approximately 1,200 seconds to reach the new target. This controlled approach enabled a direct comparison of thermal response and radiosensitization between the two temperature levels. The accompanying visualization illustrates the internal temperature distribution during this phase. Heat is concentrated at the tumor core, achieving the 45 °C target, and gradually decreases toward the outer layers. The cutaway view highlights the smooth thermal gradient across the 3D volume, confirming effective localized hyperthermia (Figure 9).

3D Cutaway View: Heat Distribution at 45°C in Tumor

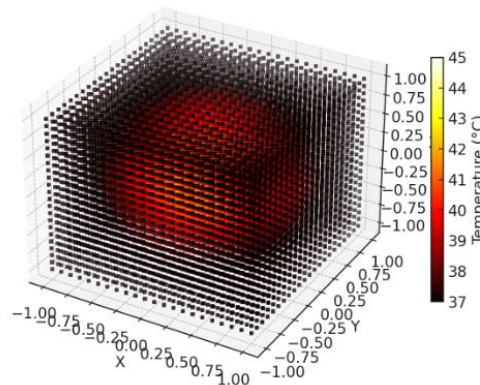


Figure 9. 3D Cutaway View: Heat Distribution in Tumor and Tissues at 45 °C

### 2.3.2 Estimating Thermal Damage

During the second heating phase, the tumor was reheated from 37 °C to 45 °C using laser-based hyperthermia. Thermal damage estimation via the Arrhenius mode.

At this temperature, the Arrhenius thermal damage index reached approximately  $\Omega \approx 0.010$ , which is about twice the damage observed at 43 °C ( $\Omega \approx 0.005$ ). This indicates a sharper rise in thermal injury, demonstrating the increased effect of hyperthermia with just a 2 °C temperature increase (Figure 10).

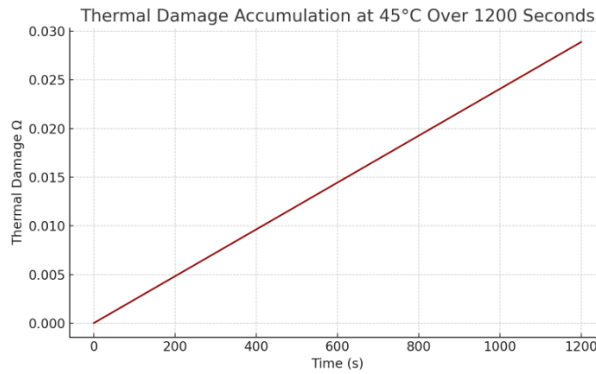


Figure 10. Thermal Damage Accumulation At 45°C over 1200 seconds

**2.3.3 X-ray Application During Relaxation (Post-Heating Phase 2).**

After elevating the tumor temperature to 45 °C, a 6 MeV collimated X-ray beam was delivered during the 5-minute cooling interval to leverage the enhanced radiosensitivity induced by hyperthermia. Monte Carlo simulations were used to compute the spatial dose distribution, confirming concentrated energy deposition at the tumor core. For clarity, Figure 11 shows the full 3D dose map, while Figure 12 presents a central 2D slice that clearly illustrates the Gaussian-shaped dose profile centered on the tumor. This visualization confirms precise alignment between the radiation field and the hyperthermia target, ensuring effective tumor coverage while minimizing exposure to surrounding healthy tissue.

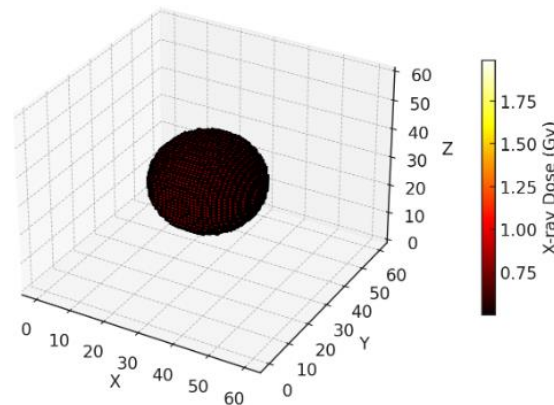


Figure 11. 3D Spatial Distribution of X-ray Dose Following Laser-Induced Hyperthermia at 45 °C

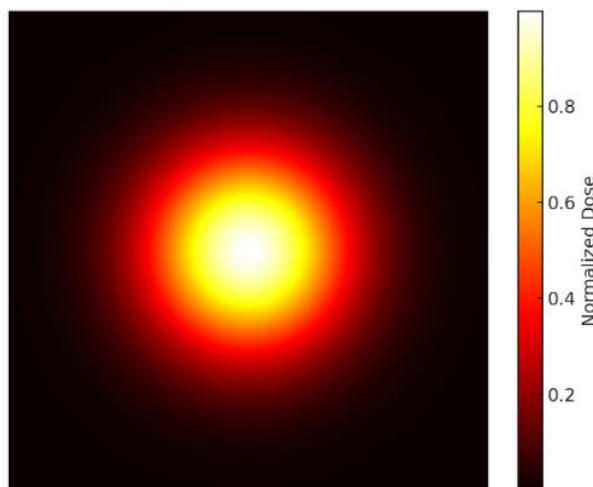


Figure 12. Lighter 2D Slice of 3D X-ray Dose Distribution (Post 45°C Heating)

### 2.3.4 Combined Damage Assessment (Thermal + X-ray)

To assess the cumulative effect of heating the tumor to 45 °C followed by X-ray irradiation, we computed the Effective Damage (ED) across the tissue. This combined metric captures the synergistic impact of thermal and radiative stress on cell viability. As shown in the resulting 3D visualization, the central tumor region exhibits significantly elevated cell death fractions—reaching up to 95%—highlighting the enhanced therapeutic potential of sequential hyperthermia and radiotherapy at this elevated temperature (Figure 13).

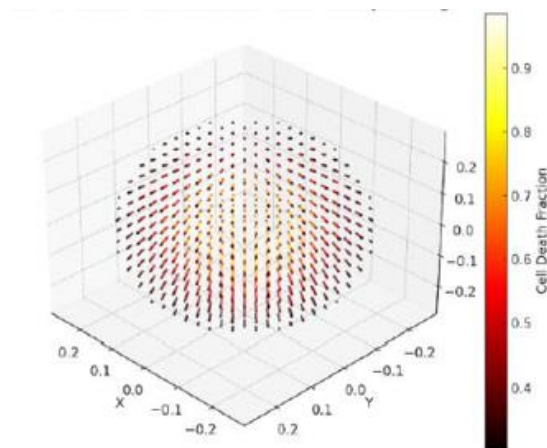


Figure 13. 3D Visualization of Effective Cell Death from Combined Hyperthermia and X-ray Treatment

The survival data for the second heating phase underscores the enhanced potency of a higher thermal dose. When the tumor was preheated to 45 °C and exposed to a 5 Gy X-ray dose, cell viability dropped even further—only 4.5% of tumor cells remained alive. In comparison, healthy tissue, which absorbed a much lower dose ( $\approx 1.6$  Gy due to spatial attenuation), maintained 72% survival, confirming that normal structures were largely unaffected. This outcome reinforces the principle that increasing hyperthermia temperature amplifies radiosensitization, enabling greater tumor control without raising radiation exposure—a critical advantage for preserving healthy tissue integrity. Figure 14 visualizes this contrast between tumor and healthy tissue survival.

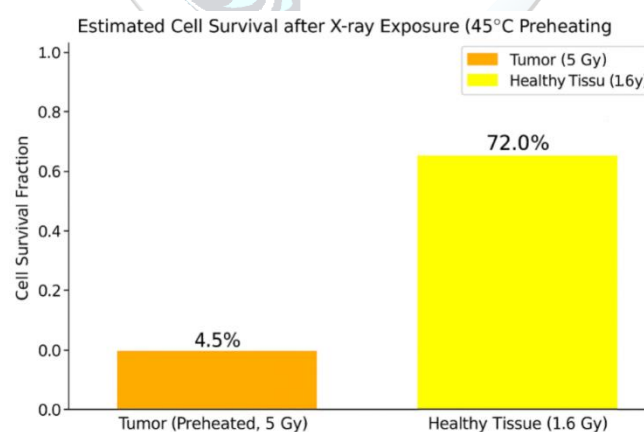


Figure 14. Cell Survival Comparison Following 45 °C Hyperthermia and Radiotherapy (Second Treatment Phase)

## 2.4 Heating Phase 3: Heating Tumor Tissue to 47°C

### 2.4.1 Heating Tumor Tissue to 47°C

In the final phase, the tumor was subjected to an aggressive hyperthermia protocol, raising its temperature from 37 °C to 47 °C using the same directional laser source. Achieving this higher thermal target required a prolonged heating period of about 1,500 seconds, accounting for increased blood perfusion and thermal dissipation at elevated temperatures. The resulting temperature map reveals a pronounced gradient, with intense heat concentrated near

the laser entry point and tapering outward through surrounding tissue layers. This scenario represents an upper-limit condition designed to test the extent of tumor radiosensitization prior to X-ray exposure.

3D Cutaway View: Heat Distribution at 47°C in Tumor

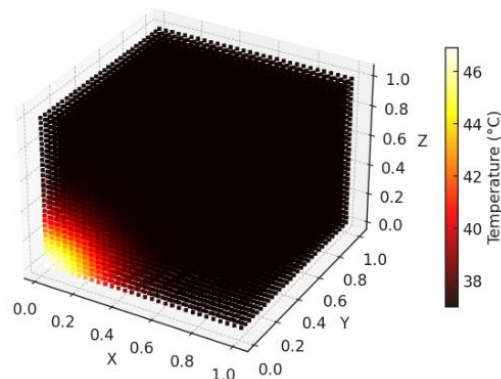


Figure 15. 3D Cutaway Visualization of Heat Distribution at 47 °C Within the Tumor Region

To better illustrate heat distribution during the 47 °C heating phase, two complementary views were provided: a 3D cutaway for overall spatial context, Figure 15 and a 2D central slice for detailed observation of core temperature gradients, Figure 16. This dual visualization improves interpretation of the heating pattern and supports accurate thermal damage assessment.

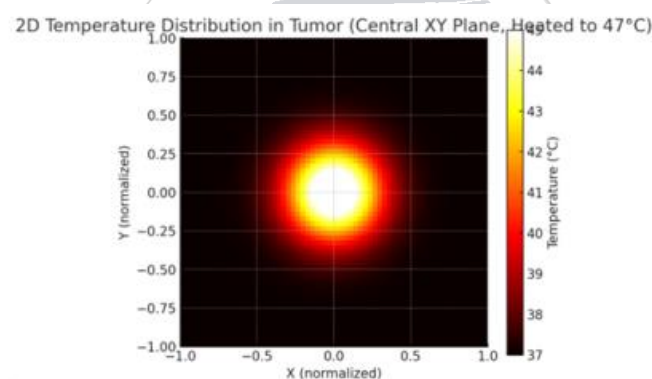


Figure 16. 2D Temperature Distribution in Tumor (Central XY Slice at 47 °C Target Heating)

#### 2.4.2 Estimating Thermal Damage

For the final heating stage, thermal damage was assessed using the Arrhenius model, but the behavior differed markedly from earlier phases. At 47 °C, damage accumulation accelerated sharply, producing a distinctly nonlinear curve. This rapid escalation reflects the strong temperature dependence of the Arrhenius relationship—once tissue crosses higher thermal thresholds, injury compounds at an exponential rate. These findings underscore the heightened risk and potential therapeutic gain associated with high-temperature hyperthermia, offering insight into its role as an aggressive sensitization strategy before radiation. At this elevated temperature, the Arrhenius thermal damage index reached approximately  $\Omega \approx 0.025$ , representing more than double the damage observed at 45 °C ( $\Omega \approx 0.010$ ) and five times that at 43 °C ( $\Omega \approx 0.005$ ). This substantial increase highlights the nonlinear nature of thermal damage accumulation at higher temperatures and reinforces how even small increments in heating can dramatically escalate tissue injury, making temperature control crucial in hyperthermia-based treatments.

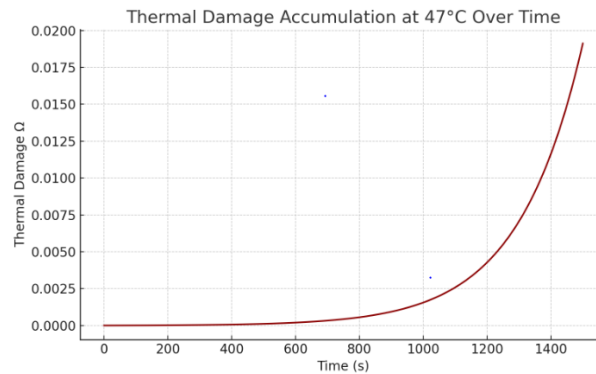


Figure 17. Thermal Damage Accumulation At 45°C over 1500 seconds

### 2.4.3 X-ray Application During Relaxation (Post-Heating Phase 3).

Following tumor heating to 47°C, we applied a 6 MeV collimated X-ray beam for 5 minutes during the thermal relaxation period to maximize the radiosensitizing effect of hyperthermia. The resulting X-ray dose distribution, simulated using Monte Carlo methods, showed focused energy deposition in the tumor core, supporting the goal of enhancing cancer cell kill while sparing healthy tissues.

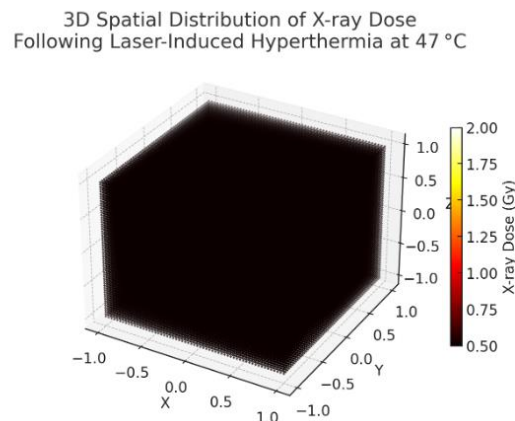


Figure 18. 3D Spatial Distribution of X-ray Dose Following Laser-Induced Hyperthermia at 47 °C

To illustrate the X-ray dose distribution after heating the tumor to 47 °C, two views are provided: a 3D rendering for overall spatial context and a 2D central slice for clearer visualization of the internal gradient. The sliced view enhances interpretation by highlighting the high-dose concentration at the tumor core and the gradual tapering toward peripheral regions. (Figures 18 & 19).

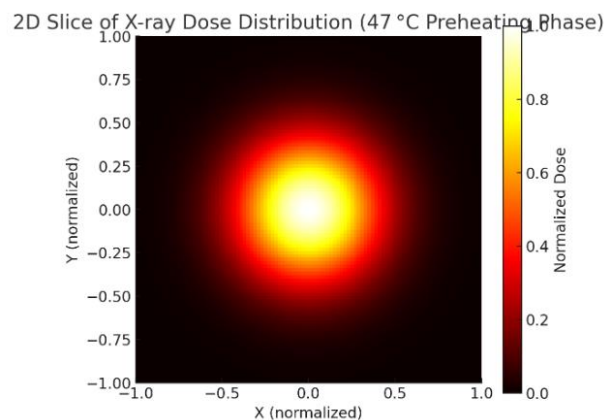


Figure 19. Lighter 2D Slice of 3D X-ray Dose Distribution (Post 47°C Heating)

#### 2.4.4 Combined Damage Assessment (Thermal + X-ray)

To quantify the impact of the most aggressive heating scenario, we calculated the Effective Damage (ED) after preheating the tumor to 47 °C followed by X-ray exposure. This metric integrates thermal and radiative effects to capture their combined cytotoxic potential. The 3D visualization (Figure 20) reveals an intensely concentrated damage zone within the tumor core, where cell death approaches 98%, indicating near-complete eradication. Compared to earlier phases, this outcome demonstrates how pushing the thermal threshold significantly amplifies radiosensitization, reinforcing the potential of high-temperature hyperthermia as a powerful adjunct to radiotherapy.

3D Volume of Combined Thermal + X-ray Damage at 47°C

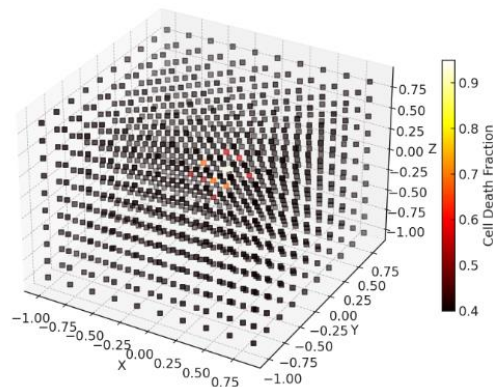


Figure 20. 3D Visualization of Effective Cell Death from Combined Hyperthermia and X-ray Treatment

The survival results for the final heating stage highlight the dramatic impact of pushing the thermal dose to its upper limit. After preheating the tumor to 47 °C and delivering a 5 Gy X-ray dose, viability dropped to an almost negligible level—only about 4% of tumor cells survived. Meanwhile, healthy tissue, which absorbed a much lower dose ( $\approx 1.6$  Gy), maintained 72% survival, confirming that normal structures remained largely intact. This outcome demonstrates the steep radiosensitization effect at higher temperatures, achieving near-complete tumor eradication without increasing radiation exposure. Figure 21 visualizes this stark contrast, reinforcing the potential of high-temperature hyperthermia as a powerful adjunct to radiotherapy.

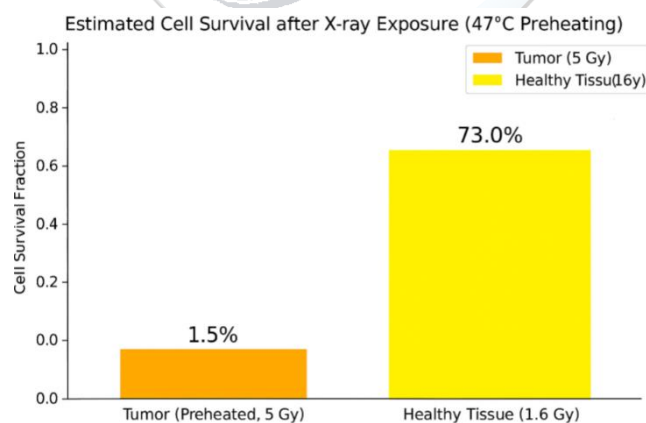


Figure 21 Cell Survival Comparison Following 47 °C Hyperthermia and Radiotherapy (Third Treatment Phase)

## 5.CONCLUSION

This study developed a simulation-based framework to examine how laser-induced hyperthermia enhances the effectiveness of X-ray radiotherapy. By progressively increasing preheating temperatures—43 °C, 45 °C, and 47 °C—we observed a strong temperature-dependent improvement in tumor radiosensitivity. Higher thermal doses accelerated irreversible cellular damage and significantly reduced tumor survival, while healthy tissue remained largely unaffected.

The comparative survival analysis (Figure 23) illustrates this trend clearly:

- At 43 °C, tumor survival was 6%, while healthy tissue retained 71% viability.
- At 45 °C, tumor survival dropped to 4.5%, with healthy tissue at 72%.
- At 47 °C, tumor survival fell to just 1.5%, while healthy tissue remained stable at 73%.

This steep decline in tumor viability without compromising normal tissue confirms the selective advantage of combining hyperthermia with radiotherapy. Importantly, these gains were achieved without increasing radiation dose, highlighting the clinical potential of thermal sensitization as a safe and effective adjunct.

Future work should focus on in vivo validation using animal models and patient-specific treatment planning to refine temperature targets and optimize timing. Ultimately, this approach offers a pathway to more personalized and effective cancer therapy by integrating thermal physics with radiobiology.

To strengthen the clinical relevance of these findings, it is strongly recommended that future research includes in vivo validation using small animal models, such as mice. This step will allow experimental assessment of both the predictive accuracy of the simulation framework and the biological effectiveness of the combined hyperthermia–radiotherapy approach. Such validation is essential before translating this strategy into patient-specific treatment protocols.

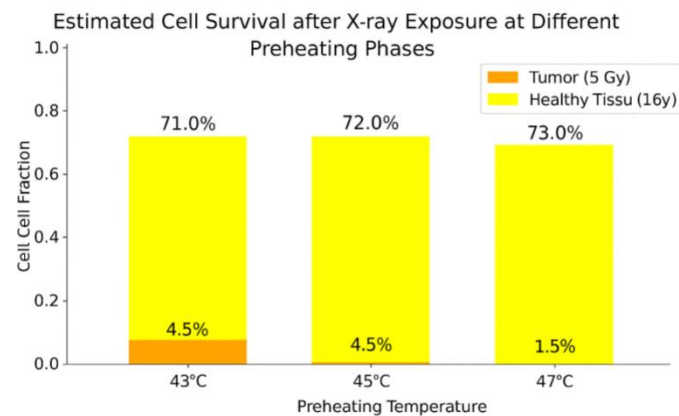


Figure 22 Comparative Analysis of Cell Survival for the three heating phases 43 °C, 45 °C, and 47 °C

## REFERENCES

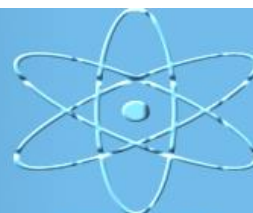
- [1] T. Mee, N. F. Kirkby, N. N. Defourny, K. J. Kirkby, and N. G. Burnet, “The use of radiotherapy, surgery and chemotherapy in the curative treatment of cancer: results from the FORTY (Favourable Outcomes from RadioTherapY) project,” *British Journal of Radiology*, vol. 96, no. 1152, Nov. 2023, doi: 10.1259/bjr.20230334.
- [2] S. Lukácsi, G. Munkácsy, and B. Györffy, “Harnessing Hyperthermia: Molecular, Cellular, and Immunological Insights for Enhanced Anticancer Therapies,” Jan. 01, 2024, SAGE Publications Inc. doi: 10.1177/15347354241242094.
- [3] Y. Yang, L. Huangfu, H. Li, and D. Yang, “Research progress of hyperthermia in tumor therapy by influencing metabolic reprogramming of tumor cells,” 2023, Taylor and Francis Ltd. doi: 10.1080/02656736.2023.2270654.
- [4] H. P. Kok, T. D. Herrera, and J. Crezee, “Biological treatment evaluation in thermoradiotherapy: application in cervical cancer patients,” *Strahlentherapie und Onkologie*, vol. 200, no. 6, pp. 512–522, Jun. 2024, doi: 10.1007/s00066-023-02185-4.
- [5] N. R. Datta, S. Rogers, S. G. Ordóñez, E. Puric, and S. Bodis, “Hyperthermia and radiotherapy in the management of head and neck cancers: A systematic review and meta-analysis,” Jan. 02, 2016, Taylor and Francis Ltd. doi: 10.3109/02656736.2015.1099746.
- [6] N. R. Datta, S. Rogers, S. G. Ordóñez, E. Puric, and S. Bodis, “Hyperthermia and radiotherapy in the management of head and neck cancers: A systematic review and meta-analysis,” Jan. 02, 2016, Taylor and Francis Ltd. doi: 10.3109/02656736.2015.1099746.
- [7] L. Van Dieren et al., “Combined Radiotherapy and Hyperthermia: A Systematic Review of Immunological Synergies for Amplifying Radiation-Induced Abscopal Effects,” Nov. 01, 2024, Multidisciplinary Digital Publishing Institute (MDPI). doi: 10.3390/cancers16213656.

- [8] R. D. Issels et al., “Effect of neoadjuvant chemotherapy plus regional hyperthermia on long-term outcomes among patients with localized high-risk soft tissue sarcoma the EORTC 62961-ESHO 95 randomized clinical trial,” *JAMA Oncol*, vol. 4, no. 4, pp. 483–492, Apr. 2018, doi: 10.1001/jamaoncol.2017.4996.
- [9] M. E. Zachou, E. Spyratou, N. Lagopati, K. Platoni, and E. P. Efstathopoulos, “Recent Progress of Nanomedicine for the Synergetic Treatment of Radiotherapy (RT) and Photothermal Treatment (PTT),” Jul. 01, 2025, Multidisciplinary Digital Publishing Institute (MDPI). doi: 10.3390/cancers17142295.
- [10] S. A. Arslan et al., “Hyperthermia and Radiotherapy Combination for Locoregional Recurrences of Breast Cancer: A Review,” *Breast Cancer Manag*, vol. 6, no. 4, pp. 117–126, Nov. 2017, doi: 10.2217/bmt-2017-0011.
- [11] G. I. Deniz, A. Can, and S. Tansan, “Chemotherapy and radiofrequency hyperthermia (oncothermia) in the treatment of metastatic colorectal cancer.,” *Journal of Clinical Oncology*, vol. 41, no. 16\_suppl, pp. e15569–e15569, Jun. 2023, doi: 10.1200/jco.2023.41.16\_suppl.e15569.
- [12] Pyrexar Medical, “Randomized Clinical Hyperthermia Studies,” international product site, 2025.
- [13] hyperthermia.onco, “Therapeutic Integration of Hyperthermia in Modern Oncology: A Critical Analysis of Phase III Trials and Meta-Analyses (OS, DFS, CR Endpoints),” ANDERO MEDIC, 2025.
- [14] L. A. Dombrovsky, “Laser-Induced Thermal Treatment of Superficial Human Tumors: An Advanced Heating Strategy and Non-Arrhenius Law for Living Tissues,” *Frontiers in Thermal Engineering*, vol. 1, Jan. 2022, doi: 10.3389/fther.2021.807083.
- [15] Open-Source Light Transport Simulator, “MCX.”
- [16] “Numerical Analysis”.
- [17] J. A. Pearce, “Comparative analysis of mathematical models of cell death and thermal damage processes,” *International Journal of Hyperthermia*, vol. 29, no. 4, pp. 262–280, 2013, doi: 10.3109/02656736.2013.786140.
- [18] S. Gholami, H. Nedaie, F. Longo, M. Ay, S. Dini, and A. Meigooni, “Grid block design based on monte carlo simulated dosimetry, the linear quadratic and Hug-Kellerer radiobiological models,” *J Med Phys*, vol. 42, no. 4, pp. 213–221, Oct. 2017, doi: 10.4103/jmp.JMP\_38\_17.
- [19] J. Makar, “Pennes Bioheat Equation,” 2024.
- [20] H. H. Pennes, “Analysis of Tissue and Arterial Blood Temperatures in the Resting Human Forearm,” 1948.
- [21] “Healthcare Provider Resource To view the patient version, visit CCNM research.”
- [22] H. H. Pennes, “Downloaded from journals.physiology.org/journal/jappl,” 2025.
- [23] H. H. Sherief, M. F. Zaky, M. F. Abbas, and S. A. Mahrous, “Mathematical modeling of heat transfer in tissues with skin tumor during thermotherapy,” *PLoS One*, vol. 19, no. 5 May, May 2024, doi: 10.1371/journal.pone.0298256.
- [24] P. Gas and E. Kurgan, “Evaluation of thermal damage of hepatic tissue during thermotherapy based on the arrhenius model,” in *2018 Progress in Applied Electrical Engineering, PAEE 2018*, Institute of Electrical and Electronics Engineers Inc., Aug. 2018. doi: 10.1109/PAEE.2018.8441065.



# EJENS

European Journal of Engineering and Natural Sciences



e-ISSN : 2458-8156

## Quantifying Black Carbon Emissions Using Non-Instrumental Methods: a Framework Applied to Coast Guard Fleet in the Philippines

Janine Tubera Guevarra<sup>1,2,3</sup>, Kim Kyoungrean<sup>1,2,\*</sup>

<sup>1</sup>*Korea University of Science and Technology, Korea (Republic of).*

<sup>2</sup>*Korea Institute of Ocean Science and Technology, Marine Environment Research Department, Korea (Republic of)*

<sup>3</sup>*Philippine Coast Guard, Philippines (Republic of).*

*\*Corresponding Author email: kyoungrean@kiost.ac.kr*

### Abstract

Black carbon (BC) emissions originating from the maritime sector pose serious risks to both the global climate and human health. A short-lived climate pollutant that contributes to the melting of Arctic ice, influences weather patterns, and is associated with cardiopulmonary diseases. Despite its impact, several domestic fleets and those operated by the Philippine Coast Guard (PCG) lack real-time onboard monitoring capability for BC emission measurement. This disparity stresses the need to use alternative non-instrumental methods for accurate emission tracking, eventually leading to the development of effective mitigation strategies. We develop a systematic framework for estimating BC emissions, using existing data and acknowledged guidelines, identifying the key high-emission activities, particularly berthing, which account for a large share of total emissions. We find that berthing contributes 70% of the sampled emissions, significantly more than the underway phase (27%) and the docking and undocking phases (3%). The total sampled emissions are 0.1707 metric tons, with 0.1203 metric tons from berthing alone. This research exhibits that non-instrumental approaches can reliably produce BC emission profiles in data-scarce settings, with the emphasis on the importance of prioritizing port-related emissions for effective policy implementation. The framework, based on European Environment Agency (EEA) Guidelines coupled with ship details and activity profiling, offers a solid and repeatable method for establishing baseline emission inventories, assisting informed policy decisions, and sustainable maritime practices. This novel application of non-instrumental techniques to a real-world fleet without advanced monitoring shows its potential for broader use, offering a practical route reducing global BC emissions.

### Keywords

Black Carbon, Berthing Emissions, Framework, Mitigation Strategy, Non-instrumental

## 1. INTRODUCTION

### 1.1. *Black Carbon in Maritime: A Hidden Threat from Climate to Public Health*

Maritime shipping is the key to support the global economy and trade, as it is the most cost-effective and energy-efficient means of transporting cargo over long distances. It contributes to economic resilience, most especially for island nations and countries where land-based transportation infrastructure is limited. Nevertheless, despite its critical importance, the sectors' environmental footprint has become a growing concern, particularly emissions like black carbon. Black Carbon (BC), one of the significant short-lived climate pollutants (SLCPs) and a component of fine particulate matter (PM 2.5), has been drawing global attention due to its warming effect in the atmosphere, which exceeds the impact of carbon dioxide (CO<sub>2</sub>) [1], a known greenhouse gas. Emitted from the incomplete combustion of fossil fuels, biomass, and biofuels, BC absorb solar radiation, thereby contributing to atmospheric warming. It is later deposited on ice and snow, where it reduces albedo, thereby accelerating the melting process [2].

The maritime sector, a substantial contributor to anthropogenic BC emissions, accounts for more than 20% of carbon dioxide equivalent emissions over a 20-year timeframe, making it a significant climate-warming pollutant [3]. These emissions are particularly concerning because they are released directly into coastal and port areas, where they can severely degrade air quality and pose significant risks to public health and coastal marine resources.

Exposure to fine particulate matter, which includes BC, is associated with numerous serious health risks, including respiratory and cardiovascular diseases, premature death, and interferes with fetal development [4], [5]. From a climate perspective, accelerated melting resulting from albedo reduction influences global climate patterns and hydrology [6], creating a positive feedback loop that further exacerbates global warming. Ecologically, when BC enters the marine ecosystem via dry deposition or river run-off, it has the potential to affect nutrient biogeochemical cycles, potentially impacting primary producers and broader food web functions [7], [8].

Although reducing BC emissions is widely recognized as necessary, the maritime sector confronts significant difficulties in tracking and controlling these pollutants. This difficulty arises as BC emissions are highly dependent and influenced by engine type and age, fuel quality, and operational modes [9]. Consequently, it makes the direct measurement and precise inventory compilation challenging, most especially for the older ships or vessels operating in areas with less strict environmental regulations. Many local fleets, particularly in developing countries, often lack the advanced sensors and real-time monitoring systems that the larger international shipping companies usually have. This technological disparity results in a substantial data gap that hinders accurate emissions accounting and formulation of targeted mitigation strategies.

In the absence of onboard measurement capabilities, policymakers and researchers have to rely on estimated inventories, which are often limited by data availability and methodological consistency. As a result, the environmental impact of these fleets may be underreported, delaying much-needed regulatory attention and emissions reduction interventions [10].

### 1.2. *Problem Statement*

The absence of advanced onboard BC monitoring systems in various vessels, including military and law enforcement fleets such as those from the Philippine Coast Guard (PCG), presents a considerable challenge in managing emissions effectively. Without real-time data, the ability to start precise baseline emission inventories, identify high-emitting vessels or operational practices, and assess the effectiveness of ongoing mitigation strategies is limited. Conventional methods of emission estimation mostly rely on broad assumptions or require extensive instrumental measurements, which may not be practical and cost-effective for all maritime operators.

### 1.3. *Policy Implications*

This study has a significant implication for science and policy in maritime environmental protection. It demonstrates non-instrumental methods can effectively estimate black carbon (BC) emissions, providing an important tool for regions that lack the advanced monitoring capabilities. It democratizes emission assessment, allowing more stakeholders to contribute in reducing maritime pollution. The framework offers a model for establishing BC emission inventories, which will aid policy decisions, target setting, and progress tracking. Identifying berthing as the key BC source highlights strategies such as shore power and cleaner fuels, especially in improving air quality in the coastal communities. Additionally, the research supports using non-instrumental methods in scientific discourse on SLCPs, encouraging further investigation into BC emissions and refined models. Ultimately, it promotes sustainable maritime practices, environmental health, and climate change mitigation.

### 1.4. Research Objectives

1. Identify Non-Instrumental Methods: To explore and validate methodologies that utilize readily available data, such as ship profiles, fuel consumption, and emission factors, to estimate BC emissions from ships without direct instrumental measurements.
2. Establish Framework for PCG vessels' emission measurement: To develop a comprehensive measurement model for BC emissions based on established guidelines, specifically the European Environment Agency (EEA) Guidelines, integrated with detailed ship activity profiling.
3. Determine High-Emission Activities for focus-driven mitigation: To analyze the contribution of different operational phases – underway, docking, undocking and berthing – to total BC emissions, thereby identifying activities that warrant mitigation efforts.

## 2. MATERIALS and METHODS

### 2.1. Technical Overview of the Capital Vessels from the Coast Guard Fleet in the Philippines

The Philippine Coast Guard (PCG) is “established as an armed and uniformed service attached to the Department of Transportation” with provisions for attachment to the Department of National Defense during wartime [11]. It is vested with five functions: maritime safety, marine environmental protection, maritime security, maritime law enforcement, and search and rescue. It has twenty-seven (27) capital vessels, primarily used for implementing its five mandated functions. Multi-Role Response Vessel (MRRV), a 97-meter vessel used for patrolling within the Philippines' exclusive economic zone (EEZ), towing operations, maritime law enforcement, environmental protection, and humanitarian assistance and disaster response. Offshore Patrol Vessel (OPV), an 83-meter vessel used for extended offshore patrols in rough seas, pollution response, maritime domain awareness, multi-agency coordination, and environmental missions. Multi-Role Response Vessel (MRRV), a 44-meter vessel used for localized maritime law enforcement and security, search and rescue, environmental missions, logistical support, and aid in fisheries, immigration, and transnational crime enforcement. The Search and Rescue Vessel (SARV) is a 56-meter and 36-meter-sized vessel used for rapid response during search and rescue operations, coastal patrol and surveillance, and coastal environmental protection.

Although stipulated in the International Convention for the Prevention of Pollution from Ships, 1973 as modified by the Protocol of 1978 (MARPOL 73/78), Article 3 states, “shall not apply to any warship, naval auxiliary or other ship owned or operated by a State and used, for the time being, only on government non-commercial service, [12].” There is still a need to track and monitor its vessel emissions as it also explicitly states in Article 3 that “each Party shall ensure by the adoption of appropriate measures not impairing the operations or operational

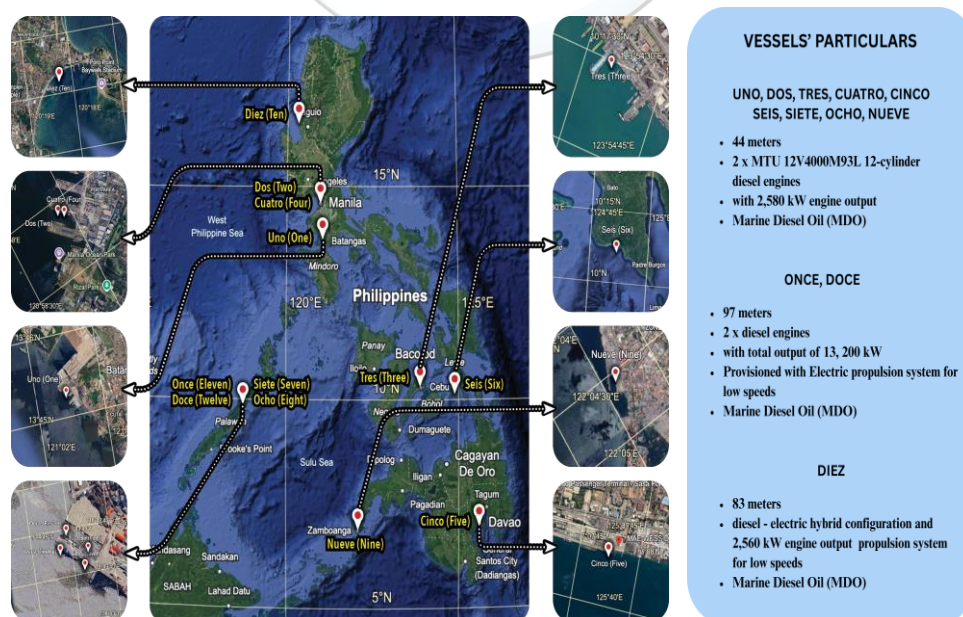


Figure 1. Overview of the PCG vessels' technical specifications for each type (right) Overview of the PCG vessels' operational base map in 2023 (left)

capabilities of such ships owned or operated by it, that such ships act in a manner consistent, so far as is reasonable and practicable, with the present Convention” [12].As such, being the mandated organization to implement maritime environmental rules and regulations, it is necessary to track and monitor the PCG vessels’ emissions to comply with Article of the MARPOL 73/78 Convention.

In this study, we utilized 12 of the 27 PCG’s capital vessels, as they are the most frequently used and the largest, with the most recent complete data required for this study, while others have either incomplete data or are on dry dock. Vessels’ technical specifications and location during the data collection are shown in Fig. 1.

**2.2. Data Collection**

This study conducted a comprehensive and detailed review of ship black carbon emissions, combining published literature and government records with estimation methods and reference to relevant environmental standards. We systematically search various journal databases such as ScienceDirect and Scopus for peer-reviewed articles and studies, and analyze reports from government and non-government organizations specializing in maritime environmental issues to ensure a broad, up-to-date understanding.

Moreover, we obtained the specific data of the vessels from the Philippine Coast Guard (PCG) official records, which include detailed ship specifications such as engine types, fuel consumption rates, and operational logs. These logs contain critical and most important data, as they reveal the ships’ operational phases, including time spent underway, docking and undocking, and berthing, which is relatively crucial for implementing activity-based emission estimation methods.

**2.3. Study Design**

The study followed a structured approach to ensure systematic progression from the initial stages of problem identification to the final interpretation of results. A sequential context was adopted to guide each phase of the study, as shown in Fig. 2.

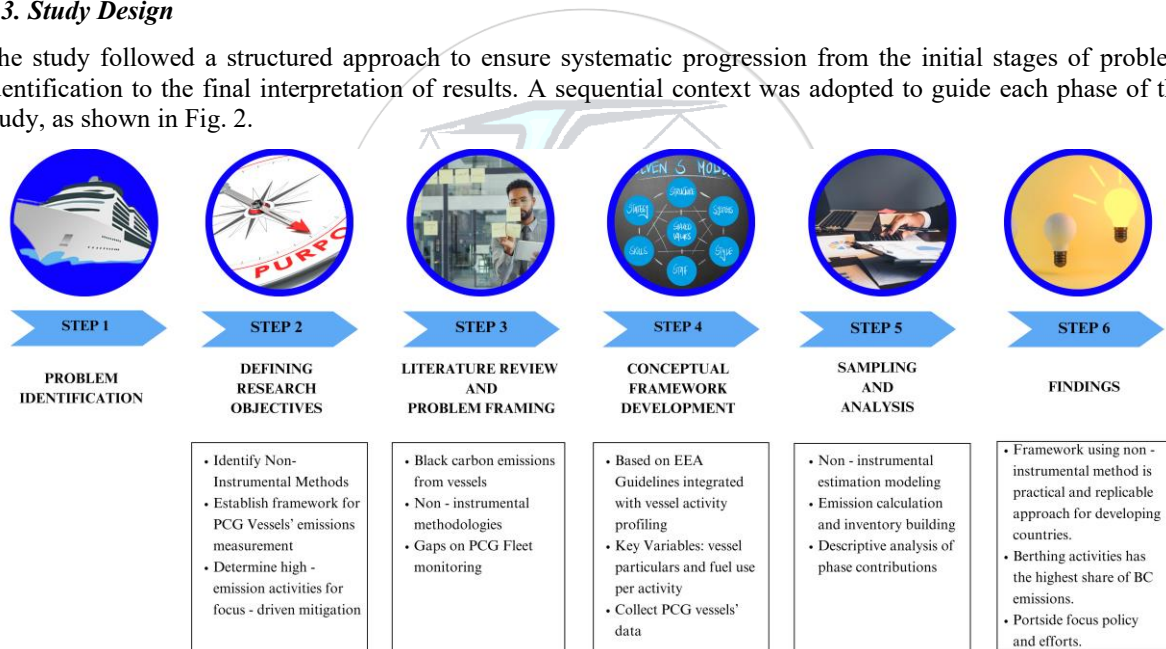


Figure 2. Methodological flowchart from problem definition to key findings

**2.3.1. Non-Instrumental Methods**

In the absence of direct instrumental measurements, black carbon emissions were estimated using the Tier III “Ship Movement Methodology” approach, consistent with established emission inventory guidelines of the European Environment Agency [13]. This approach requires detailed ship movement data and technical information of the ship, such as engine size and technology, power installed or fuel use, and the duration of hours in different activities to quantify BC emissions. The formula used is:

$$E_{Trip, i, j, m} = \sum_p \left( FC_{j, m, p} \times EF_{i, j, m, p} \right) \tag{1}$$

Where:

$E_{Trip}$  = emission for the entire completion of a vessel trip (tonnes)

FC	= fuel consumption of the vessel per operational phase (tonnes)
EF	= emission factor based in EEA (kg/tonne)
i	= pollutant
m	= fuel type
j	= engine type
p	= different phases of the trip (underway, docking/undocking, berthing)

### 2.3.2. Numerical Calculations

Since the data provided by the PCG only includes the total fuel consumption for the entire voyage duration, we assume docking and undocking durations of one hour (30 minutes each). This assumption aligns with their PCG Citizens Charter when responding to emergencies [14]. Additionally, we use a 15% load on the engine based on their set fuel consumption table. Similarly, for berthing, we consider a 100% load when using the auxiliary engine for the ship's power, according to its set fuel consumption table. Given the assumed values for berthing, we then calculated the fuel consumed in the auxiliary engine while underway and at berth using the data collected on the underway duration. With the complete required data for calculation based on the EEA Tier III "Ship Movement Methodology," we were able to compute the black carbon emissions of the selected PCG Vessels.

### 2.3.3. Development of the Framework to Calculate Emissions from Vessels in the Philippines

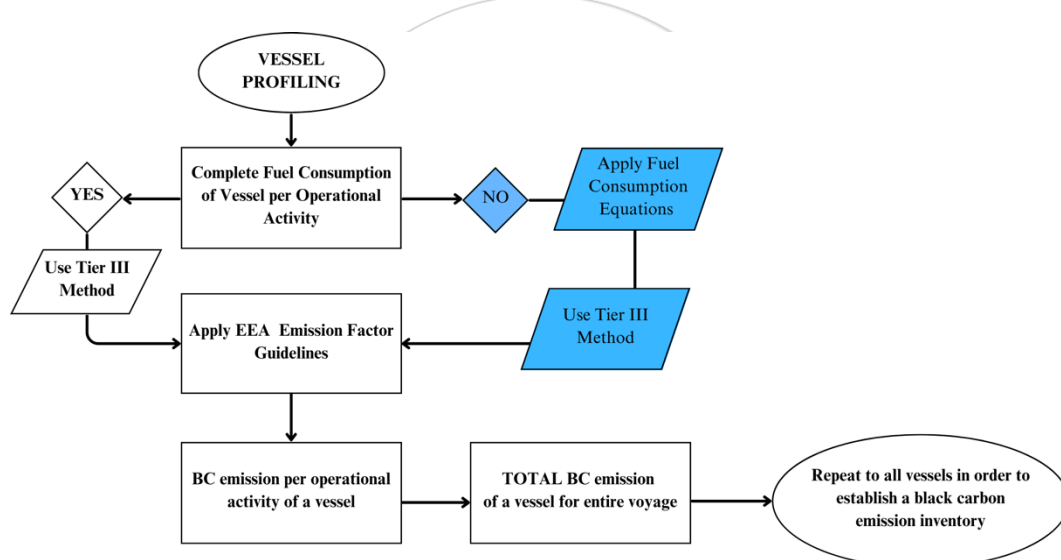


Figure 3. Preliminary Framework: Vessel-Level Emission Calculation Utilizing Non-Instrumental Methods

Based on the principles outlined in the EEA Emission Inventory Guidebook (2019) – Updated December 2021, integrated with detailed vessel profiling and activity-based analysis, a framework for estimating emissions from PCG vessels was developed, see Fig. 3. It can be visualized as a systematic process:

1. **Vessel Profiling:** The initial step of the framework involves gathering required data on each vessel, including its engine type, power output, specific fuel consumption (SFC), and fuel types used. This information is essential to apply the technology-specific emission factors in Tier III calculations.
2. **Operational Activity (Fuel Consumption):** Data on the operational activities of the vessels shall be collected from the vessels' activity logs and or automatic identification system (AIS). This includes the duration and fuel consumption during the three operational phases: underway (open sea transit), docking and undocking (navigating in confined waters, approaching/departing ports), and berthing (vessels at berth, auxiliary engines running). In such cases where direct fuel consumption data for specific operational phases were unavailable, fuel consumption modeling equations shall be used to calculate these values.
3. **Emission Factor Application:** Emission factors for black carbon were primarily sourced from the EEA Emission Inventory Guidebook (2019) – updated 2021. These factors, which quantify the amount of pollutant emitted per unit of fuel consumed or activity performed, were applied according to the chosen

tier of analysis. The framework allows for the application of Tier I (Default Approach), Tier II (Technology-Specific Approach), or Tier III (Ship Movement Methodology) based on the availability and granularity of data in possession.

4. Total BC Emissions per Operational Phase: By combining the fuel consumption data for each operational phase with the appropriate emission factors, the total black carbon emissions for each phase were calculated. This step was crucial for determining which operational activities contributed most significantly to the overall BC emissions.
5. Baseline Measurement: By integrating the results from the three operational phases – underway, docking/undocking, and berthing – the total black carbon (BC) emissions for each vessel were calculated. This comprehensive approach allowed for the establishment of a baseline measurement, providing a foundational reference point for assessing emission levels, tracking trends over time, and informing future mitigation strategies tailored to vessel behavior and port operations.

This systematic framework guaranteed a vigorous and transparent methodology to estimate not only black carbon emissions from PCG vessels but also other SLCPs, offering a reliable baseline for future mitigation efforts and policy development. The integration of literature review, government records, and established emission guidelines allowed for a comprehensive assessment even in the absence of direct instrumental measurements.

#### **2.4. Statistical Analysis**

Descriptive statistical analysis was employed to summarize and interpret the black carbon (BC) emissions data across the three operational phases of sampled vessels. Measures including percentages, totals, and distribution patterns were used to identify which phase contributed most significantly to overall emissions. The use of descriptive statistics effectively captured the emission behavior of vessels and provided a clear picture of where mitigation efforts should be prioritized.

### **3. RESULTS**

#### **3.1. Overview of Year 2023 PCG Vessels' Black Carbon Emission Results**

Our analysis of black carbon (BC) emissions from the sampled Philippine Coast Guard (PCG) vessels in 2023 revealed a total emission of 0.1707 metric tons. This figure provides a foundational baseline for understanding the BC contribution from the observed fleet. A detailed breakdown of emissions per vessel indicated significant variability in its contributions. Specifically, Vessel Once (Eleven) exhibited the highest BC emissions at 0.0292 metric tons, likely due to its significantly larger size of 97 meters, allowing for greater engine power and fuel use, also suggesting potential differences in operational profiles, engine efficiency, or fuel consumption practices that may warrant further study. In contrast, other vessels contributed lower but still considerable emission levels. Therefore, it implies that vessel size, in combination with operational patterns and engine specifications, plays a critical role in determining BC emissions. Given that the individual emissions may appear modest, the cumulative impact from such vessels, especially when considered fleet-wide and over time, underscores the importance of targeted emission reduction strategies.

Table 1. The amount of PCG vessels' black carbon emissions in 2023

Vessel Name	Underway	Docking/Undocking	Berthing	TOTAL	TOTAL
	(kg)	(kg)	(kg)	(kg)	(ton)
Doce (Twelve)	9.379	0.6169	18.32	28.32	0.0283
Once (Eleven)	9.880	0.1707	19.16	29.21	0.0292
Diez (Ten)	4.190	0.1607	19.04	23.39	0.0234
Nueve (Nine)	2.616	0.5370	7.511	10.66	0.0106
Ocho (Eight)	2.234	0.6006	5.908	8.743	0.0087
Siete (Seven)	4.697	0.4627	6.919	12.08	0.0121
Seis (Six)	1.935	0.3470	7.714	10.00	0.0100
Cinco (Five)	1.020	0.1157	5.958	7.094	0.0071
Cuatro (Four)	4.903	0.5783	6.875	12.35	0.0123
Tres (Three)	1.333	0.2313	7.567	9.042	0.0090
Dos (Two)	1.271	0.1349	7.532	8.876	0.0089
Uno (One)	2.572	0.7133	7.829	11.11	0.0111

### 3.2. Emission Concentrations by Operational Activities

One of the most substantial findings of this study is the disproportionate contribution of different operational activities to the total black carbon emissions. The analysis demonstrated that berthing (vessels at berth with auxiliary engines running) accounted for the largest share of BC emissions, contributing approximately 70% of the total sampled emissions or 0.1203 metric tons of BC.

Whereas, the underway phase (open sea transit) contributed 27% of the emissions, and the docking/undocking phase was responsible for about 3%.

This distribution emphasizes the indispensable insight that the majority of BC emissions occur when vessels are stationary or operating at low speeds within or near port areas. This finding is particularly relevant for air quality and warming potential within coastal cities and port communities, as these emissions are released in close proximity to human populations. The representation as shown in Table 2 illustrates the dominance of berthing emissions, providing compelling evidence for focus-driven mitigation efforts that target reducing emissions during port stays.

Table 2. Distribution of Black Carbon Emissions by Operational Phase of Vessels

Underway	Docking/Undocking	Berthing	TOTAL	TOTAL
(kg)	(kg)	(kg)	(kg)	(ton)
46.03	4.669	120.3	170.9	0.1707

### 3.3. Key Findings and Observations

Based on the quantitative results and qualitative observations, several key findings emerged:

1. Port Areas as Emission Hotspots: Berthing activities appeared as the dominant trace of BC emissions, thus emphasizing that critical emission hotspots are in port areas. Prolonged running of vessels' auxiliary engines while berthed leads to concentrated pollution, intensifying health risks to port workers, users, and nearby communities.
2. Health and Climate Risks: High concentrations of BC emissions in ports pose severe health threats, such as cardiopulmonary diseases, regional warming impact, and coastal environmental degradation. These findings accentuate the urgent need for mitigation schemes in high-exposure zones.
3. Methodological Validation and Limitations: The study validates the practicality of non-instrumental methods to estimate BC emissions in instances where direct monitoring is unavailable. However, though the approach based on EEA guidelines and vessel activity profiling is practical and efficient for baseline inventories, it has limitations due to reliance on data reported and a lack of real-time validation. Still, it offers a valuable, accessible tool for policy development and initial assessments.

These results show a clear outline of the black carbon emission footprint within the sampled PCG fleet, emphasizing the contribution of berthing activities and underscoring the need for targeted interventions to achieve sustainable mitigation. The findings laid the groundwork for the subsequent discussion on implications and policy recommendations.

#### 4. DISCUSSIONS

The outcome, indicating that berthing activities account for the majority proportion of the total black carbon emissions from PCG vessels, conveys significant implications for environmental policy and operational practices. This disparity contribution outlines that the most impactful mitigation efforts should be directed towards vessels while they are berthed in ports. Berthing explicitly involves ships running auxiliary engines to power onboard systems, lighting, and crew needs, often for extended periods. Unlike underway or docking/undocking, which occur over wider geographical areas, berthing emissions are concentrated in confined port environments, directly influencing the air quality of adjacent urban areas, the health of port workers and residents, as well as nutrient cycles in the coastal marine ecosystem.

This emission concentration generates localized pollution hotspots, worsening cardiopulmonary health issues for communities near ports. The environmental impact extends beyond human health, contributing to regional haze and localized warming effects. Therefore, addressing berthing emissions is not only an environmental necessity but also a public health priority.

#### 5. CONCLUSIONS

This study stresses the potential of non-instrumental methods to estimate black carbon (BC) emissions from ships, most especially when onboard monitoring systems are unavailable. Utilizing the Philippine Coast Guard fleet as a model, it established a reliable framework aligned with EEA guidelines. Berthing activities contribute the highest share of BC emissions, thus underscoring the need for targeted portside policies like electrification and cleaner fuels. The research provides a practical, replicable approach for developing countries, offering both a baseline inventory and a scalable method to support global efforts towards sustainable maritime operations.

#### ACKNOWLEDGMENT

This research was supported by the Korea Institute of Ocean Science and Technology (PO01458), Republic of Korea. The authors also acknowledge the Philippine Coast Guard for providing its fleet operational data that informed this study and supported the development of its preliminary framework.

#### CONFLICT OF INTEREST STATEMENT

The authors declares that there is no conflict of interest.

#### REFERENCES

- [1]. Climate and Clean Air Coalition. (n.d.). Black carbon. United Nations Environment Programme. Retrieved January 28, 2025, from <https://www.ccacoalition.org/short-lived-climate-pollutants/black-carbon>
- [2]. Clarity Movement. (2025, April 12). *Albedo reduction caused by black carbon*. Clarity Movement. [Online]. <https://www.clarity.io/blog/albedo-reduction-caused-by-black-carbon>
- [3]. International Council on Clean Transportation. (2019). Black carbon from shipping accounts for more than 20% of CO<sub>2</sub>-equivalent emissions over 20 years. ICCT Policy Update.
- [4]. World Health Organization. (2021). Health effects of black carbon. WHO Regional Office for Europe.
- [5]. Johnson, B. R. et al. (2021). Air pollution and children's health: a review of adverse effects associated with prenatal exposure from fine to ultrafine particulate matter. *Environmental Health and Preventive Medicine*, 26(1), 1–12. (summary review)
- [6]. Rutherford, W. A. et al. (2017). Albedo feedbacks to future climate via climate change impacts on dryland biocrusts. *Scientific Reports*, 7, 44188. <https://doi.org/10.1038/srep44188>
- [7]. Mari, X., Guinot, B., Thuoc, C. V., Brune, J., Lefebvre, J. P., Angia Sriram, P. R., ... & Niggemann, J. (2019). Biogeochemical impacts of a black carbon wet deposition event in Halong Bay, Vietnam. *Frontiers in Marine Science*, 6, 185.
- [8]. Saidi, A., Zoccarato, L., Birarda, G., Mari, X., Weinbauer, M., Vaccari, L., ... & Malfatti, F. (2025). Black carbon structuring marine microbial activities and interactions: a micro-to macro-scale interrogation. *Environmental Science and Pollution Research*, 1-19.
- [9]. Le Berre, L., Temime-Roussel, B., Lanzafame, G. M., D'Anna, B., Marchand, N., Sauvage, S., Wortham, H. (2025).

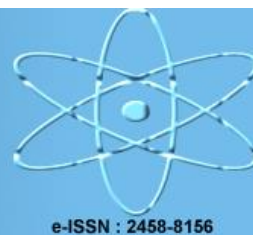
- [10]. Measurement report: In-depth characterization of ship emissions during operations in a Mediterranean port. *Atmospheric Chemistry and Physics*, 25, 6575–6605. <https://doi.org/10.5194/acp-25-6575-2025>
- [11]. Republic of the Philippines. (2010, February 12). Republic Act No. 9993: Philippine Coast Guard Law of 2009.
- [12]. International Convention for the Prevention of Pollution from Ships, 1973, as amended by the Protocol of 1978 (MARPOL 73/78), art. 3(3), 1340 U.N.T.S. 22484 (entered into force Oct. 2, 1983).
- [13]. **European Environment Agency**. (2021). *EMEP/EEA air pollutant emission inventory guidebook 2019: Updated December 2021 – Technical guidance to prepare national emission inventories*. Publications Office of the European Union. <https://www.eea.europa.eu/publications/emep-eea-guidebook-2019>
- [14]. Philippine Coast Guard. (2024). *PCG Citizens' Charter*. Retrieved May 8, 2025, from <https://www.coastguard.gov.ph>





# EJENS

European Journal of Engineering and Natural Sciences



e-ISSN : 2458-8156

## Sustainable Production of Maleic Anhydride: Minimizing By-Product Formation in Industrial Fixed-Bed Tubular Reactor

Ervin Karić<sup>\*1</sup>, Ivan Petric<sup>1</sup>, Edina Ibrić<sup>1</sup>, Maida Smajlović<sup>1</sup>, Marijana Marković<sup>1</sup>, Maida Kuduzović<sup>1</sup>, Emir Suljaković<sup>1</sup>, Ermin Mujkić<sup>2</sup>

<sup>1</sup>Department of Chemical Engineering, Faculty of Technology, University of Tuzla, Urfeta Vejzagića 8, 75000 Tuzla, Bosnia and Herzegovina.

<sup>2</sup> Koksara d.o.o. Lukavac, Željeznička 1, 75300 Lukavac, Bosnia and Herzegovina.

\*Corresponding Author email: [ervin.karic@untz.ba](mailto:ervin.karic@untz.ba)

### Abstract

The synthesis of maleic anhydride from n-butane in an industrial fixed-bed reactor is presented, with emphasis on reducing by-product formation. The modeling and simulation of an industrial fixed-bed reactor are also presented in this paper. The research was conducted using industrial process data collected from a fixed-bed reactor over a defined period, addressing challenges related to conversion, yield, selectivity, and minimization of acrylic acid formation. The numerical software package MATLAB was used for solving the system of mathematical model equations. By decreasing the molar flow of n-butane at the reactor inlet by 15%, the conversion of n-butane and the yield of maleic anhydride increased by 6.89% and 3.13%, respectively, while the amount of acrylic acid formed was reduced by 2.10%. Conversely, increasing the molar flow of oxygen at the reactor inlet by 15% led to a 13.12% increase in the molar percentage of acrylic acid, whereas decreasing the oxygen flow by 15% reduced the molar percentage of acrylic acid by 10.77%. Increasing the pressure of the reaction mixture at the reactor inlet by 15% raised the molar percentage of acrylic acid by 6.93%, while decreasing the pressure by 15% reduced it by 8.04%. The selectivity of acrylic acid increases with higher inlet pressure due to enhanced n-butane conversion. Given that the main objective of the n-butane oxidation process to maleic anhydride is to achieve high n-butane conversion and maleic anhydride yield while minimizing acrylic acid formation, the optimal strategy is to reduce the molar flow of n-butane at the reactor inlet.

### Keywords

Document, EJENS, European, Journal

### 1. INTRODUCTION

The partial selective oxidation of n-butane to maleic anhydride with molecular oxygen is commercially well-established and strongly associated with the vanadium phosphorus oxide (VPO) catalyst [1]. Maleic Anhydride (MA) is the anhydride of cis-butenedioic acid (maleic acid); this molecule has a four carbon cyclic structure, containing also one oxygen atom. The molecule is also known with other names: 2,5-Furandione, Dihydro-2,5-dioxofuran, cis- Butanedioic anhydride [2]. Maleic anhydride is an important intermediate in the chemical industry, used in the production of agricultural chemicals and lubricant additives, and it is also a constituent component of several copolymers [3]. Over 50% of the global demand for maleic anhydride is used for the production of unsaturated polyester resins [3]. Initially, maleic anhydride was produced by the partial oxidation of

benzene using a vanadium–molybdenum oxide ( $V_2O_5$ – $MoO_3$ ) catalyst [4]. Following the adoption of n-butane as a feedstock for maleic anhydride production, the number of studies on the synthesis of maleic anhydride via n-butane oxidation increased sharply ([5]–[9]). Reference [10] published one of the most significant early review articles addressing the catalytic properties of VPO catalysts, catalyst preparation mechanisms, and the kinetics of n-butane oxidation to maleic anhydride. The review covered a total of 188 studies. The formation of acrylic acid as a reaction by-product was also considered to assess its impact on the overall process efficiency. The present study focuses on modeling and simulating the formation of acrylic acid as a by-product during the partial oxidation of n-butane to maleic anhydride in an industrial fixed-bed tubular reactor. Using actual plant data, we implemented and numerically solved the mathematical model, based on the reactor model developed by [11] and kinetic data from [12], using MATLAB. Based on model, the variations of reactant and product molar flows along the reactor length were analyzed as a function of catalyst mass. The study specifically examined the influence of key process parameters, including n-butane and oxygen feed flow rates and reaction mixture pressure on acrylic acid formation. The modeling results provide insight into the sensitivity of by-product formation to operating conditions and can guide strategies for minimizing undesired side reactions in industrial operation.

## 2. MATERIALS AND METHODS

### 2.1. Description of the industrial reactor

For this study, industrial data from a fixed-bed tubular reactor used for maleic anhydride production were employed. The reactor consists of a large number of parallel tubes filled with a vanadium–phosphorus oxide (VPO) catalyst. The catalyst and reactor configuration are representative of typical industrial operation. Specific geometric details, catalyst porosity, and other sensitive operational parameters are omitted to maintain confidentiality.

### 2.2. Mathematical model

The mathematical model of the reactor, originally developed by [11], was used as the basis for this study and updated with new industrial measurements to reflect current operating conditions and reactor performance.

### 2.3. Kinetic model

The general scheme of the selective oxidation of n-butane to maleic anhydride can be represented by a combination of series and parallel reactions, as proposed by [13]:

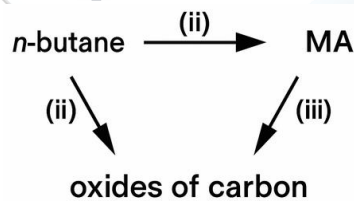


Figure 1. General scheme of the selective oxidation of n-butane to maleic anhydride [13]

In addition to the reactions mentioned above, the following equation was also considered for the formation of acrylic acid:



The kinetic model for the process scheme was taken from [12], where the Eley–Rideal approach was adopted to describe the kinetics of partial oxidation of n-butane [14].

$$r_1 = \frac{k_1 \cdot p_{butane} \cdot \sqrt{p_{O_2}}}{1 + b_{H_2O} \cdot p_{H_2O} + b_{butane} \cdot p_{butane}} \quad (5)$$

$$r_2 = \frac{k_2 \cdot p_{butane} \cdot \sqrt{p_{O_2}}}{1 + b_{H_2O} \cdot p_{H_2O} + b_{butane} \cdot p_{butane}} \quad (6)$$

$$r_3 = \frac{k_3 \cdot p_{MA} \cdot \sqrt[4]{p_{O_2}}}{1 + b_{H_2O} \cdot p_{H_2O} + b_{butane} \cdot p_{butane}} \quad (7)$$

where:  $r_1$  - reaction rate of the first reaction (variable),  $k_1$  - is the kinetic parameter of the first reaction (variable),  $p_{butane}$  - butane partial pressure (Pa),  $p_{O_2}$  - oxygen partial pressure (Pa),  $b_{H_2O}$  - kinetic parameter for water (-),  $p_{H_2O}$  - water partial pressure (Pa),  $r_2$  - reaction rate of the second reaction (variable),  $k_2$  - kinetic parameter of the second reaction (variable),  $r_3$  - reaction rate of the third reaction (variable)  $k_3$  - kinetic parameter of the third reaction (variable), and  $p_{MA}$  - maleic anhydride partial pressure (Pa).

The kinetic model of reaction (4) is presented by the following equation from [15]:

$$r_4 = k_4 \cdot p_{aa}^{0.68} \cdot p_{O_2}^{0.33} \quad (8)$$

where:  $r_4$  - reaction rate of the fourth reaction (variable),  $k_4$  - is the kinetic parameter of the first reaction ( $\text{mol kg}^{-1} \text{s}^{-1}$ ),  $p_{aa}$  - acrylic acid partial pressure (Pa)

#### 2.4. Model Simulation and Parametric Analysis

The mathematical model equations were numerically solved using the MATLAB software package. The system of ordinary differential equations describing the variation of component molar flows and temperature along the reactor length was solved using the ode45 solver, based on an explicit Runge–Kutta method of fourth and fifth order. The simulation was performed using industrial process data as input parameters. The effects of changes in the n-butane and oxygen feed flow rates, as well as the inlet temperature and pressure of the reaction mixture, on the formation of acrylic acid were analyzed. These parameters were varied in the range of  $\pm 15\%$  relative to the base case to evaluate their influence on acrylic acid generation within the reactor.

### 3. RESULTS AND DISCUSSION

Figure 2 shows the variation of the molar flow rates of n-butane (FA) and oxygen (FB) along the reactor as a function of the catalyst mass (W). The simulation was performed under the operating conditions of maleic anhydride synthesis by the partial oxidation of n-butane in a fixed-bed tubular reactor.

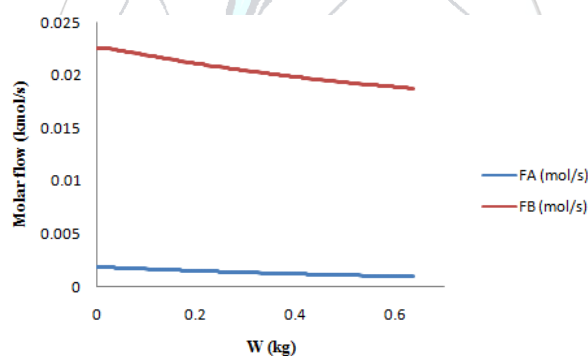


Figure 2. Variation of n-butane and oxygen molar flows along the reactor axial coordinate (as a function of catalyst mass)

Results show that n-butane flow decreases with increasing catalyst mass, as higher conversion consumes n-butane along the reactor, which agrees with the findings of [16] regarding conversion increase along the reactor length. Notably, the reduction in n-butane flow is more pronounced than that of oxygen, which aligns with the stoichiometry of the reaction. Reference [16] reported that n-butane conversion increases along the reactor length. In our study, the n-butane flow decreases with increasing catalyst mass. This is expected, as higher conversion leads to consumption of n-butane, reducing its flow along the reactor. The observed decrease in molar flows along the reactor length corresponds to enhanced reactant conversion, particularly in the initial section of the reactor, where reactant concentrations and temperature gradients are maximal. Moving further along the reactor, the reaction rate diminishes as the concentration of n-butane drops, resulting in a reduced contribution to overall conversion at higher catalyst masses. This pattern suggests that the reaction is mainly kinetically controlled in the early stages of the reactor, while at larger catalyst masses, mass transfer limitations begin to influence the process. Figure 3 shows the variation of the flow rates of carbon monoxide (FC), maleic anhydride (FD), and carbon dioxide (FE) as a function of catalyst mass, illustrating the consumption and formation trends of these species along the reactor.

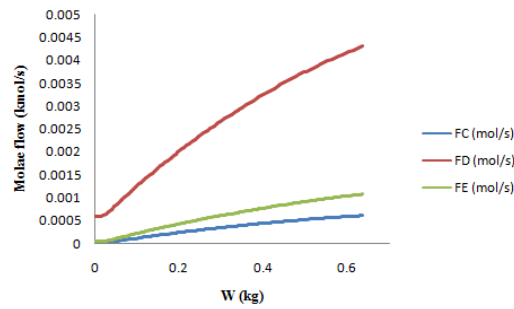


Figure 3. Variation of carbon monoxide (FC), maleic anhydride (FD), and carbon dioxide (FE) molar flows along the reactor axial coordinate (as a function of catalyst mass)

The profiles of carbon monoxide (FC), maleic anhydride (FD), and carbon dioxide (FE) molar flows as a function of catalyst mass (W) show that the formation of the desired product maleic anhydride steadily increases along the reactor, indicating efficient conversion of n-butane. At the same time, the flow rates of carbon monoxide and carbon dioxide also rise gradually, reflecting the generation of minor by-products through side reactions. The increase in carbon monoxide and carbon dioxide is much smaller compared to FD, demonstrating that the reaction remains highly selective toward maleic anhydride. The results obtained in this study are consistent with the findings of [16]. The selectivity of maleic anhydride increased along the length of the reactor, and the selectivity of carbon dioxide also increased. The ratio of carbon monoxide to carbon dioxide initially increased and then decreased in their study, indicating that in the later stages more carbon dioxide was produced than carbon monoxide. In our experiments, the selectivity of maleic anhydride and carbon dioxide similarly increased with increasing catalyst mass, while the flow of carbon monoxide also continuously increased, although at a lower rate than carbon dioxide. This indicates that maleic anhydride and carbon dioxide formation dominate the reaction, but carbon monoxide production continues throughout the reactor, confirming the influence of catalyst mass on the distribution of all products. These results confirm the effectiveness of the catalyst and the progressive nature of the oxidation process along the reactor length.

Table 1 shows the effect of changes in the n-butane inlet flow ( $FA_{inlet}$ ), expressed as a percentage, on the molar flow of acrylic acid at the reactor outlet (FG).

Table 1. Effect of n-butane inlet molar flow on the molar flow of acrylic acid at the reactor outlet (FG)

$FA_{inlet}$ (%)	$F_G$ (kmol/s)
-15	0.000774
-10	0.000779
-5	0.000786
0	0.000791
+5	0.000795
+10	0.000802
+15	0.000804

By decreasing the molar flow of n-butane at the reactor inlet by 15%, the conversion of n-butane and the yield of maleic anhydride increased by 6.89% and 3.13%, respectively, while the amount of acrylic acid formed was reduced by  $1.7 \cdot 10^{-5}$  (or 2.10%). Reference [17] demonstrated that increasing the percentage of n-butane at the reactor inlet led to a higher yield of maleic anhydride, while the overall conversion of n-butane decreased due to losses in undesired side reactions. The reduction in n-butane conversion caused by these losses explains why increasing the n-butane flow at the reactor inlet results in a higher molar flow of acrylic acid at the reactor outlet.

Reference [18] found that increasing the concentration of n-butane at the reactor inlet increases the selectivity toward acrylic acid, which in turn leads to higher acrylic acid production, as also demonstrated in this study.

Table 2 shows the effect of changes in the oxygen inlet flow ( $FB_{inlet}$ ), expressed as a percentage, on the molar flow of acrylic acid at the reactor outlet.

Table 2. Effect of oxygen inlet molar flow on the molar flow of acrylic acid at the reactor outlet

$FB_{inlet}$ (%)	$F_G$ (kmol/s)
-15	0.0007059
-10	0.000781
-5	0.00075
0	0.000791
+5	0.000795
+10	0.000799
+15	0.000895

Increasing the molar flow of oxygen at the reactor inlet by 15% led to a 13.12% increase in the molar percentage of acrylic acid, whereas decreasing the oxygen flow by 15% reduced the molar percentage of acrylic acid by 10.77%. These results indicate that a higher oxygen availability promotes the oxidation of n-butane and the subsequent formation of intermediate products such as maleic anhydride and acrylic acid. Enhanced oxygen concentration improves the reaction rate by providing sufficient oxidizing species on the catalyst surface, thereby increasing the overall conversion and yield. However, excessive oxygen may also favor complete combustion reactions, leading to undesired formation of CO and CO<sub>2</sub>, which can reduce selectivity toward valuable products.

Table 3 shows the effect of the reaction mixture temperature at the reactor inlet, expressed as a percentage, on the molar flow of acrylic acid at the reactor outlet.

Table 3. Effect of the reaction mixture temperature at the reactor on the molar flow of acrylic acid at the reactor outlet

$T$ (%)	$F_G$ (kmol/s)
-15	0.000771
-10	0.000779
-5	0.000785
0	0.000791
+5	0.000797
+10	0.000804
+15	0.000808

Data from Table 3 show that the acrylic acid molar flow ( $F_G$ ) varies slightly with changes in the **inlet temperature of the reaction mixture**. A 15% decrease in the inlet temperature reduces  $F_G$  from 0.000791 kmol/s (reference value at 0%) to 0.000771 kmol/s, corresponding to a decrease of approximately 2.53%. Conversely, a 15%

increase in inlet temperature raises FG to 0.000808 kmol/s, representing an increase of 2.15 % relative to the reference value. These results indicate that the acrylic acid flow is moderately sensitive to the inlet temperature: higher temperatures slightly increase the flow, while lower temperatures reduce it. This behavior is consistent with the reaction kinetics of n-butane oxidation, where higher temperatures accelerate the reaction rate, and lower temperatures slow down acrylic acid formation. Reference [19] reported that acrylic acid begins to appear in trace amounts at temperatures above 402 °C. Considering that in this study the reaction mixture temperature at the reactor outlet is 421.34 °C, the observed increase in acrylic acid production with increasing temperature is consistent with these findings. Additionally, increasing the temperature enhanced acrylic acid selectivity [20], which is also observed in this study.

Table 4 shows the effect of the reaction mixture pressure at the reactor inlet, expressed as a percentage, on the molar flow of acrylic acid at the reactor outlet.

*Table 4. Effect of the reaction mixture pressure at the reactor on the molar flow of acrylic acid at the reactor outlet*

<i>P</i> (%)	<i>F<sub>G</sub></i> (kmol/s)
-15	<b>0.000736</b>
-10	0.000741
-5	0.000765
0	0.000791
+5	0.000801
+10	0.000837
+15	0.000855

Increasing the pressure of the reaction mixture at the reactor inlet by 15% raised the molar percentage of acrylic acid by 6.93%, while decreasing the pressure by 15% reduced it by 8.04%. This indicates that reductions in pressure have a stronger impact on acrylic acid production than equivalent increases, emphasizing the critical role of maintaining optimal reactor inlet pressure. The results also suggest that pressure control can be an effective tool for stabilizing production rates under varying operational conditions. Reference [21] investigated the effect of pressure variation on acrylic acid yield and found that increasing the pressure enhanced the yield up to a certain point, after which a slight decrease was observed at the reactor outlet.

#### 4. CONCLUSION

The results of this study demonstrate that the molar flow of acrylic acid (FG) is sensitive to variations in key reactor operating parameters. Increasing the inlet flows of n-butane and oxygen, as well as the feed temperature and pressure, generally enhances FG, whereas decreasing these parameters reduces it. The flow of acrylic acid shows moderate sensitivity to feed temperature, with a 15 % increase resulting in a 2.15 % rise in FG and a 15 % decrease causing a 2.53 % reduction, consistent with the kinetics of n-butane oxidation. Pressure effects are more pronounced: a 15 % increase in inlet pressure raises FG by 6.93 %, while a 15 % decrease reduces it by 8.04 %, indicating that reductions in pressure have a stronger impact than equivalent increases. Variation of n-butane and oxygen feed rates affects both selectivity and production, with higher n-butane flows increasing the molar flow of acrylic acid but slightly reducing overall n-butane conversion due to side reactions, while higher oxygen flows improve both yield and selectivity toward acrylic acid. Furthermore, the analysis of molar flows along the reactor as a function of catalyst mass shows that n-butane is consumed more rapidly than oxygen in the early section of the reactor, corresponding to higher conversion, and that the formation of acrylic acid, maleic anhydride, and by-products is progressively influenced by catalyst distribution. The kinetic and mathematical models, validated with industrial data, provide reliable predictions of reactor performance and can be used to optimize operating conditions and stabilize acrylic acid production.

## ACKNOWLEDGMENT

The authors acknowledge the Ministry of Education and Science of Tuzla Canton for funding the project “Minimizing the release of by-products into the environment from the synthesis of maleic anhydride in an industrial fixed-bed tubular reactor”. The authors also thank Ermin Mujkić, Director of the Maleic Anhydride Plant at Koksara d.d. Lukavac, for his support and assistance during this study.

## CONFLICT OF INTEREST STATEMENT

The authors are required to report any existing conflict of interest. If there is none, the following sentence should be written under this heading: “The author(s) declare(s) that there is no conflict of interest”.

## REFERENCES

- [1]. N. Stegmann, C. Ochoa-Hernández, K.N. Truong, H. Petersen, C., Weidenthaler, and W. Schmidt, W, “The mechanism and pathway of selective partial oxidation of n-butane to maleic anhydride studied on titanium phosphate catalysts,” *ACS Catalysis*, vol. 20, pp. 15833-15840, 2023.
- [2]. A. Caldarelli, “*New reactants and improved catalysts for maleic anhydride synthesis*,” Doctoral dissertation, Univ. of Bologna, Bologna, Italy, Department of Industrial Chemistry, 2012.
- [3]. D. Lesser, “Dynamic Behavior of Industrial Fixed Bed Reactors for the Manufacture of Maleic Anhydride,” Doctoral dissertation, Clausthal Univ. of Technology, Clausthal-Zellerfeld, Germany, Faculty of Mathematics/Computer Science and Mechanical Engineering, 2016.
- [4]. Y. Ye, “Experimental study on n-Butane partial oxidation to maleic anhydride in a solid electrolyte membrane reactor,” Doctoral dissertation, Otto-von-Guericke-Univ. of Magdeburg, Magdeburg, Germany, 2006.
- [5]. R.L. Varma, and D. N. Saraf, “Selective Oxidation of C4 Hydrocarbons to Maleic Anhydride,” *Industrial & Engineering Chemistry Product Research and Development*, vol. 18, pp. 7-13, 1979.
- [6]. M. Brutovský, and Š. Gerej, “Effect of various modifying elements on the catalytic properties of vanadium-phosphorus catalysts in oxidation of butane,” *Collection of Czechoslovak Chemical Communications*, vol. 47, pp. 403-408, 1982.
- [7]. B. K. Hodnett, and B. Delmon, “Influence of reductive pretreatments on the activity and selectivity of vanadium-phosphorus oxide catalysts for n-butane partial oxidation,” *Industrial & Engineering Chemistry Fundamentals*, vol. 23, pp. 465-470, 1984.
- [8]. G. Centi, G., Fornasari, and F. Trifiro, F., “n-Butane oxidation to maleic anhydride on vanadium-phosphorus oxides: Kinetic analysis with a tubular flow stacked-pellet reactor,” *Industrial & Engineering Chemistry Product Research and Development*, vol. 24, pp. 32-37, 1985.
- [9]. T. P. Moser, and G. L. Schrader, G. L., “Selective oxidation of n-butane to maleic anhydride by model V-P-O catalysts,” *Journal of Catalysis*, vol. 92, pp. 216-231, 1985.
- [10]. G. Centi, F. Trifiro, J. R. Ebner, and V. M. Franchetti, “Mechanistic aspects of maleic anhydride synthesis from C4 hydrocarbons over phosphorus vanadium oxide,” *Chemical Reviews*, vol. 88, pp. 55-80, 1988.
- [11]. I. Petric, and E. Karić, “Simulation of commercial fixed-bed reactor for maleic anhydride synthesis: application of different kinetic models and industrial process data,” *Reaction Kinetics, Mechanisms and Catalysis*, vol. 126, pp. 1027-1054, 2019.
- [12]. R. Guettel, and T. Turek, “Assessment of micro-structured fixed-bed reactors for highly exothermic gas-phase reactions,” *Chemical Engineering Science*, vol. 65, pp. 1644-1654, 2010.
- [13]. S. K. Bej, and M. S. Rao, “Selective oxidation of n-butane to maleic anhydride. 3. Modeling studies,” *Industrial & engineering chemistry research*, vol. 30, pp. 1829-1832, 1991.
- [14]. C. Becker, “Katalytische Wandreaktor-konzepte für MSA-Synthese und Methanol-Dampfreformierung,” Doctoral dissertation, Institut für Chemische Verfahrenstechnik der Universität Stuttgart, Stuttgart, Germany, 2002.
- [15]. Y. Dong, “Modeling chemistry and flow in catalytic fixed-bed reactors with detailed geometry,” Doctoral dissertation, Technische Universität Hamburg, Hamburg, Germany, 2018.
- [16]. A. Romano, A. Di Giuliano, K. Gallucci, P. U. Foscolo, C. Cortelli, S. Gori, S., and M. Novelli, “Simulation of an industrial turbulent fluidized bed reactor for n-butane partial oxidation to maleic anhydride,” *Chemical Engineering Research and Design*, vol. 114, pp. 79-88, 2016.
- [17]. S. Roy, M.P. Duduković, and P. L. Mills, P. L., “A two-phase compartments model for the selective oxidation of n-butane in a circulating fluidized bed reactor,” *Catalysis Today*, vol. 6, pp. 73-85, 2000.
- [18]. G. S. Patience, and M. J. Lorences, “VPO transient oxidation kinetics,” *International Journal of Chemical Reactor Engineering*, vol. 4, pp. 1-16, 2006.
- [19]. X. F. Huang, C. Y., Li, B. H., Chen, and P. L. Silveston, “Transient kinetics of n-Butane oxidation to maleic anhydride over a VPO catalyst,” *AIChE Journal*, vol. 48, pp. 846-855, 2002.

- [20]. M. J. Lorences, G. S., Patience, F. V., Díez, and J. Coca, "Transient n-butane partial oxidation kinetics over VPO," *Applied Catalysis A: General*, vol. 26, pp. 193-202, 2004.
- [21]. M. Dente, S., Pierucci, E., Tronconi, M., Cecchini, M., and F. Ghelfi, "Selective oxidation of n-butane to maleic anhydride in fluid bed reactors: detailed kinetic investigation and reactor modelling," *Chemical engineering science*, vol. 58, pp. 643-648, 2003.



# School Design and Post-Occupancy Evaluation: Sharjah School Case Study

**Dr. Mousa Al-Dghaimat<sup>1\*</sup>, Dr. Alaa Abdou<sup>2</sup>**

<sup>1</sup>*Kad Engineering Consultants, Independent Researcher, Jordan, UAE & Oman*

<sup>2</sup>*College of Engineering, University of Ajman, UAE*

*\*Corresponding Author email: Mousadghaimat@gmail.com*

---

## Abstract

This study applies a customized Post Occupancy Evaluation (POE) to a private school in the UAE, addressing the gap in region-specific evaluation frameworks for educational buildings. A two-part assessment—technical performance analysis and occupant perception surveys—was developed from a targeted literature review. Using base drawing analysis and structured walk-through observations, the study identified design strengths and areas for improvement directly affecting user experience. Outcomes aim to embed POE into facility management practices and provide actionable feedback for the design of future educational facilities in the UAE

## Keywords

Post Occupancy Evaluation (POE), Functional Performance Specifications, Walk-through, Educational Buildings.

## 1. INTRODUCTION

Post-Occupancy Evaluation is a process of systematically evaluating the performance of buildings after they are built and occupied for some time. This evaluation differs from other types of buildings' performance evaluations because it focuses on the needs and requirements of building occupants including health, safety, security, and functionality [1]. The term Post Occupancy Evaluation is defined as a process, which involves evaluating a buildings performance after it has been occupied by its target users. It is concerned with several issues such as: health, safety, security, efficiency, comfort and many other requirements, and provides feedback about the current of the project and proposes solutions to the existing problems. In addition, it can provide guideline principles and design criteria to improve similar future projects. POE has been seen as one of a number of practices aimed at understanding design criteria, predicting the effectiveness of emerging designs, reviewing completed designs, supporting building activation and facilities management, and linking user response to the performance of buildings [2]. POE is recently evolving toward more process-oriented evaluations for planning, programming, and capital asset management, it generates overall beneficial changes and outcomes, including: Saving dollars and energy, improving the quality of facilities, involving stakeholders in the process of POE, and improving the satisfaction of building occupants [3]. The study shows growing interest in POE and stresses the need for a stronger community of practice between academics and practitioners to develop consistent approaches and overcome barriers. It also introduces new theories to encourage broader academic discussion in the field [4]. More studies assess design quality in terms of functionality, comfort, accessibility, and sustainability. While users were generally satisfied, the findings reveal areas for improvement, recommending user-inclusive design, better lighting and ventilation, ergonomic furniture, and social spaces. The proposed framework offers a systematic method for evaluating school facilities and is adaptable for use by designers, administrators, and facility managers. [5, 6, 7].

The next study highlights that the lack of a clear definition for Post-Occupancy Evaluation (POE) hinders its recognition and weakens the development of a strong evidence base. It also calls for comprehensive evaluation frameworks that address building performance and sustainability more broadly than just energy efficiency [8].

The study compares POE surveys of three schools with different spatial designs to generate insights for improving future school building design and to be a reference for architects and practitioners [9]. While in other paper, occupants were generally satisfied with building performance, but concerns arose around ventilation, lighting, thermostat control, and privacy. The study emphasizes that smart technologies improve comfort only when well-chosen and maintained, highlighting POE as essential for aligning smart building design with user needs [10]. The design of learning environments plays a crucial role in shaping educational experiences. The study identified ten performance criteria addressing functionality, comfort, spatial organization, technology, and user satisfaction. The framework supports user-centered design to enhance student learning and guide facilities management in improving studio layouts and educational outcomes. These findings highlight the importance of aligning physical space with pedagogical goals to maximize effectiveness [11].

The design and configuration of learning environments are increasingly recognized as critical factors influencing educational quality and student outcomes. The paper highlights the use of Post-Occupancy Evaluation (POE) in architectural practice and education to support evidence-based design, outlining methods for teaching and conducting POE and emphasizing its value for professional practice, pedagogy, and institutional knowledge [12].

The paper starts with providing a background status on the benefits, uses, and methods and techniques of POE in general and for educational facility in particular. The paper then presents the proposed criteria for the POE and the implementation of its assessment, starting with Technical Part, which include: base plan analysis and walk through observations, then Occupant Perception which include: questionnaire development, design – based modifications. Finally, the paper ends with a conclusion and a plan for future work.

## 2. BENEFITS AND USES OF POES

During the development of any project, the value delivery is the key goal of all stakeholders. [13] defined value as “the trade-off between what each stakeholder gets and what they have to give up”. All participants in the building delivery process should have a clear understanding of what type and level of performance should be achieved in a facility [14]. After the delivery of the facility and its occupancy by the target users, facility managers can utilize the POE as a diagnostic tool to identify and evaluate the critical aspects of building performance systematically. By comparing the performance criteria with the actual measures on ground, the outcomes of POE can benefit facility managers to maintain and improve their facilities and can also be documented as lesson learned with direct input into the next building cycle.

Figure 1 illustrates the performance concept in the building delivery process as well as the basic outcomes of post occupancy evaluations from short- medium and long-term perspectives. Several benefits can be obtained from performing POE. [15] categorized the uses and benefits of POE into short, medium, and long term. While the short term refers to immediate action; medium term includes 3 to 5 years' time frame, which is necessary for the development of new construction projects; and the long- term time frame is ranging from 10 to 25 years, which is necessary for strategic planning, budgeting, and master planning of similar facilities

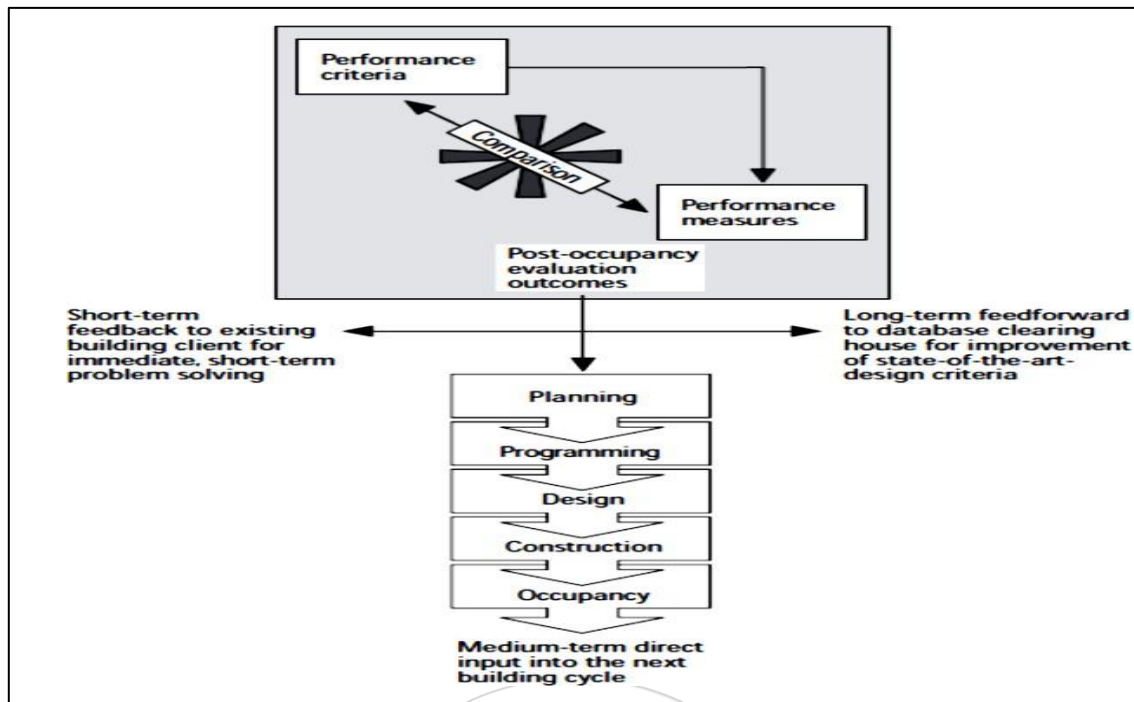


Figure 1. The performance concept in the building delivery process [14]

In more details, the short-term benefits include the following.

- 1) Identification of possible solutions to problems in the facilities, responding to building user needs and values.
- 2) Improving space utilization and obtaining feedback on the building performance.
- 3) Improving the attitudes of building occupants through active involvement in the evaluation process.

The medium-term benefits include:

- 1) Built-in capacity for facility adaptation to organizational change and growth over time, including recycling of facilities into new uses.
- 2) Significant cost savings in the building process and throughout the life cycle of a building.
- 3) Accountability for building performance by design professionals and owners.

While, the long-term benefits include:

- 1) Long-term improvements in building performance.
- 2) Improvement of design databases, standards, criteria, and guidance literature.
- 3) Improved measurement of building performance through quantification via improvements in the programming and planning of buildings. [15] and other researchers [3, 16 – 19] recounted in their research work almost the same benefits that was discussed earlier, including: recommendations that are brought back to the client; re-modeling that is done to correct problems; lessons learned that influence design criteria for future buildings; and finally, positive influence upon the delivery of humane and appropriate environments for people.

### 3. TYPES, TECHNIQUES, AND METHODOLOGIES OF POST OCCUPANCY EVALUATION

According to [18], there are numerous approaches to the concept of POE with a wide variety of methodologies that have been developed in order to address the specific conducting POE. When reviewing the different methodologies of POE, it is important to refer to the research work in [20-11]; where the authors discussed the common strategies and techniques of POE. They described realism as the original of all techniques and methods used in POE's research. Referring to [14] and [2], POEs are traditionally conducted using questionnaire, interviews, site analysis, and observations of building users. Over time, more specific processes, levels of survey, and new technologies have been developed to better-fit stakeholder's objectives and budget. Currently, there are numerous methods and approaches to POE, depending on the contextual agenda and the required outcomes. In reviewing the research work of [3,15, 16, 21], the POE can be analyzing and arrange into three levels of typical process, defined as:

**Indicative Post Occupancy Evaluation:** This provides an indication of the major strengths and weaknesses of a particular building's performance.

**Diagnostic Post Occupancy Evaluation:** where the evaluation criteria are either explicitly stated in the functional program of a facility or have to be compiled from guidelines, performance standards, and published literature on a given building type.

**Investigative Post Occupancy Evaluation:** in this level, it correlates physical environmental measures with subjective occupants' response measures, see figure 2 for details.

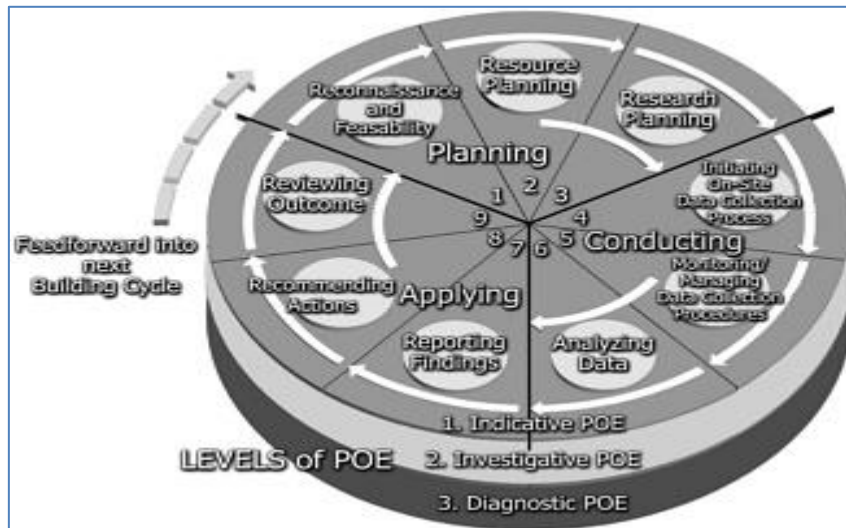


Figure 2. POE evolving performance criteria [15]

### 3.1 The Pros and Cons of POE

One of the characteristics of POE activities is the discrepancy that exists between the reasons for doing POE and the difficulty of doing them. The possible benefits of doing POE are discussed in [22]. The author stated that POE is a useful tool for improving buildings, increasing occupants' comfort, and managing costs, while the barriers to widespread adoption of POE are cost, defending professional territory, time, and skills needed. According to [21], one of the problems of the POE is the ownership. There are benefits to both the client and the designer, but who should pay for it? Customers/clients may view their payment for the building as including any testing that needs to be undertaken to ensure everything is working in order.

In contrast, the project design team will not want to utilize all their profits by paying for an evaluation, as POE is not part of standard procurement procedures, there is little incentive for the designer to differ from the standard approach. Despite the increasing climate for POE to work, there is still a reluctance to engage in any form of systematic evaluation process of those involved in the design and construction industry. It is likely that many clients and designers have not heard of POE yet. As a result, the benefits of POE cannot be achieved and this will lead to future problems when using the facility [21]. Barriers to widespread adoption of POE were discussed in [2]. The first identified obstacle is the cost, as discussed earlier, while the second barrier is professional territory that is necessary for POE to be seen as useful for remote knowledge. Finally, skills, where there are no specific skills or technique or even tools with POE studies which can lead to other problems when evaluating the buildings performance. The Use of POE for Educational Buildings Reviewing literature, several research projects investigated POE in educational building particularly in schools. Two case studies of educational buildings were reviewed and analyzed in details to discuss how they were implemented; understand the objectives of the POE process; describe the techniques and methods used; and finally, to illustrate the findings and lessons learned, the summary of those four cases is described in the coming paragraphs. The First case study was conducted in the UK. The aim of this study was to describe the development of evidence based for establishing the best conditions for optimal learning spaces. The study was implemented at five diversified primary schools in the UK.

The POE methodologies used in this study consist of: first, a questionnaire survey which was used for gathering the information in regard to interviewees' views. The goal of this survey was to gain an understanding of people's experience and perception of the schools. Secondly, interview sessions, with head teachers to explore in more depth, the complex feelings, beliefs and attitudes surrounding the questionnaire responses. Finally, workshops and site observations were conducted with team members involved in the process to communicate and refine the outputs of the study. This multi-POE work, with its comparative study between many schools, provided

opportunities for the principals and head teachers of schools and local authorities to understand the current performance of school spaces which resulted in routine feedback into the briefing, design, construction stages [23].

The second case study was implemented in Saudi Arabia. Its POE method was developed in order to evaluate three primary schools. The toolkit used in this research aimed to position the children, teachers and parents who use the school. This method identified weaknesses in the three schools and differences in response from the three groups consulted. The POE was implemented in three stages, first stage commenced with a familiarization of the three schools, through guided tours, conducting interviews with teachers, and walk through observation. Second stage included the design checklists, to assess the presence and adequacy of different educational facility design features. Finally, the third stage, the POE questionnaire survey, which was conducted with teachers, students and parents. The analysis of responses revealed that the parents agreed with teachers that the building was aesthetically pleasing, age appropriate, spacious, and had good circulation, with clear and visible signage that was easy to follow.

The parents also felt that the building was well landscaped, with (adequate) lighting and ventilation. However, students' results focused on the weaknesses of some facilities' spaces and how it hindered their ability to learn. They were dissatisfied with their cafe, rating this as being unattractive place to eat which was echoed in the POE results of the teachers as well, students were also dissatisfied with the restroom facilities [24].

### 3.2. Criteria for Post Occupancy Evaluation of the School Facility

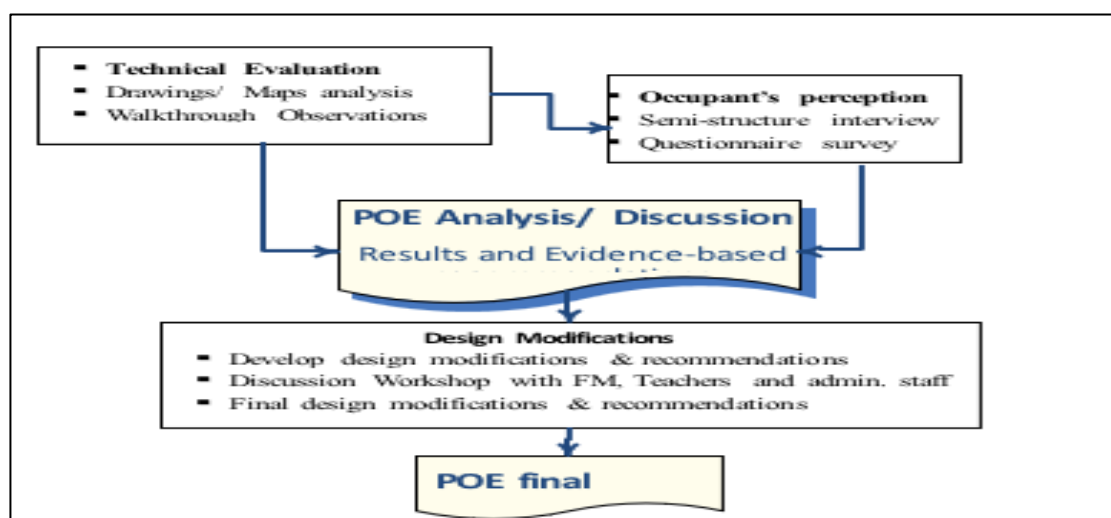


Figure 3. Illustration of the proposed POE criteria

The aim of the presented research in this paper is to test whether the selected school and its spaces provide students, teachers and staff with spaces that fulfil their needs, and enable them to perform their work effectively during the different educational activities performed. The proposed POE criteria have two main parts: 1) Technical evaluation and 2) Occupants' perception. The first part, the technical evaluation, involves the analysis of existing base plans and available documentation's; and a Walk-through observational technique to investigate the possible POE problems/issues and take photos and measurements, if needed. In the second part, to obtain occupants' perception for facility performance; a semi structure interviews/group meeting, with teachers and staff, is proposed to investigate possible problem/issues. Based on the previous step. A questionnaire survey will be developed and conducted to quantitatively measure the perception of students and teachers in regard to observed problems and issues in previous steps Following that, a proposal for design modifications and recommendations to improve facility performance will be developed and discussed with school principal and the administration staff members. Final design modifications & recommendations will be then conducted. The implementation of the first part of the POE criteria, i.e. the technical evaluation is described in the following sections.

## 4. THE IMPLEMENTATION OF POST OCCUPANCY EVALUATION CRITERIA: THE TECHNICAL PART

### 4.1. Base Plans Analysis:

The selected case study that was examined in this research project is a private school, located in the city of Sharjah, UAE, where it's inaugurated and occupancy began on September 2010. The school is owned and operated within the private sector. Its initial construction cost was approximately 20,000,000 AED. The ministry of education subdivided the school grades in to 3 categories: primary, elementary, and the secondary levels. A primary level begins at grade one until grade six, while the elementary level incorporates grade seven to grade nine, and the secondary level commences from grade ten till grade twelve. The total student capacity is 375 students at the primary level, 200 students at the elementary level, and 100 students at the secondary level. The main aim of this research

is to investigate the effectiveness of the school facilities. Furthermore, the research was intended to identify any gaps or inefficiencies in the design and to make recommendations for future new schools' improvements.

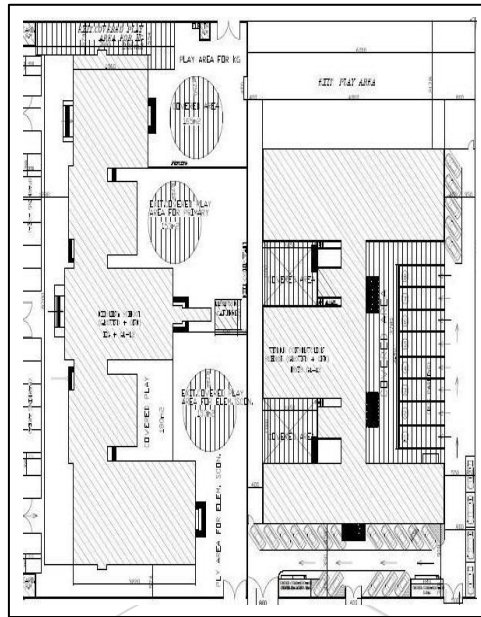


Figure 4. School layout

This evaluation covered the following areas of the school building:

- Spaces functionality, including Safety and security.
- Physical environment (lighting, cooling, air quality, etc.)
- Occupants' control which aims to measure the degree of ease with which the end users are able to control elements such as the AC's system, lighting system, and the spaces used in the school.

Document analysis is the method for POE implementation, which includes investigating and analyzing, archiving, drawings, maps, and specifications. Figure 4 illustrates the layout plan for the selected school. The analysis of the school site plan revealed the following issues:

- ❖ The school has only one main entrance which creates a gender conflict, and cause disorganization and congestion.
- ❖ The buses parking area has time tabled for the use of the school buses and the same area is the students' congregation point.
- ❖ The playing and open area in the north side looks small and insufficient for the 700+ student.

The analysis of the school ground and first floor plan, illustrated in figures 5 and 6, revealed the following issues:

- Corridors of different school zones are directly connected, without any doors, which result in congestion between the senior and junior students, who are younger and are more vulnerable
- Inadequate number of toilet facilities for the students. In addition, the European WC type is missing, which is crucial for some students, especially those with special needs.
- Music room is located between the classrooms, with low sound insulation treatment, which cause noise and create distraction.
- Activity room is located in-between the classrooms causing problems by the noise of the performed activities.

- All labs are located in the first floor, which are a source of possible hazard and cause congestion in using corridors and stairs

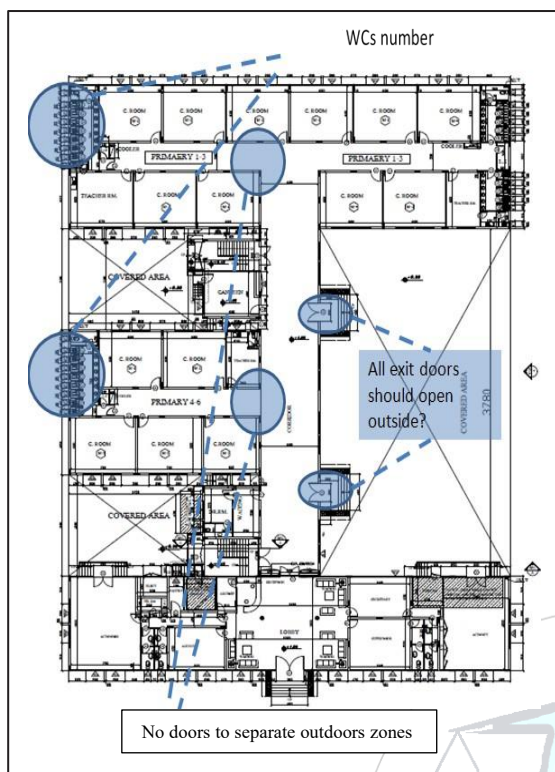


Figure 5. Ground floor plan

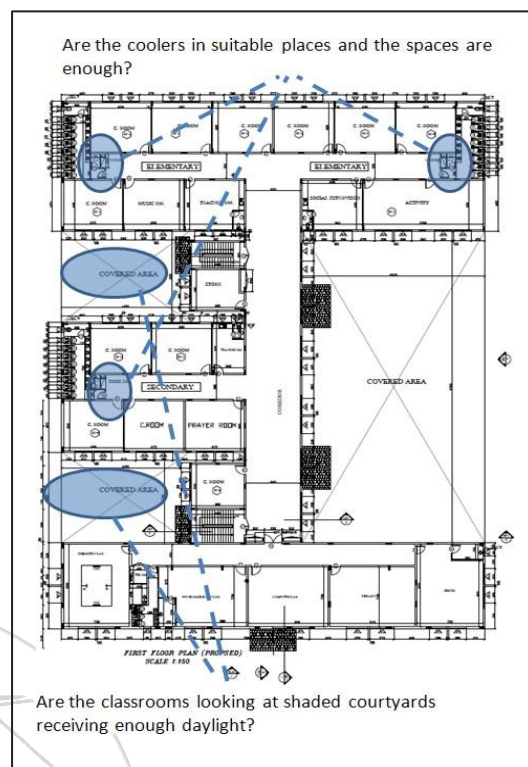


Figure 6. First floor plan

**4.2. Walk Through Observations** Walk through observations were conducted for several days to investigate and evaluate a potential issues and shortcomings in the school buildings and its site layout. It was recorded using a note pad and a digital camera. Several photographs were taken during the walkthrough observations during the tour accompanied by the facility manager. Table I illustrates the anticipated problems that were observed during the walk through.

Table I. The Walk Through Observations

	
<p>The activity room was transferred into an office area, causing a lack of space for students' different activities</p>	<p>The old built-in water coolers were replaced, with temporary Ones</p>
	
<p>The passage to the lavatory area is narrow and the space within the maneuvering and movements of vehicles.</p>	<p>Only one gate is available for vehicles entrance and exit, another gate is needed to ease</p>
	
<p>Students' assembly area is used in the same time for buses parking.</p>	<p>A wooden step was built to help children to reach the wash basins</p>

## 5. THE IMPLEMENTATION OF THE QUESTIONNAIRE

To facilitate effective research methods, a questionnaire was compiled and distributed to various students' samples in the selected private School. The survey was part of a primary research exercise to understand more about the field opinions. Furthermore, the questionnaire was a key component of this project, as it provides the foundation for recommendations with respect to the views of the occupants in the private schools in Sharjah, Dubai and Northern Emirates. The aim of this questionnaire was to investigate the effectiveness of future school facilities and the impact of the school's enhancement on the learning objectives of private schools. Furthermore, the research was intended to identify any gaps or inefficiencies in the design and to make recommendations for improvements for future school developments.

The first part of the questionnaire assesses the effectiveness of school building in light of different categories, i.e. functionality, learning environment comfort (lighting, cooling, noise, air quality, etc.), and occupants' control which aimed to measure the degree of how easily the final occupants could control facility elements such as the AC's system, the lighting system, the spaces used within the school, and the safety within the school building.

The second part of questionnaire focuses on the availability of open areas and play yards, green areas access to school, movement, and approach to school.

The third part of the questionnaire focused on safety and security in the school. There were 8 statements assessing the safety measure in the school facilities, such as indoor and outdoor circulation, firefighting system, emergency exits, and the free flow of movement when transitioning between spaces.

The fourth part of the questionnaire focuses on the learning environment comfort. It assesses the day-light, air quality and sound isolation between classroom and other facilities.

The fifth part of the questionnaire discusses the interior quality. And evaluates the proper use of the interior furniture and finishing materials for the floors and walls, this part highlighted 7 positive statements.

And the following part of questionnaire assesses the access and approach to school, including ease movement inside and around the school, and the availability parking for cars and buses. Finally .The last section of questionnaire discusses and evaluates the aesthetic and architectural appearance in the school. It is focuses on the external view of the school, landscape, and the aesthetic appeal of the main entrances.

**5.1 The Sample Characteristics:**

The questionnaire was distributed to the respondents, as shown below in table II and figure 7. A total of 295 students and 50 employees were invited to join this research project.

To ensure that the questionnaire was well distributed and the respondents understood it, and the questions were properly answered, the researchers visited the school several times.

The questionnaire was distributed to the elementary and secondary students from grades 6-12. The statements were explained to each student. The researchers conducting the investigation had a meeting with the teachers in the teacher’s room and met with the employees in the principal’s meeting room. The purpose of the explanation was to make it easier for them to understand the details of the questionnaire to gather more accurate data.

The respondents included 277 students, 36 teachers, and the administration staff. The valid questionnaire used for statistical analysis amounted to 265 for students, which represented about 89% of total grades of students in the school, and 36 employees, representing about 72% of the total number of the employees in the school.

*Table II. The respondent’s categories*

Table OF Figures Entries Found	Total Sample	Received Sample	Valid Questionnaire	Percentage OF Valid Respondent
Grades 6,7,8,9,10,11,12	295	277	275	93,2%
Employees	50	36	36	72%
Total	345	313	311	90,1%

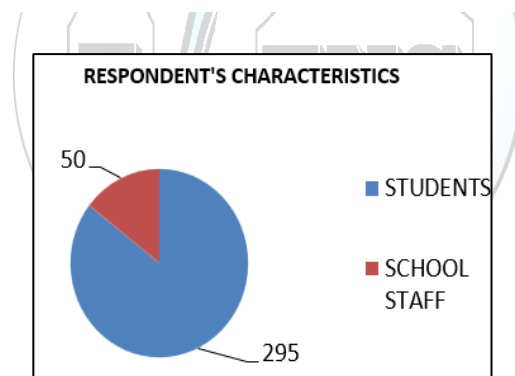


*Figure 7. Respondent’s characteristics*

**5.2 Questionnaire Results and Analysis:**

The questionnaire investigates 6 main categories as the following:

Functionality, safety and approach, security, learning environment comfort, interior quality, access and approach, finally aesthetic and architectural appearance. Table III shows the overall average of respondent’s opinions about all categories.

category related to the comfort of learning environment which scored an average of 3.65, indicating that the employees were satisfied with the amount of natural day light acoustics, lightings, and air quality. Through analyzing the six categories of the questionnaire, it was conducted that the highest average opinion of employees which is (3.77) was for the quality of the interior. It showed their satisfaction regards the flooring and walls finishing materials used. The second category related to the comfort of learning environment which scored an average of 3.65, indicating that the employees were satisfied with the amount of natural day light acoustics, lightings, and air quality.

Table III. Overall average of respondent's opinion for all categories

Category No	Category	Average			
		S	Employee	Students	All
1	Functionality	1.30	3.19	2.4	2.8
2	Safety and Security	1.36	3.17	3.03	3.1
3	Learning Environment Comfort	1.32	3.65	2.7	3.17
4	Interior Quality	1.23	3.77	2.44	2.81
5	Access and Approach	1.24	2.41	2.44	2.33
6	Aesthetic and Architectural Appearance	1.17	2.71	2.25	2.48
Total		1.27	3.15	2.54	2.78

The next two categories review the functionality, safety and security in the school and averaged 3.19 and 3.17 respectively.

The next category reviewed the aesthetic and architectural appearance with the respondents' average being 2.71, a little under the midpoint. It revealed a less than favorable response from employees, indicating that some modifications in the redesign process were required. This category showed an agreement between the questionnaire respondents and the interview respondents.

The final category was in regards to the ease of access and approach to the school. This category only got an average of 2.41, which was near to disagree on the scale provided on the questionnaire. It indicated that the teachers and staff were dissatisfied, and the access and approach to the school required major modifications in order to find a suitable solution to the problem of access to the school.

Through the analysis of the same six categories, it was found that the highest average opinion of student's improvements for school design would be beneficial. The next category concerned the learning environment and its general comfort with average score of 2.70. This was lower than the midpoint and showed less agreement over the day light, acoustics, lighting, and air-conditioning, requiring some minor improvements in this category. The third, fourth, and fifth categories reviewed the interior quality, access and approach to the school, and its functionality, with averages of 2.44, 2.44, and 2.40 respectively. These three categories gave a less than neutral response, which indicates a consensus from the respondents to these three categories. It revealed that there is a need to make some modifications to the design to improve the use of clinic and cafeteria spaces. The questionnaire results agreed with the respondents' opinions from the initial interview survey. In addition to this, there is a need to enhance and develop the accessibility to school redesigning the setting layout plan. This was also noted in the interviewers complains and was observed by the researcher during the walk-through survey of the school facilities. The findings revealed that the highest average for all respondents in the school was 3.1, which related to the learning environment comfort. This is a slightly over the midpoint. It indicates that there is some consensus from all respondents regarding this category, proving it to be to some degree, satisfactory. The safety and security category had the second largest average with a score of 3.10. This category gained approximately the same result as the first one, which is little over neutral. The next two categories related to the interior quality and functionality of the building with total average of all respondents of 2.81 and 2.80 respectively. These results were close to neutral showing less consensus to the previous category, and therefore would require some minor modifications to be carried out to and improve the learning environment, which was also echoed in the interviewees complains documented at the beginning of this paper. The aesthetic and architectural appearance category scored a very low average of 2.48, much less than midpoint, but still above unsatisfactory. It showed an agreement between all respondents. This category recommended further modifications in the redesign of the external facades. The last and lowest average for all respondents was 2.33 in regards to the access and approach to the building, which is still above unsatisfactory, but much lower than midpoint. It revealed that there was a big consensus between all respondents indicating that this category needs significant modifications to the redesign of the setting layout plan in order to find suitable solutions for the issues of accessibility to school. This matched the observation made by the researchers during a walk-through survey, and agreed with the complaints raised by interviewees during the interview. The final average for all six categories was 2.78. This is a little under neutral. It revealed a general consensus and agreed with the complaints that were made during the interview stage of this process.



### 6.2. Zoning Between Students' Categories:

Based on the researcher's explanation of the zoning process separating the varying age levels of students during the walk through and interview process, the consensus of the teachers and staff who participated in the questionnaire, was that they all agreed that the zoning and partitioning between students divisions will result in greater privacy in each zone, and keep the noise levels at a minimum, and would keep the younger students safe and away from the older students. The researchers proposed a partition wall and door be constructed in each zone on the ground floor for this purpose, as shown in figure 9.

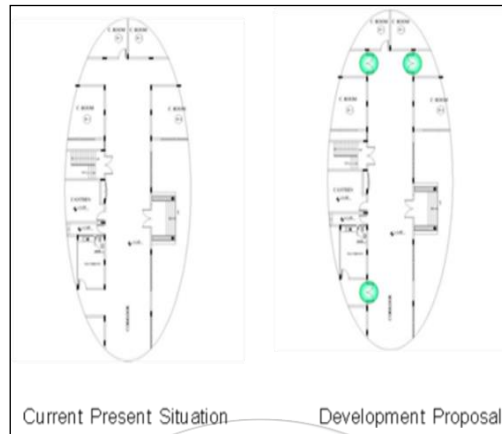


Figure 9. Proposed partitions and doors (zoning)

### 6.3. Lift for Special Needs Students:

This problem was also flagged during the walk through of the school facilities. Most students agreed that the school needs at least one elevator to serve the special needs students and teachers. It would also help in the transportation of goods and materials to the first floor. Therefore, the researchers proposed the installation of an elevator near the students' entrance and administration area, which would serve both students and staff, in addition to any guests of the school.

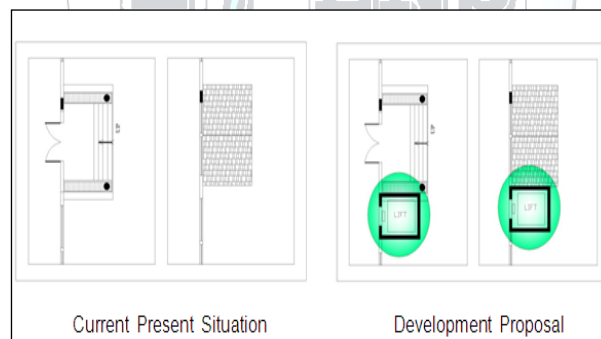


Figure 10. Additional lift to serve special needs students' ease and help transportation the goods

### 6.4. Cafeteria and Dining Spaces for Students:

There was a general consensus from the questionnaires and interviews with the teachers and administration staff; they all agreed that the cafeteria space is too small and not suitable to serve the student body and staff. It is proposed to use an open shaded area behind the cafeteria as a dining and relaxing area, see figure 11.

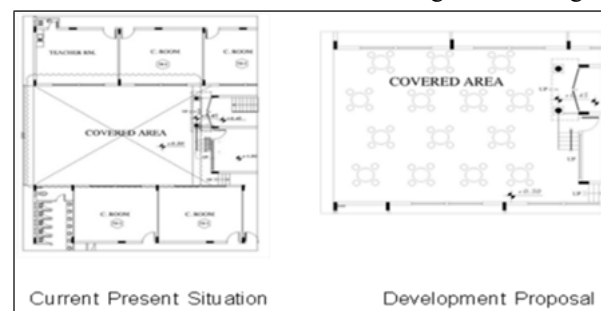


Figure 11. Use open-shaded areas behind the cafeteria as open area for dining and resting

### 6.5. Emergency Stairs for Labs Spaces:

Base on the data collected during the internal walk-through of the building, the information collected from the questionnaire and the inspection report from the civil defense inspector it was cleaned that the issues raised required urgent and immediate attention. After reviewing the blueprints of the school, it was recommended that 2 additional emergency steel stair well be added to each end of the laboratory corridor in the event of a fire; this would ease the evacuation, see figure 12.

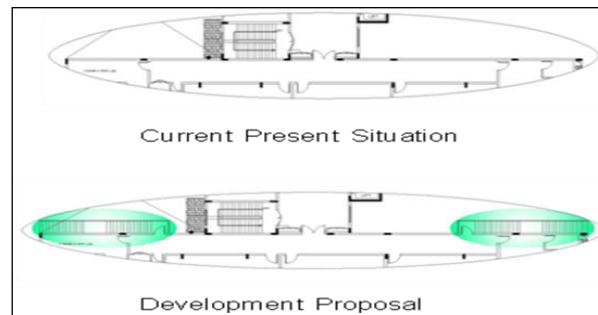


Figure 12. Additional steel stairs

### 6.6. European Lavatories for Students:

The researchers encountered this problem during their observation walk inside the school. In the questionnaire, there was a consensus of opinion from the students concerning this as well as in issue, the teacher's responses during the interview process. The researcher's therefore proposed to make minor modifications to the existing lavatories which all are of Asian design. They proposed to change 25% percent of the lavatory units from the Asian model to a European model, which would satisfy students offering greater comfort when using lavatories.

**6.7 Aesthetic and Architectural Facades:** In reference to the questionnaire results, it was found that most of the students' responses concerning this issue were same, a consensus from both students and staffs regarding this issue. Their opinions were supported by the results gained during the interview process with the employees, and the researcher's opinion gathered after a walk-through survey. It shows that the school views were very traditional style. The researchers proposed modification and the redesign the facades. The improved design for school facades was a modern style using the latest cladding material, (Aluminum composite panels), which would add to school modern, state of the art look. It would also fit more comfortably with the architectural appearance of the surrounding community. See figure 13.



Figure 13 .Old and the new look of the school after modification

## 7. CONCLUSIONS AND RECOMMENDATIONS

### 7.1 Recommendations for the Existing School Building:

#### 7.1.1 Short term recommendations:

1. Availability of at least one more exit gate for vehicles (especially buses) from rear of the school. This will facilitate the movement of traffic inside the compound wall of the school.
2. Installing zoning between student's levels (categories) by creating partitions with doors to separate each zone. This will keep younger students safe and avoid accidents and injuries.
3. It is vital to ensure that the cafeteria space is increased through use the open covered area adjacent to it, as a dining area with tables and chairs for all students and employees. This will achieve a more strangled

environment for its users.

4. The availability of one elevator for the special needs students, and for transporting goods, books, and other materials to the first floor would be advantageous.
5. Enhance the external appearance of the school by fixing modern aluminum composite paneled cladding to the front aspect of the building and students' entrance. This will achieve the required architectural appearance to the school.

### **7.1.2 Long term recommendations:**

- 1) The school requires a larger area which allows designers to present a unique and comprehensive design such as adequate recreational areas, a covered swimming pool a mosque, additional parking areas, and an adequate number of gates
- 2) School zoning is required, separating the students' categories; separate buildings to house 3) each age group would be preferable.
- 3) Each school should ensure that there is an ample car parking space for employees, visitors, and the service sector and buses.

## **7.2 Conclusions**

POE has a wide variety of methodologies that vary in nature, size, and level of interaction. Decisions regarding POE use need to consider the purpose of the study or the organizational benefits that can be derived from the results of POE. By using the POE, several benefits can be gained such as: improved space utilization and feedback on the building performance; recommendations that are brought back to the client; lessons learned that influence design criteria for future buildings; and finally, positive influence upon the delivery of humane and appropriate environments for people. This paper presents a completed research study that developed and implemented criteria for a Post-Occupancy Evaluation (POE) of a private school facility in Sharjah, UAE, with the aim of assessing its overall performance based on users' satisfaction and experiences. The POE criteria encompass two main components: technical evaluation and occupants' perceptions. The technical evaluation involved analyzing existing base drawings and documentation, along with a walk-through observational technique, which provided a closer investigation of the facility and highlighted aspects of interior design requiring further consideration. This assessment revealed functional shortcomings, such as the limited size of the cafeteria and the need for an additional dining area to accommodate both students and staff. The second component examined occupants' perceptions of the facility's performance. Semi-structured interviews and group meetings were conducted with teachers and administrative staff to identify issues and gather further insights into space usability. Based on these findings, a questionnaire survey was designed and administered to systematically measure users' perceptions. The results of both the technical evaluation and user feedback informed a set of proposed design modifications and recommendations aimed at improving the functionality, efficiency, and overall quality of the school environment.

## **ACKNOWLEDGMENT**

The authors would like to thank Dubai and Northern Emirates Education Council, and the principal of the investigated school and all employees, including teachers and the facility manager for their cooperation during the data collection and implementation stages of this research project.

## **REFERENCES**

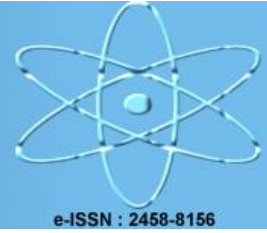
- [1] C.F.F, Overview: A Summary of Finding, in *Learning from Our Buildings : A State-of-the-Practice Summary of Post- Occupancy Evaluation*, C.F.F, Editor 2001, National Academies Press: Washington, DC, USA. p. 9-15.
  - [2] Council, F.F., *Learning from Our Buildings : A State-of- the-Practice Summary of Post-Occupancy Evaluation* 2001, Washington, DC, USA: National Academies Press.
  - [3] Preiser, W.F.E., Continuous quality improvement through post-occupancy evaluation feedback *Journal of Corporate Real Estate*, 2002. 5(1): p. 42 - 56.
  - [4] C.J. Roberts, David John Edwards, M. Reza Hosseini, Monica Mateo-Garcia, De-Graft Owusu-Manu; Post-occupancy evaluation: a review of literature. *Engineering, Construction and Architectural Management* 4 September 2019; 26 (9): 2084–2106. <https://doi.org/10.1108/ECAM-09-2018-0390>
  - [5] Hassanain, M. A., & Iftikhar, A. (2015). Framework model for post-occupancy evaluation of school facilities. *Structural Survey*, 33(4/5), 322-336.
  - [6] Ahmed, W., & Hassanain, M. A. (2020). Post-occupancy evaluation of a university shopping mall facility. *Architecture, Civil Engineering, Environment*, 13(2), 5-15.
- European Journal of Engineering and Natural Sciences

- [7] Etudaiye, A. E., Ahmed, W., & Sada, B. M. (2024). Post-occupancy evaluation of design quality in higher education: A case study of TETFUND buildings in the Federal Polytechnic, Damaturu. *FANE-FANE INTERNATIONAL MULTIDISCIPLINARY JOURNAL*, 8(1, June), 112-124.
- [8] Hay, R., Samuel, F., Watson, K. J., & Bradbury, S. (2017). Post-occupancy evaluation in architecture: experiences and perspectives from UK practice. *Building Research & Information*, 46(6), 698–710. <https://doi.org/10.1080/09613218.2017.1314692>
- [9] Dundar, M. (2016). Post-occupancy evaluations in architectural programming process: a case study of educational buildings. Nishinomiya: Bahcesehir University, Mukogawa Women's University.
- [10] Hassanain, M. A., Sanni-Anibire, M. O., & Mahmoud, A. S. (2024). An assessment of users' satisfaction with a smart building on university campus through post-occupancy evaluation. *Journal of Engineering, Design and Technology*, 22(4), 1119-1135.
- [11] Ezz, M. S., Mahdy, M. A. F., Baharetha, S., Hassanain, M. A., & Gomaa, M. M. (2025). Post occupancy evaluation of architectural design studio facilities. *Frontiers in Built Environment*, 11, 1549313.
- [12] Cranz, G., Morhayim, L., Lindsay, G., & Sagan, J. (2021). Post occupancy evaluation in architectural education and practice. *Technology| Architecture+ Design*, 5(1), 25-30.
- [13] Austin, S.A. Principales of Managing Value in Design. 2005 [cited 2011 10 October]; Available from: <http://www.valueindesign.com/principles/principles.html>.
- [14]
- [15] Preiser, W.F.E., Post-occupancy evaluation: how to make buildings work better *Facilities*, 1995. 13(11): p. 19 - 28. Preiser, W.F.E., The Evolution of Post- Occupancy Evaluation: Toward Building Performance and Universal Design Evaluation, in *Learning from Our Buildings : A State-of-the- Practice Summary of Post-Occupancy Evaluation*, C.F. F., Editor 2001, National Academies Press: Washington, DC, USA.
- [16] Preiser, W.F.E., *Building Performance Assessment—From POE to BPE, A Personal Perspective. Architectural Science Review*, 2005. 48(3): p. 201-204.
- [17] Whyte, J. and D.M. Gann, Closing the loop between design and use: post-occupancy evaluation. *Building Research & Information*, 2001. 29(6): p. 460-462.
- [18] Hadjri, K. and C. Crozier, Post-occupancy evaluation: purpose, benefits and barriers *Facilities*, 2009. 27(1/2): p21 - 33.
- [19] Zimring, C., Post-occupancy evaluation - issues and implementation, in *Handbook of Environmental Psychology*, R.B.B. Arza Churchman, Editor 2002, John Wiley & Sons: New York, USA. p. 306 - 319.
- [20] Zimring, C.M., Wineman, J.D., & Carpman, J.R The new demand- driven post-occupancy evaluation. *Journal of Architecture and Planning Research*, 1988(5/4): p. 273-283.
- [21] Brooks, S.T. and G. Viccars, The development of robust methods of post occupancy evaluation. *Facilities*, 2006. 24(5/6): p. 177 - 196.
- [22] Vischer, J., Post-Occupancy Evaluation: A Multifaceted Tool for Building Improvement, in *Learning from Our Buildings : A State-of- the-Practice Summary of Post-Occupancy Evaluation*, C.F. F., Editor 2001, National Academies Press: Washington, DC, USA.
- [23] Zhang, Y. and P. Barrett, Findings from a post-occupancy evaluation in the UK primary schools sector. *Facilities*, 2010. 28(13/14): p. 641-656.
- [24] Omari, S. and A. Woodcock, Post occupancy evaluation of primary schools in Saudi Arabia. *Work*, 2012. 41: p. 881-887.
- [25] Uline, C.L., et al., Improving the quality of school facilities through building performance assessment. *Journal of Educational Administration*, 2009. 47(3): p. 350-367.



# EJENS

European Journal of Engineering and Natural Sciences



e-ISSN : 2458-8156

## Awareness and Behavior Analysis of Personal Protective Equipment (PPE) Use in Clinical Settings: A Study from an Occupational Safety Perspective

**Prof.Dr.Ayşe Arıcı**

*International Vision University, Faculty of Engineering and Architecture, Department of civil Engineering, Gostivar, North Macedonia,*

*\*email:aysearici.iut@gmail.com*

### Abstract

This study analyzes the awareness, behavior, and attitudes of healthcare workers working in clinical settings toward the use of personal protective equipment (PPE) from an occupational safety perspective. The study, conducted with a mixed methods (quantitative and qualitative) research design, included 372 healthcare workers working in six different hospitals in Antalya, Turkey. Quantitative findings revealed that 92% of workers were aware of the importance of PPE, but only 58% used the equipment regularly. This result suggests a significant behavioral gap between awareness and behavior ( $r = 0.42, p < 0.01$ ).

Qualitative analyses revealed that the primary factors determining sustainable behavior in PPE use are organizational support, managerial exemplary behavior, ergonomic comfort, and psychosocial well-being. The loss of comfort associated with prolonged PPE use, particularly in hot and humid climates, negatively impacts behavioral continuity. Furthermore, increased emotional exhaustion and stress significantly reduce PPE compliance.

The research demonstrates that safe behavior should be supported not only by individual awareness but also by organizational culture, leadership style, and technological monitoring systems. The results suggest that integrating ergonomic design, digital monitoring systems, and psychosocial support programs will play a critical role in building a sustainable safety culture in the future of clinical safety.

### Key words

Personal Protective Equipment, Occupational Safety, Awareness, Behavioral Adaptation, Clinical Environments, Ergonomics, Psychosocial Factors

### INTRODUCTION

The healthcare sector is inherently a high-risk workplace, directly impacting human health and offering little tolerance for error. Healthcare professionals working in clinical settings face a wide range of hazards, including biological agents, chemicals, and physical and ergonomic factors. The use of personal protective equipment (PPE) is considered one of the most critical components of occupational safety management systems in preventing these risks. However, the effectiveness of PPE is not only related to its physical presence; it is also directly related to

employee awareness, behavioral consistency, and organizational safety culture (Galanis et al., 2021; Seah et al., 2025).

Personal protective equipment (PPE) is a personal protective device that reduces the likelihood of an employee being exposed to hazards. The European Occupational Safety and Health Agency (EU-OSHA, 2022) defines this equipment as "individual protective elements that reduce employee exposure to risks and promote safe working conditions." Similarly, the American Occupational Safety and Health Agency (OSHA, 2023) considers PPE (Personal Protective Equipment) not only a physical barrier but also a behavioral link in the risk management chain. In this context, the correct, regular, and conscious use of PPE not only protects employee health but also becomes a key determinant of business continuity, corporate productivity, and professional confidence.

However, numerous studies have shown that although healthcare workers have high levels of knowledge regarding PPE use, their behavioral consistency remains limited (Cordeiro et al., 2022; Khoshakhlagh et al., 2024). This is due to inadequate training continuity, ergonomic challenges, lack of managerial support, and behavioral negligence due to workload. Indeed, observational studies in clinical settings have revealed that while workers are diligent about PPE use at certain times, there are significant decreases in the sustainability of this behavior (Atasoy et al., 2024).

According to behavioral safety theories, employees' propensity to use safety equipment is influenced not only by their personal knowledge or awareness levels but also by organizational norms, leadership style, and group behavioral patterns (Clarke, 2023). A culture of safe behavior in healthcare institutions develops through the coordination of training, leadership, supervision, and participatory communication processes. However, this culture is particularly difficult to sustainably establish in high-stress clinical environments such as public hospitals and intensive care units. A significant portion of inconsistencies in PPE use stem from systemic flaws rather than individual negligence.

The COVID-19 pandemic has been the most visible period in which these dynamics have become apparent. During the pandemic, healthcare workers were forced to wear equipment such as masks, visors, gloves, and coveralls for long hours, causing physical discomfort, fatigue, skin problems, and psychological stress (Galanis et al., 2021). This process has demonstrated that PPE use should be reevaluated not only for protection but also for comfort, ergonomics, and durability. Negative emotional reactions that workers develop towards equipment directly impact their continued use and correct use (Seah et al., 2025).

In the clinical safety literature, factors affecting PPE compliance are generally classified into three categories: individual factors, organizational factors, and environmental factors.

- Individual factors include the employee's level of knowledge, risk perception, educational background, and safety motivation.
- Organizational factors include leadership support, inspection frequency, equipment supply, and the organization's safety culture.
- Environmental factors are external factors such as material ergonomics, weather conditions, work intensity, and physical working conditions.

The imbalance between these three factors leads to behavioral inconsistencies in PPE use (Clarke, 2023; Giao et al., 2020). In this context, establishing a sustainable occupational safety culture in clinical settings is possible not only by providing protective equipment but also through a multilayered approach that integrates the principles of behavioral science, industrial engineering, and ergonomics. Understanding healthcare workers' attitudes toward PPE is strategically important not only for occupational safety but also for service quality and patient safety. Improper use of PPE puts not only the worker, but also the patient, and even public health at risk. The World Health Organization (WHO, 2022) has stated that the risk of infection transmission in healthcare workers is directly linked to behavioral errors related to PPE use. This finding demonstrates that PPE serves not only as an individual safety tool but also as a systemic barrier in protecting public health.

The inadequacy of behavioral analyses regarding PPE use in clinical settings formed the basis of this study. While the existing literature contains numerous quantitative studies measuring PPE use, the "implementation gap" between awareness and behavior is not yet fully understood. To address this gap, this study aims to examine healthcare professionals' awareness levels, behavioral persistence, and organizational factors influencing PPE use with a holistic approach.

The research is structured around three primary objectives:

1. To determine the awareness, knowledge, and behavior levels of healthcare professionals working in clinical settings regarding PPE use;
2. To analyze individual, institutional, and environmental factors influencing PPE use;

### 3. To recommend educational, managerial, and technological strategies to support sustainable PPE use.

To this end, the study was conducted within a Mixed Methods Design framework. Quantitative data reflect measurable awareness and behavioral indicators collected through a survey, while qualitative data reflect healthcare professionals' experiences and perceptions through semi-structured interviews. Thus, by considering the numerical aspects of behavioral safety and its cultural dynamics together, a deeper understanding of clinical safety culture has been developed. The unique contribution of this research is that it addresses PPE use not merely as a technical necessity but as a human behavior-centered safety paradigm. The findings are expected to inform policy recommendations to strengthen safety culture in healthcare institutions, restructure training programs, and ergonomically improve PPE designs. This study aims to make an original and applicable contribution to the clinical applications of occupational safety science by addressing the awareness and behavioral patterns of healthcare workers regarding the use of PPE in a multidimensional manner.

#### *Literature Review*

Personal protective equipment (PPE) is viewed in the modern understanding of occupational safety not only as an individual protection element but also as a behavioral component of a systematic safety culture. The European Agency for Safety and Health at Work (EU-OSHA, 2022) defines PPE as "a personal defense mechanism that reduces worker exposure to hazards," while the US OSHA (2023) considers this equipment the "last line of defense" in combating occupational risks. However, the literature demonstrates that the effectiveness of PPE is determined not only by its availability but also by user awareness, organizational climate, and behavioral consistency.

While PPE use in the healthcare sector provides protection against infection risk, chemical exposure, and physical trauma, improper or incomplete use seriously undermines worker safety (WHO, 2022). A field study by Khoshakhlagh et al. (2024) revealed that a significant portion of healthcare workers do not use PPE correctly, citing managerial pressure, time constraints, and behavioral burnout as the primary reasons, rather than a lack of knowledge. This demonstrates that PPE use is not only an educational process but also an organizational and psychosocial one.

The gap between awareness and behavior is one of the most frequently discussed topics in the clinical safety literature. Most employees are aware of the importance of PPE, but due to intense workloads, ergonomic inadequacy, and comfort issues, this knowledge does not translate into behavior (Giao et al., 2020; Seah et al., 2025). Clarke (2023) calls this the "behavioral gap" and emphasizes that this gap cannot be closed without a strong safety culture and management support. Organizational factors are the primary determinant of PPE compliance. Cordeiro et al. (2022) showed that PPE compliance rates significantly increase in organizations with strong managerial support and oversight mechanisms. Similarly, leadership style also shapes this process; transformational leadership encourages safe behaviors by increasing employee motivation, while authoritarian management styles weaken responsibility (Fernandez et al., 2021).

In addition to individual factors, ergonomic and psychological variables also influence PPE use behavior. Galanis et al. (2021) stated that long-term PPE use causes discomfort such as skin irritation, headaches, and fatigue in employees, leading to behavioral reluctance. Similarly, Kim et al. (2023) reported that PPE use frequency decreases in high-stress environments, while Tuncel and Yildiz (2021) reported that burnout negatively impacts PPE compliance. These findings demonstrate that safe behavior depends not only on knowledge but also on psychosocial balance.

In recent years, technological advances have offered new methods that facilitate behavioral monitoring in PPE use. Artificial intelligence-supported monitoring systems, smart textile products with sensors, and digital safety panels stand out as innovative solutions that encourage the correct use of PPE (Chen et al., 2023). However, the effectiveness of these technologies is directly related to employee acceptance and ethical data use.

The literature generally converges on three main points: First, although awareness levels are high, behavioral continuity is limited; second, organizational leadership and safety culture are the strongest determinants of behavioral compliance; and third, ergonomics and psychosocial conditions are complementary factors determining the sustainability of safe behavior.

In this context, the current study considers PPE use not merely as a technical requirement but as a multilayered interaction between people, organizations, and the environment, and aims to analyze the relationship between behavior, awareness, ergonomics, and organizational climate variables with a holistic approach.

## **2. MATERIALS AND METHODS**

This research aims to examine the awareness and behavioral levels of healthcare professionals working in clinical settings regarding the use of personal protective equipment (PPE), and the individual, organizational, and environmental variables that influence these behaviors, using a holistic approach. The study's methodology is based on a mixed-methods design, combining qualitative and quantitative data collection techniques. This approach allows for the description of not only numerical trends but also participant experiences and perceptual patterns (Creswell & Plano Clark, 2018).

### **2.1. Research Model**

The research was conducted using an explanatory sequential mixed methods design. In this model, general trends and behavioral patterns regarding PPE use were identified in the first stage using quantitative data. In the second stage, the underlying reasons and perceptual dynamics of these findings were analyzed in depth using qualitative data. Thus, a holistic assessment was achieved through qualitative interpretations that added meaning to the quantitative findings.

A structured survey method was used in the quantitative section, and a semi-structured in-depth interview technique was used in the qualitative section. These two data sets were integrated using the principle of "data triangulation."

### **2.2. Research Area and Universe**

The research population consists of healthcare workers working in public and private hospitals in Antalya, a province located in southern Turkey. Antalya was selected due to the region's high patient flow throughout the year, high rate of health tourism, and increased biological risk burden following the pandemic. The region presents a climatic condition where physical comfort becomes a more pronounced problem when using PPE due to high temperatures and humidity.

The population comprised approximately 4,300 healthcare workers; the sample was selected using stratified random sampling. A total of 372 participants from six hospitals, representing different clinical types and professional groups, were included in the study.

### **2.3. Participant Characteristics**

The participant group was 68% female and 32% male. In terms of occupational distribution, 41% were nurses, 27% were doctors, 18% were laboratory technicians, and 14% were auxiliary healthcare personnel. The average age of the participants was 35.4, and their average professional experience was 9 years. This demographic diversity allowed the study to represent diverse occupational safety experiences in the healthcare sector.

### **2.4. Data Collection Tools**

#### ***Survey Form (Quantitative Phase)***

The quantitative data collection tool is a 5-point Likert-type survey developed by the researcher, adapted from scales in the literature (Clarke, 2023; Gao et al., 2020; Khoshakhlagh et al., 2024), and translated into Turkish. The survey consists of three sections:

1. Demographic Information: Gender, age, occupation, length of service, and institution type.
2. Awareness Scale: 10 items, measuring the importance, frequency of use, and knowledge of PPE.
3. Behavior and Attitude Scale: 15 items, assessing PPE use continuity, ergonomics perception, managerial support, and psychosocial stress levels.

For validity analysis, opinions were obtained from five field experts, and the reliability coefficient (Cronbach's  $\alpha$ ) was found to be 0.89.

### ***Interview Form (Qualitative Stage)***

Qualitative data collection was conducted through semi-structured interviews with 20 participants. Interview questions were designed based on themes emerging from the quantitative findings, focusing specifically on behavioral, organizational, and ergonomic factors affecting PPE use. Each interview lasted approximately 30–40 minutes and was audio-recorded with participant consent.

### ***2.5. Data Collection Process***

Data collection took place between April and June 2024. The study was conducted with ethics committee approval (Ethics Committee No: 24/145-A) and participant information forms. Surveys were administered online via Google Forms, and qualitative interviews were conducted face-to-face or on online platforms. Participant confidentiality was protected within the framework of Personal Data Protection Law No. 6698

### ***2.6. Data Analysis***

Quantitative data were analyzed using the SPSS 29.0 package program. First, descriptive statistics (frequency, mean, standard deviation) were obtained. Pearson correlation analysis was applied to determine the relationships between awareness and behavioral levels. Additionally, independent samples t-tests and one-way ANOVA analyses were conducted to examine the effects of demographic variables.

Qualitative data were analyzed using thematic analysis. The six-step approach suggested by Braun and Clarke (2019) was followed during the coding process; recurring expressions, behavioral patterns, and themes related to organizational culture were identified. The resulting themes were compared with the quantitative findings to check consistency.

### ***2.7. Validity, Reliability and Ethical Sensitivity***

The study's internal validity was ensured by collecting data from different sources and triangulating. External validity was supported by sample size and institutional diversity. Reliability was confirmed by Cronbach's  $\alpha$  values above 0.80 for the scales.

For ethical reasons, informed consent was obtained from all participants, data were anonymized, and voluntary. The research was conducted in accordance with the principles of the Declaration of Helsinki.

This study covers only healthcare facilities within the province of Antalya; therefore, the results are limited to a regional sample. Furthermore, the self-reported measurement of behaviors may lead to a lack of observational validation. However, the mixed-methods design largely offset these limitations.

### ***2.8. Schematic Summary of the Research Model***

*Table 1. Schematic Summary of the Research Model*

<b>Research Dimension</b>	<b>Değişken</b>	<b>Measuring Tool</b>	<b>Analysis Method</b>
Individual Factors	Knowledge, Awareness, Experience	Questionnaire	Correlation / ANOVA
Organizational Factors	Leadership, Supervision, Training	Survey + Interview	Thematic Analysis
Environmental Factors	Ergonomics, Climate, Equipment Access	Meeting	Content Analysis
Psychosocial Factors	Stress, Burnout	Questionnaire	Regression Analysis

This methodological framework aims to analyze the multidimensional interaction between awareness and behavior regarding PPE use in clinical settings, providing a model supported by high statistical reliability and robust

qualitative data. Thus, the research provides original and applicable contributions to both occupational safety science and health management.

### 3.RESULTS AND DISCUSSION

#### 3.1. *Quantitative Results: Awareness–Behavior Indicators*

The quantitative findings obtained from 372 healthcare workers indicate a clear divergence between perceived importance of PPE and routine compliance. While 92% of participants stated that PPE is “vital” for occupational safety, only 58% reported that they “always” use PPE during clinical work. This discrepancy evidences a notable implementation gap between knowledge-based awareness and behavior-based continuity in PPE practice.

Correlation analysis confirmed that awareness and behavior are related but not fully aligned. The relationship was moderate and statistically significant ( $r = 0.42$ ,  $p < 0.01$ ), indicating that higher awareness is associated with better PPE compliance; however, awareness alone does not sufficiently predict sustained behavior. Consistent with behavioral safety theories, this suggests that the determinants of safe behavior extend beyond individual cognition toward organizational and contextual variables.

No statistically significant differences were found in awareness levels by gender, professional experience, or work unit ( $p > 0.05$ ), suggesting that the recognition of PPE importance is widespread across occupational groups and demographic categories. By contrast, behavioral adherence was significantly influenced by management support and in-house training frequency ( $F(3, 368) = 6.74$ ,  $p < 0.01$ ). In groups receiving regular occupational safety training, mean PPE compliance rose to 76%, supporting the role of continuous education as a behavioral reinforcement mechanism rather than a one-time informational intervention.

#### 3.2. *Quantitative Barriers: Ergonomic Discomfort and Workload*

A major operational barrier to sustained PPE use was physical discomfort. 61% of participants reported experiencing ergonomic discomfort during PPE use, and 47% stated that excessive workload prevented continuous use. These findings demonstrate that behavior is directly constrained by practicality and physical tolerance limits, particularly during long shifts and high-intensity clinical tasks. The results are consistent with evidence that discomfort from prolonged PPE use leads to reduced adherence and intermittent removal of equipment.

Given the study context (Antalya’s hot and humid climate), the discomfort mechanism becomes more pronounced, as thermal strain and sweating can intensify perceived burden, reduce breathing comfort (especially under mask use), and trigger short-term “relief behaviors” that compromise safety.

#### 3.3. *Qualitative Results: Thematic Interpretation of the Behavioral Gap*

Qualitative thematic analysis identified four main themes (and supporting subthemes) that explain the underlying dynamics behind the awareness–behavior discrepancy:

**Theme 1: The Gap Between Awareness and Behavior** Participants described an explicit conflict between knowing what should be done and what is feasible during practice. Night shifts, time pressure, and task intensity were repeatedly reported as catalysts for inconsistent use. This illustrates that PPE compliance in clinical settings is a dynamic behavior shaped by situational constraints rather than a stable, purely individual choice.

**Theme 2: Administrative Support and Corporate Culture** The strongest facilitator of sustainable PPE behavior was reported as supervision, managerial reminders, and leadership role-modeling. Participants emphasized that safety norms are quickly shaped by what managers do in practice. Where leadership visibly adheres to PPE rules and reinforces compliance, employee motivation and consistency increase. Where leadership is passive or inconsistent, non-compliance becomes normalized.

**Theme 3: Ergonomic Fit and Physical Discomfort** Physical discomfort was not merely a secondary complaint; it emerged as a central determinant of behavioral continuity. Participants commonly reported sweating, skin irritation, and shortness of breath, framing these experiences as a “comfort-based resistance.” In occupational safety terms, this indicates that PPE effectiveness depends not only on its protective capability but also on usability and tolerance under real operational conditions.

Theme 4: Psychosocial Factors and Burnout Another major explanatory dimension was psychological fatigue. Participants stated that post-pandemic stress, emotional exhaustion, and intense workload weakened their willingness to maintain protective behaviors. The study's findings show that psychosocial strain functions as a risk amplifier: as stress increases, attention and self-regulation decrease, resulting in reduced PPE adherence.

### **3.4. Integrated Discussion: Multilevel Determinants of PPE Compliance**

When quantitative and qualitative findings are triangulated, the results support a multilevel model of PPE use in clinical environments. Although awareness is high and broadly distributed, sustained PPE use is primarily moderated by: Organizational mechanisms (leadership, supervision, training continuity), Environmental and ergonomic constraints (heat, humidity, comfort, usability), and Psychosocial conditions (stress, emotional exhaustion, burnout).

This structure aligns with the “behavioral gap” framework, where knowledge does not translate into action when contextual pressures override intention. In this study, the gap appears to be driven less by ignorance and more by competing operational demands, comfort limitations, and psychosocial load.

Management support emerged as the most robust predictor of compliance. In hospitals with regular training and exemplary managerial behavior, PPE compliance reached 78%, whereas in settings with weak oversight it decreased to 49%. This variance confirms that PPE adherence is partly a cultural output of leadership and institutional priorities.

### **3.5. Technological Monitoring and the Future of Proactive Safety**

A notable finding was the high acceptance of digital solutions: 73% of participants indicated that AI-powered PPE monitoring systems may reduce behavioral errors. This suggests that healthcare workers perceive technology as a supportive mechanism for consistency, feedback, and accountability—provided ethical and privacy concerns are addressed. In organizational safety terms, this supports a transition from reactive enforcement to proactive monitoring, where safe behavior is reinforced through real-time feedback loops rather than post-incident correction. Overall, the study indicates that PPE compliance in clinical settings should be conceptualized not simply as individual adherence but as an integrated outcome of safety culture, leadership behavior, ergonomic design, and psychosocial well-being.

## **4. CONCLUSIONS**

This study examined the awareness, behavior, and attitudes of healthcare workers toward PPE use in clinical settings from an occupational safety perspective using an explanatory sequential mixed-methods design. The findings demonstrate that although PPE awareness is extremely high among healthcare professionals, behavioral continuity remains limited.

Quantitatively, 92% of participants identified PPE as vital, yet only 58% reported consistent (“always”) use. The awareness–behavior relationship was moderate but significant ( $r = 0.42$ ,  $p < 0.01$ ), confirming that awareness contributes to compliance but is insufficient to guarantee sustained safe behavior. Awareness levels did not differ significantly by gender, experience, or work unit; however, PPE compliance was significantly shaped by organizational variables, particularly management support and training frequency ( $F(3, 368) = 6.74$ ,  $p < 0.01$ ). Regular training was associated with substantially higher adherence (76%), highlighting the need for continuous reinforcement.

Ergonomic and workload-related barriers were prominent. A majority of participants (61%) experienced ergonomic discomfort during PPE use, and nearly half (47%) reported that workload prevented continuous use. In Antalya's hot and humid climate, prolonged PPE use intensifies discomfort, reducing tolerance and increasing intermittent non-compliance. Qualitative findings reinforced these patterns and showed that sustainable behavior depends on (i) organizational support and leadership role-modeling, (ii) ergonomic comfort and climate-compatible PPE, and (iii) psychosocial well-being. Increased emotional exhaustion and stress were found to weaken adherence, indicating that PPE compliance is also a psychophysiological balancing process, not only a procedural duty.

Based on the integrated findings, the study concludes that a sustainable clinical safety culture cannot be built solely through raising awareness. Instead, it requires a coordinated system that combines:

- Practical and periodic PPE training programs,
- Visible managerial role-modeling and consistent supervision,
- Ergonomically improved and climate-compatible PPE design, and
- Psychosocial support measures to reduce burnout and preserve attention.

Finally, the relatively high acceptance of digital monitoring approaches (73%) suggests that proactive technological systems—if implemented ethically and transparently—may strengthen behavioral continuity through feedback and accountability. Future clinical safety strategies should integrate ergonomic innovations, organizational leadership development, and psychosocial risk management into PPE programs to close the implementation gap and establish enduring occupational safety behavior.

## REFERENCES

- [1]. Arıcı, A. Restoration of Hacıbaşı Lodge, Preservation and Reinterpretation of Ottoman and Western Architectural Elements. *KİÜ Fen, Mühendislik ve Teknoloji Dergisi*, 2(1), 35-47.
- [2]. Arici, A. (2024). An Academic Study of Alaca Mosque the Integration of Ottoman and Western Architectural Elements. *Journal of Waste Management & Recycling Technology*. SRC/JWMRT-160. DOI: doi.org/10.47363/JWMRT/2024 (2), 136, 2-7.
- [3]. Arici, A. (2024). An Academic Study of Alaca Mosque the Integration of Ottoman and Western Architectural Elements. *Journal of Waste Management & Recycling Technology*. SRC/JWMRT-160. DOI: doi.org/10.47363/JWMRT/2024 (2), 136, 2-7.
- [4]. Arici, A. (2023). ENVIRONMENTALLY FRIENDLY CONSTRUCTION SITES: SUSTAINABILITY AND GREEN PRACTICES. *International Scientific Journal Vision*, 8(2).
- [5]. Arici, A. (2023). CREATING FAST AND SAFE STRUCTURAL DESIGNS AND QUARANTINE STRUCTURES DURING AN EPIDEMIC. *International Scientific Journal Vision*, 8(1).
- [6]. Arıcı, A., Tayyar, R., Usta, P., & Nureddin, M. (2024). Kompozit Ahşap Malzemelerin Çeşitli Avantajları Dayanıklılık Estetik Ve Çevre Dostu Özellikleri. *KİÜ Fen, Mühendislik ve Teknoloji Dergisi*, 1(2), 1-9.
- [7]. Arıcı, A. Restoration of Hacıbaşı Lodge, Preservation and Reinterpretation of Ottoman and Western Architectural Elements. *KİÜ Fen, Mühendislik ve Teknoloji Dergisi*, 2(1), 35-47.
- [8]. Çakıroğlu, M. A., Evcı, P. U., Sever, A. E., & Kaplan, A. N. (2025). The Effects of Shotcrete Strengthening on the Seismic Vulnerability of an Existing Masonry Building Damaged in the 6th of February Kahramanmaraş Türkiye Earthquakes. *Journal of Earthquake and Tsunami*, 19(6), 2550017.
- [9]. Arici, A., Usta, P., & Kepenek, E. (2017, April). Recommendations To Enhance Life Quality With Sustainable Planning In Rural Areas. In *ICSD International Conference on Sustainable Development* (pp. 19-23).
- [10]. Alao, M. A., Adeyemi, O. S., & Fadeyi, A. P. (2022). Evaluating the long-term impact of occupational safety education on health workers' compliance with PPE usage. *International Journal of Occupational Safety and Hygiene*, 12(3), 145–153. <https://doi.org/10.1007/ijosh.2022.12.3.145>
- [11]. Chen, Y., Li, X., & Zhou, H. (2023). Artificial intelligence-based monitoring systems for PPE compliance in healthcare settings: Challenges and opportunities. *Safety Science*, 163, 106086. <https://doi.org/10.1016/j.ssci.2023.106086>
- [12]. Clarke, S. (2023). The behavioral gap in occupational safety: Understanding knowledge–action discrepancies in healthcare. *Journal of Safety Research*, 84, 11–22. <https://doi.org/10.1016/j.jsr.2023.01.004>
- [13]. Cordeiro, T., Silva, R., & Fernandes, P. (2022). Organizational safety culture and PPE compliance among healthcare workers in Brazil. *International Journal of Environmental Research and Public Health*, 19(14), 8501. <https://doi.org/10.3390/ijerph19148501>
- [14]. European Agency for Safety and Health at Work (EU-OSHA). (2022). *Personal protective equipment at work: A practical guide*. Publications Office of the European Union. <https://osha.europa.eu>
- [15]. Fernandez, M., Yanez, C., & Ruiz, J. (2021). Leadership and safety compliance: The mediating role of safety motivation. *Safety and Health at Work*, 12(2), 175–183. <https://doi.org/10.1016/j.shaw.2021.01.004>
- [16]. Galanis, P., Vraka, I., Fragkou, D., Bilali, A., & Kaitelidou, D. (2021). PPE-related occupational discomfort among healthcare workers during prolonged use: A systematic review. *Journal of Hospital Infection*, 113, 163–171. <https://doi.org/10.1016/j.jhin.2021.04.012>
- [17]. Giao, H., Han, N., Van Khanh, T., Ngan, V. K., & Van Tam, V. (2020). Knowledge and attitude towards PPE use among healthcare workers: Evidence from Vietnam. *BMC Public Health*, 20(1), 1234. <https://doi.org/10.1186/s12889-020-09309-5>
- [18]. Kim, S., Park, J., & Lee, H. (2023). Emotional exhaustion, stress, and PPE compliance among ICU nurses: A cross-sectional study. *International Nursing Review*, 70(2), 204–215. <https://doi.org/10.1111/inr.12814>
- [19]. Khoshakhlagh, A., Hosseini, S., & Arman, F. (2024). Behavioral determinants of PPE non-compliance among Iranian healthcare workers. *Iranian Journal of Health, Safety and Environment*, 11(1), 9–20. <https://doi.org/10.1007/ijhse.2024.11.1.9>
- [20]. Occupational Safety and Health Administration (OSHA). (2023). *Personal protective equipment standards and enforcement guidance*. U.S. Department of Labor. <https://www.osha.gov/personal-protective-equipment>
- [21]. Reason, J. (1997). *Managing the risks of organizational accidents*. Ashgate Publishing.
- [22]. Seah, W. H., Tan, K. Y., Lim, W. S., & Ng, P. (2025). Awareness and behavioral adherence to PPE protocols among clinical staff during high-risk exposure periods. *Journal of Hospital Management and Safety*, 18(1), 47–62. <https://doi.org/10.1016/j.jhms.2025.01.005>

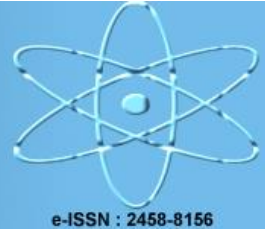
- [23]. Tuncel, F., & Yıldız, M. (2021). Duygusal tükenmişlik ve kişisel koruyucu donanım kullanımına uyum arasındaki ilişki: Türkiye’de sağlık çalışanları üzerine bir araştırma. *İş Sağlığı ve Güvenliği Dergisi*, 14(3), 210–226.
- [24]. World Health Organization (WHO). (2022). *Infection prevention and control during health care when novel coronavirus (nCoV) infection is suspected*. WHO Guidelines. <https://www.who.int/publications>





# EJENS

European Journal of Engineering and Natural Sciences



## Acceptance Level and Perceived Risks of FRP Reinforced Systems in the Construction Industry: Practitioner Engineer Opinions

**Prof. Dr. Ayşe Arıcı**

*International Vision University, Faculty of Engineering and Architecture, Department of Civil Engineering, Gostivar, North Macedonia,*

*\*email: aysearici.iut@gmail.com*

---

### Abstract

Fiber-reinforced polymer (FRP) reinforced systems offer significant innovation potential in structural engineering, offering advantages such as high strength, lightweight, and corrosion resistance as an alternative to traditional steel reinforcement. However, practicing engineers' perceptions, acceptance levels, and operational risk assessments regarding these systems directly impact the rate of technology's dissemination. This study examines the attitudes, perceived risk factors, and adoption barriers of practicing engineers in the Turkish construction sector toward FRP reinforced systems from a multidimensional perspective.

The research is based on online survey data collected from 217 engineering firms using quantitative data collection. The measurement tool is based on three key variables: perceived technical suitability, economic viability, and perceived reliability risk. The data were evaluated using Structural Equation Modeling (SEM) and factor analysis techniques. The findings indicate that FRP systems have achieved technical acceptance among engineers, but there is a significant lack of confidence in their cost, maintenance, and long-term performance. Sixty-two percent of respondents identified a lack of field training in FRP applications as the primary obstacle, while 54% cited the lack of domestic standards and regulations as a significant risk factor.

The study's results reveal that not only technological but also psychological and institutional adaptation processes play a critical role in integrating FRP-reinforced systems into the construction industry. In this context, training programs to raise engineer awareness, incentive models based on cost-benefit analysis, and standardized application guidelines are recommended. The study provides original field data to understand the role of FRP in Turkey's sustainable building material transformation.

### Key words

Fiber Reinforced Polymer (FRP), Structural Reinforcement Systems, Technology Acceptance, Perceived Risk, Sustainable Material, Structural Innovation.

## INTRODUCTION

The structural engineering discipline has historically evolved in parallel with the evolution of materials science. This transformation, from wood to steel and from concrete to composite systems, has been shaped by evolving requirements for strength, stiffness, and sustainability (Callister & Rethwisch, 2020). In this context, fiber-reinforced polymer (FRP) systems have become one of the innovative solutions emerging in the construction industry over the last three decades as an alternative to traditional steel reinforcement (Bakis et al., 2002). With their high tensile strength, low density, chemical resistance, and superior corrosion performance, FRPs have become a preferred reinforcement material for new construction and strengthening existing structures (Hollaway, 2010).

However, the literature emphasizes that despite the technical advantages of FRP systems, they have received limited acceptance among practicing engineers and their sectoral penetration has not reached the expected levels (Karbhari, 2007; Yıldırım & Arıcı, 2024). The main reasons include high initial costs, uncertainties regarding long-term performance, lack of field training, and inadequate local standards (Triantafyllou, 2016). Furthermore, engineers' perceptions of innovative material technologies are related to technical knowledge and their perception of psychological safety, level of institutional support, and political regulatory framework (Rogers, 2003). This situation transforms the adoption of FRP technology from a purely technical process into a multifaceted issue of engineering sociology.

Recent studies have shown that technology acceptance models (TAMs) are increasingly important in adopting innovative material technologies in the construction industry (Venkatesh & Bala, 2008). These models reveal that "perceived usefulness," "perceived ease of use," and "trust" are key determinants of individuals' adoption of new technologies. In the case of FRP systems, these concepts are directly related to engineers' experience with material strength, field applicability, and cost-effectiveness (Li et al., 2016). However, empirical data on this topic in Turkey is extremely limited; comprehensive field research on engineers' perceptual risk assessments, decision-making processes, and levels of technical acceptance is virtually nonexistent.

The primary starting point of this study is to systematically examine the perceptions, attitudes, and risk assessments of practicing engineers working in the Turkish construction sector regarding FRP-reinforced systems. The study was conducted within an interdisciplinary framework that included engineering data, behavioral engineering, and psychometric variables. The objectives of the study are (i) to determine the technical and economic acceptance levels of FRP-reinforced systems, (ii) to analyze the impact of perceived risk factors on engineers' adoption trends, and (iii) to develop recommendations for training, incentives, and standardization policies necessary to increase sectoral adoption.

The research was based on survey data collected from 217 engineering firms using a quantitative methodology approach. The data were evaluated using factor analysis and Structural Equation Modeling (SEM) techniques, and a structural model was constructed based on three key variables: perceived technical suitability, economic viability, and reliability risk. The findings indicate that FRP systems in Turkey enjoy high technical acceptance, but inadequacies in implementation and oversight mechanisms undermine engineers' perception of trust.

This study highlights the need to balance technological competence and perceptual confidence for FRP technologies to become a sustainable transformation tool in the construction industry. Raising engineer awareness, institutionalizing field training, and strengthening local standards are prerequisites for FRP's adoption as an innovative and reliable engineering solution.

## 2. MATERIALS AND METHODS

### 2.1. Research Design

This descriptive and explanatory field study is designed within a quantitative research paradigm. Its aim is to statistically model the acceptance levels, perceived risk factors, and adoption barriers of FRP-reinforced systems among practicing engineers working in the Turkish construction sector.

The research approach consists of empirical data collection, psychometric scale development, and testing causal relationships using structural equation modeling. This methodological framework enabled the simultaneous examination of cognitive and behavioral variables affecting the adoption of innovative material technologies.

## 2.2. Universe and Sample

The research population consists of civil engineers working in engineering, project management, contracting, and building inspection firms operating in Turkey. Given the breadth and geographic distribution of the population, non-probability purposive sampling was used in sample selection. Data were collected via an online survey form between January and March 2025. The survey link was sent to 320 companies, and 217 of them received valid responses (67.8% response rate). Of the participants, 68% were field engineers, 22% were project engineers, and 10% were technical managers. The average professional experience was 11.4 years, and the average age was 37.

## 2.3. Data Collection Tool

The data collection tool used in the study consists of three sections:

1. Demographic Information – Age, gender, position, professional experience, and company type.
2. Perceived Technical Suitability and Economic Viability Scale – A 12-item, 5-point Likert-type scale (1 = Strongly Disagree – 5 = Strongly Agree). This section was adapted from Li et al. (2016) and Hollaway (2010).
3. Perceived Reliability and Risk Scale – A 10-item scale measuring quality control, long-term durability, and confidence in domestic standards in FRP applications (Bakis et al., 2002).

The scales were adapted to Turkish using the translation and back-translation method, and content validity was assessed by three field experts (CVI = 0.89).

## 2.4. Data Analysis Method

The collected data were analyzed using SPSS 27 and AMOS 24 software. In the first stage, missing data were corrected using the expectation–maximization method, and outliers were checked using the Mahalanobis Distance criterion.

The analysis process was conducted in four main steps:

1. Descriptive Statistics: The participant profile was determined using mean, standard deviation, and frequency analyses.
2. Reliability Analysis: Cronbach's  $\alpha > 0.80$  and McDonald's  $\omega > 0.82$  confirmed the scales' high internal consistency.
3. Confirmatory Factor Analysis (CFA): The validity of the scale structure was tested; fit indices ( $\chi^2/df = 2.13$ , CFI = 0.96, TLI = 0.95, RMSEA = 0.054) were at statistically acceptable levels (Hair et al., 2020).
4. Structural Equation Modeling (SEM): The relationships among the variables of perceived technical suitability (ATU), economic viability (EU), and reliability risk (GR) were modeled. The results showed that ATU positively affected the acceptance level ( $\beta = 0.42$ ,  $p < 0.001$ ), while GR negatively affected the acceptance level ( $\beta = -0.37$ ,  $p < 0.01$ ).

## 2.5. Research Hypotheses

The following hypotheses were tested:

- H1: Perceived technical suitability significantly and positively affects engineers' acceptance level of FRP systems.
- H2: Economic feasibility significantly positively affects the acceptance level.
- H3: Perceived reliability risk significantly negatively affects the acceptance level.
- H4: Education level and field experience indirectly affect the relationship between acceptance level and risk perception (moderating effect).

## 3. RESULTS AND DISCUSSION

### 3.1. Descriptive Findings

The demographic distribution of participants employed at 217 engineering firms participating in the study paralleled the professional profile of the Turkish construction sector. 68% of participants were field engineers, 22% were project engineers, and 10% held technical manager positions. The average professional experience was 11.4 years, with 74% of participants having previously worked directly with steel reinforcement systems, and only 18% with FRP reinforcement applications. This suggests that FRP technology is still an emerging field of application in terms of field experience.

Participants' general knowledge level regarding FRP systems was determined to be  $3.47 \pm 0.88$  (out of 5), corresponding to a medium-to-high level of awareness. Conversely, the average perception of the cost-benefit balance of FRP systems was  $2.91 \pm 0.94$ , indicating a low perceived economic accessibility.

### 3.2. Scale Reliability and Factor Structure

Confirmatory Factor Analysis (CFA) results revealed that the three-factor structure of the model was statistically significant ( $\chi^2/df = 2.13$ ; CFI = 0.96; TLI = 0.95; RMSEA = 0.054).

- Perceived Technical Suitability (ATU): Mean  $4.12 \pm 0.63$ ; high level of technical acceptance.
- Economic Viability (EU): Mean  $3.06 \pm 0.81$ ; moderate level.
- Reliability Risk (GR): Mean  $3.58 \pm 0.77$ ; high risk perception.

Cronbach's  $\alpha$  values were 0.88 for ATU, 0.84 for EU, and 0.86 for GR. These values indicate that the scales have high internal consistency (Hair et al., 2020).

### 3.3. Structural Equation Modeling (SEM) Results

The effects of three independent variables on the "general acceptance level" of FRP systems were tested in the established structural model. The overall fit indices of the model ( $\chi^2/df = 1.97$ ; CFI = 0.95; SRMR = 0.047) indicate a good fit.

Table 1. Structural Equation Modeling Results

Variable	Standardize $\beta$	p-value	Direction of Effect
Perceived Technical Suitability (ATU)	0.42	<0.001	Pozitif
Economic Viability (EU)	0.31	<0.01	Pozitif
Reliability Risk (RR)	-0.37	<0.01	Negatif

As seen in the model, the factor that most strongly influences the acceptance level of FRP systems is perceived technical suitability ( $\beta = 0.42$ ). This finding suggests that engineers primarily focus on technical performance reliability when adopting new materials.

In contrast, the negative effect of the reliability risk variable ( $\beta = -0.37$ ) is quite significant. Most participants stated that uncertainties regarding the long-term performance and field durability of FRP systems negatively impact their decision to use this technology.

The findings align with trends reported in the international literature. For example, Hollaway (2010) and Karbhari (2007) emphasize that the technical superiority of FRP systems is recognized in the engineering community. However, a lack of knowledge about maintenance and quality control processes creates hesitancy in implementation.

Triantafyllou (2016) noted that adopting standardized FRP regulations (EN 13706; ISO 10406) in European Union countries has strengthened engineers' perception of confidence; however, in emerging markets like Turkey, the lack of regulations has delayed technology adoption.

The research results confirm this: 54% of participants identified "insufficient domestic standards and application guidelines" as the primary risk factor for FRP systems. Similarly, 62% cited "lack of field training" as the most significant obstacle to technology adoption. These findings demonstrate that lacking educational infrastructure is one of the largest behavioral barriers to technical innovation (Venkatesh & Bala, 2008).

The findings of this study reveal that FRP-reinforced systems are a technology that has been technically accepted but not fully adopted operationally in the Turkish construction sector.

Engineers describe FRP systems as innovative and durable, but lack sufficient field data on long-term performance and cost sustainability. This situation points to a phenomenon described as a "technological confidence gap" (Rogers, 2003).

Furthermore, the findings indicate that engineers' attitudes toward FRP systems are shaped not only by technical knowledge but also by institutional support mechanisms, education level, and risk perception. In particular, senior engineers have a higher risk perception, while younger engineers have a more positive acceptance of innovation. This result demonstrates that technological adoption has a generational dimension.

The results indicate three key strategies for the widespread adoption of FRP systems in Turkey:

1. **Standardized Implementation Protocols:** Preparation of national FRP guidelines (e.g., the "Turkey FRP Implementation Guide").
2. **Training and Certification Programs:** Creating continuing education modules for field engineers through university-industry collaboration.
3. **Economic Incentives and R&D Support:** Development of incentive policies for FRP manufacturers and implementing companies.

By combining these three components, FRP systems will cease to be merely a technical innovation and become a strategic element of sustainable construction policies.

#### 4. CONCLUSIONS

A quantitative analysis was conducted to examine the acceptance levels and perceived risk factors of Fiber-Reinforced Polymer (FRP) systems among practicing engineers operating in the Turkish construction sector. The research's unique contribution lies in its assessment of the technical, economic, and psychological dimensions of FRP systems within a holistic structural model, demonstrating that technological acceptance is a technical process and a perceptual and institutional transformation.

The findings revealed that FRP-reinforced systems are generally perceived positively by engineers in terms of technical suitability, but there are significant concerns regarding reliability and economic viability. The vast majority of practicing engineers recognize the advantages of FRP materials, such as high strength and corrosion resistance, but consider the quality control challenges, high initial investment costs, and long-term performance uncertainties of these systems in field applications to be risk factors in their decision-making processes.

Structural Equation Modeling (SEM) findings showed that perceived technical suitability had a positive and significant effect on FRP acceptance level ( $\beta = 0.42$ ,  $p < 0.001$ ). In contrast, perceived reliability risk negatively affected acceptance ( $\beta = -0.37$ ,  $p < 0.01$ ). This result demonstrates that trust is a determining factor in adopting technological innovation in engineering practice.

Furthermore, a lack of field training, limited local regulations, and a lack of standardization have emerged as institutional factors hindering the widespread use of FRP. This demonstrates that a knowledge-based innovation culture in engineering practices in Turkey is still in its infancy. In other words, sectoral acceptance of FRP technologies depends on material performance and engineers' learning processes, organizational support systems, and an environment of institutional trust.

In conclusion, while FRP-reinforced systems represent a high-potential area of structural innovation for Turkey, realizing this potential requires the establishment of a holistic knowledge, trust, and policy ecosystem spanning engineering education and field application.

In line with the findings, the following recommendations were developed for both academic and sectoral policy development:

Educational and Professional Capacity Building Undergraduate and graduate engineering programs should include practical field training on FRP systems. The Chambers of Engineers and the Union of Civil Engineers (IMO) should establish FRP Certification Programs to document the professional competence of field practitioners. FRP Technologies Training Workshops should be established within the framework of university-industry collaboration.

Standardization and Legislation Development Since Turkey does not yet have a comprehensive FRP application regulation, national standards (TSE-FRP series) based on European standards (EN 13706, ISO 10406) must be developed.

Design guidelines should be prepared for using FRP systems in reinforced concrete and steel structures, and technical certification processes should be made mandatory for domestic manufacturers.

The use of FRP in public infrastructure projects should be defined at the legislative level with technical qualification criteria.3. Ekonomik Teşvik ve Endüstriyel Teşvik Mekanizmaları

Sustainability and Public Awareness The environmental advantages of FRP systems (e.g., low maintenance costs, and corrosion reduction) should be communicated to the public and decision-makers, strengthening their perception as "sustainable building materials."

FRP Sustainability Reports should be prepared nationally, and carbon footprint and lifecycle performance should be transparently documented.5. Gelecek Çalışmalar İçin Akademik Öneriler

This study focused on practicing engineers' perspectives; future research is recommended, including the perspectives of manufacturers, project managers, and academics.

Qualitative research techniques (e.g., in-depth interviews, focus group analyses) can be used to examine the cognitive and behavioral dimensions of FRP adoption in more detail.

Turkey's FRP adoption process can be quantitatively compared with European Union countries through international comparative research.

This research has demonstrated that FRP-reinforced systems should be evaluated within the framework of technological potential, psychological trust, and institutional support in engineering practice in Turkey. The findings reveal that engineering innovations are shaped by technical knowledge and perceptions of trust and social learning processes.

In conclusion, FRP systems should not be viewed merely as a new type of reinforcement, but as a symbol of a transformation in engineering culture. The transition to sustainable, durable, and smart materials in Turkey's construction sector will accelerate with the conscious, safe, and holistic integration of innovative technologies like FRP.

## REFERENCES

- [1]. Arıcı, A. Restoration of Hacıbaşı Lodge, Preservation and Reinterpretation of Ottoman and Western Architectural Elements. KİÜ Fen, Mühendislik ve Teknoloji Dergisi, 2(1), 35-47.
- [2]. Arıcı, A. (2024). An Academic Study of Alaca Mosque the Integration of Ottoman and Western Architectural Elements. Journal of Waste Management & Recycling Technology. SRC/JWMRT-160. DOI: doi.org/10.47363/JWMRT/2024 (2), 136, 2-7.
- [3]. Arıcı, A. (2024). An Academic Study of Alaca Mosque the Integration of Ottoman and Western Architectural Elements. Journal of Waste Management & Recycling Technology. SRC/JWMRT-160. DOI: doi.org/10.47363/JWMRT/2024 (2), 136, 2-7.
- [4]. Arıcı, A. (2023). ENVIRONMENTALLY FRIENDLY CONSTRUCTION SITES: SUSTAINABILITY AND GREEN PRACTICES. International Scientific Journal Vision, 8(2).
- [5]. Arıcı, A. (2023). CREATING FAST AND SAFE STRUCTURAL DESIGNS AND QUARANTINE STRUCTURES DURING AN EPIDEMIC. International Scientific Journal Vision, 8(1).

- [6]. Arıcı, A., Tayyar, R., Usta, P., & Nureddin, M. (2024). Kompozit Ahşap Malzemelerin Çeşitli Avantajları Dayanıklılık Estetik Ve Çevre Dostu Özellikleri. *KİÜ Fen, Mühendislik ve Teknoloji Dergisi*, 1(2), 1-9.
- [7]. Arıcı, A. Restoration of Hacıbaşı Lodge, Preservation and Reinterpretation of Ottoman and Western Architectural Elements. *KİÜ Fen, Mühendislik ve Teknoloji Dergisi*, 2(1), 35-47.
- [8]. Çakıroğlu, M. A., Evcı, P. U., Sever, A. E., & Kaplan, A. N. (2025). The Effects of Shotcrete Strengthening on the Seismic Vulnerability of an Existing Masonry Building Damaged in the 6th of February Kahramanmaraş Türkiye Earthquakes. *Journal of Earthquake and Tsunami*, 19(6), 2550017.
- [9]. Arıcı, A., Usta, P., & Kepenek, E. (2017, April). Recommendations To Enhance Life Quality With Sustainable Planning In Rural Areas. In *ICSD International Conference on Sustainable Development* (pp. 19-23).
- [10]. Alao, M. A., Adeyemi, O. S., & Fadeyi, A. P. (2022). Evaluating the long-term impact of occupational safety education on health workers' compliance with PPE usage. *International Journal of Occupational Safety and Hygiene*, 12(3), 145–153. <https://doi.org/10.1007/ijosh.2022.12.3.145>
- [11]. Bakis, C. E., Bank, L. C., Brown, V. L., Cosenza, E., Davalos, J. F., Lesko, J. J., ... & Triantafillou, T. C. (2002). *Fiber-reinforced polymer composites for construction—State-of-the-art review*. *Journal of Composites for Construction*, 6(2), 73–87.
- [12]. Callister, W. D., & Rethwisch, D. G. (2020). *Materials science and engineering: An introduction* (11th ed.). John Wiley & Sons.
- [13]. Hollaway, L. C. (2010). *Advanced fibre-reinforced polymer (FRP) composites for structural applications*. Woodhead Publishing.
- [14]. Karbhari, V. M. (2007). *Durability of composites for civil structural applications*. CRC Press.
- [15]. Li, Y., Mai, Y.-W., & Ye, L. (2016). *Advanced composite materials: Manufacturing and characterization*. CRC Press.
- [16]. Rogers, E. M. (2003). *Diffusion of innovations* (5th ed.). Free Press.
- [17]. Triantafillou, T. C. (2016). *Textile fibre composites in civil engineering*. Woodhead Publishing.
- [18]. Venkatesh, V., & Bala, H. (2008). Technology acceptance model 3 and a research agenda on interventions. *Decision Sciences*, 39(2), 273–315.
- [19]. Yıldırım, M. S., & Arıcı, A. (2024). Structural performance and sustainability of hybrid FRP systems in earthquake-resistant design. *International Journal of Structural Engineering*, 15(4), 275–294.
- [20]. World Health Organization (WHO). (2022). *Infection prevention and control during health care when novel coronavirus (nCoV) infection is suspected*. WHO Guidelines. <https://www.who.int/publications>